

AD-A193 519

ANALYSIS OF STIFFNESS REDUCTION FAILURE AND STRESS  
CONCENTRATION IN FIBER. (U) PENNSYLVANIA UNIV  
PHILADELPHIA DEPT OF MATERIALS SCIENCE AND E.

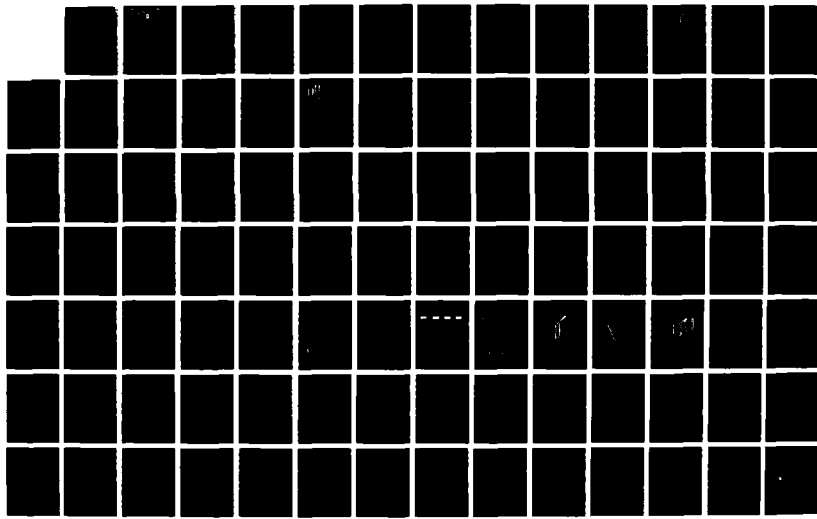
1/2

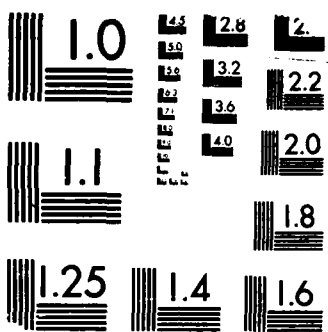
UNCLASSIFIED

2 HASHIN 31 DEC 87 AFOSR-TR-88-0367

F/G 11/4

NL





MICROCOPY RESOLUTION TEST CHART  
IRFAU STANDARDS-1963-A

**UNCLASSIFIED**

SECURITY CLASSIFICATION OF THIS PAGE

**DTIC FILE COPY**

2

**DTIC DOCUMENTATION PAGE****1a. REPORT SECURITY CLASSIFICATION****ELECTE****AD-A193 519****DR 01 1988****MODULE****D****4. PERFORMING ORGANIZATION REPORT NUMBER****HQ****6a. NAME OF PERFORMING ORGANIZATION**

University of Pennsylvania

**6b. OFFICE SYMBOL  
(if applicable)**

ORA

**6c. ADDRESS (City, State and ZIP Code)**133 S. 36th St., Suite 300  
Philadelphia, PA 19104-3246**7a. NAME OF MONITORING ORGANIZATION**

Air Force Office of Scientific Research

**8a. NAME OF FUNDING/SPONSORING  
ORGANIZATION**

AFOSR

**8b. OFFICE SYMBOL  
(if applicable)**

NA

**8c. ADDRESS (City, State and ZIP Code)**Boiling Air Force Base  
Washington, DC 20332-6448**9. PROCUREMENT INSTRUMENT IDENTIFICATION NUMBER**

AFOSR-85-0342

**11. TITLE (Indicate Security Classification)**Analysis of Stiffness  
Reduction, Failure and Stress Concentration**12. PERSONAL AUTHOR(S) in Fiber Composite Laminates**

Dr. Zvi Hashin

**13a. TYPE OF REPORT**

Final

**13b. TIME COVERED**

FROM 10/1/85 TO 12/31/87

**14. DATE OF REPORT (Yr. Mo. Day)****15. PAGE COUNT**

132

**16. SUPPLEMENTARY NOTATION****17. COSATI CODES****18. SUBJECT TERMS (Continue on reverse if necessary and identify by block number)**Crack, Damage, Delamination, Differential Scheme, Failure,  
Fiber Composite, Interlaminar, Intralaminar, Laminate, Stiff-  
ness, Thermal Expansion, Variational Method**19. ABSTRACT (Continue on reverse if necessary and identify by block number)**

A novel variational method to evaluate the stiffness reduction and the internal stresses  $[0^\circ/90^\circ]_n$  laminates has been developed and has been applied to analysis of glass/epoxy and graphite/epoxy laminates. The method has been extended to evaluate thermal expansion coefficients of cracked laminates and also internal stresses due to temperature change. Results demonstrate the stiffness, Poissons ratio and thermal expansion coefficients of cracked density. In particular, it has been shown that the values of thermal expansion coefficients of cracked laminates also depend on the signs of load and temperature change. Internal stresses obtained convey important information about sources of continued internal failure.

A comprehensive survey on damage in fiber composite materials has been prepared including classification of the various kinds of damage and description of methods of analysis.

**20. DISTRIBUTION/AVAILABILITY OF ABSTRACT**UNCLASSIFIED/UNLIMITED  SAME AS RPT.  DTIC USERS **21. ABSTRACT SECURITY CLASSIFICATION****UNCLASSIFIED****22a. NAME OF RESPONSIBLE INDIVIDUAL**

George K HARSH

**22b. TELEPHONE NUMBER  
(Include Area Code)**

(202) 767-0463

**22c. OFFICE SYMBOL**

NA

APOS.R-TK. 68-0367

19. ABSTRACT (continued).

The differential scheme approximation for effective properties of composite materials has been modified and generalized to the case of cracked materials. The method is of general nature. Specific results have been given for stiffness reduction due to cracks for isotropic materials containing many randomly oriented elliptical or penny shaped cracks and for orthotropic (fiber composite) sheets containing many aligned cracks (along fibers). The method corrects serious shortcomings of the usually employed self consistent scheme.

Accession For	
NTIS GRA&I	<input checked="" type="checkbox"/>
DTIC TAB	<input type="checkbox"/>
Unannounced	<input type="checkbox"/>
Justification	
By	
Distribution/	
Availability Codes	
Dist	Avail and/or Special
A-1	

AFOSR-TN- 88-0367

DEPARTMENT OF THE AIR FORCE  
AIR FORCE OFFICE OF SCIENTIFIC RESEARCH  
BOLLING AIR FORCE BASE, DC 20332-6448

Contract AFOSR-85-0342

ANALYSIS OF STIFFNESS REDUCTION, FAILURE AND STRESS  
CONCENTRATION IN FIBER COMPOSITE LAMINATES

Dr. Z. Hashin - Principal Investigator

Final Report  
October 1, 1985 - December 31, 1987

DEPARTMENT OF MECHANICAL ENGINEERING AND APPLIED MECHANICS  
DEPARTMENT OF MATERIALS SCIENCE AND ENGINEERING  
SCHOOL OF ENGINEERING AND APPLIED SCIENCE  
UNIVERSITY OF PENNSYLVANIA  
PHILADELPHIA, PA 19104-6315

88 3 31 005

## 1. SUMMARY

A novel variational method to evaluate the stiffness reduction and the internal stresses in  $[0^\circ_m / 90^\circ_n]_s$  laminates has been developed and has been applied to analysis of glass/epoxy and graphite/epoxy laminates. The method has been extended to evaluate thermal expansion coefficients of cracked laminates and also internal stresses due to temperature change. Results demonstrate the stiffness, Poisson's ratio and thermal expansion coefficients changes with crack density. In particular, it has been shown that the values of thermal expansion coefficients of cracked laminates also depend on the signs of load and temperature change. Internal stresses obtained convey important information about sources of continued internal failure.

A comprehensive survey on damage in fiber composite materials has been prepared including classification of the various kinds of damage and description of methods of analysis.

The differential scheme approximation for effective properties of composite materials has been modified and generalized to the case of cracked materials. The method is of general nature. Specific results have been given for stiffness reduction due to cracks for isotropic materials containing many randomly oriented elliptical or penny shaped cracks and for orthotropic (fiber composite) sheets containing many aligned cracks (along fibers). The method corrects serious shortcomings of the usually employed self consistent scheme.

## 2. RESEARCH OBJECTIVES

- (a) To develop analysis of stiffness reduction of laminates due to intralaminar crack distribution in more than one direction.
- (b) To develop analysis of change of thermal expansion coefficients of laminates due to intra-

laminar crack distributions.

- (c) To evaluate internal stresses, due to load and temperature change, in laminates with intra-laminar crack distributions and to utilize these to assess sources of progressive internal failure.
- (d) To evaluate stiffness reduction of solids due to distributions of cracks of various shapes.
- (e) To analyze by variational methods stress concentrations near edges of laminates and holes.

### 3. STATUS OF RESEARCH

Under a previous AFOSR contract we have developed a novel variational method which enabled us to evaluate stiffness reduction and approximate internal stresses in a cross-ply laminate with only one ply cracked. The stiffness reduction results were found to be in remarkable agreement with experimental results, [1]. Under the present contract we have generalized this method to cross-ply laminates in which all plies may be cracked along the fibers [2]. We have called such laminates - orthogonally cracked. It should be noted that to the best of our knowledge the literature contains only one publication on the subject of analysis of orthogonally cracked laminates which employs very extensive numerical analysis while the present analysis is mathematically so simple that the results can be evaluated on a programmable calculator.

We have obtained expressions for Youngs moduli and Poissons ratios of orthogonally cracked laminates for arbitrary crack density of intralaminar cracks as well as approximate three dimensional stresses in the laminate. We have found that only the cracks transverse to the load have a significant effect on Youngs modulus in that direction while Poissons ratio is significantly affected by the two

crack families. The internal stresses reveal that the stress normal to laminate midplane (peeling stress) is a major source of continued crack formation [2].

To complete the elastic properties of the orthogonally cracked laminate we also need the shear modulus. Unfortunately our considerable efforts to evaluate this modulus have not been successful because of some peculiar mathematical difficulties and we hope to resolve this problem at some future time.

Other important properties are the thermal expansion coefficients of the cracked laminate. We were able to evaluate these in novel and simple fashion [3] on the basis of some general theorems on thermoelasticity of composite materials and the internal stresses given in [2]. The results show that the thermal expansion coefficients diminish significantly with increasing crack density to attain asymptotic values. Furthermore, it has been shown that the values of the thermal expansion coefficients depend on the nature of the load (tension or compression) and temperature change (heating or cooling) since internal cracks may all be open, some open some closed, or all closed.

We were also able to evaluate the internal thermal stresses in an orthogonally cracked laminate [6] by utilization of variational principles of thermoelasticity and admissible stress fields of the type used in [2]. These stresses indicate which way internal failure proceeds due to temperature change.

A very important problem which has received much attention in the literature is stiffness reduction of a solid by various distributions of cracks. For example : elliptical cracks in different orientations or aligned line cracks. Exact solutions for such problems are available only for dilute concentration of cracks which implies that mutual distances between cracks are so large that they do not interact, which is not a practical situation. The current most popular approximate approach to this problem is the self consistent scheme but the results of this method are often unreliable. We have been able to devise another approximate method which is as general as the self consistent scheme but does not exhibit its shortcomings. The essence of the method is modification and generalization of the approach known as the differential scheme ,which has been employed to evaluate effective properties of composite materials, to cracked materials [5].

According to the contract statement of work we have examined the capability of our variational approach to obtain stress concentrations at edges of laminates and holes. After considerable work we have reached the conclusion that the method is too complicated for this purpose and that the appropriate approach to such problems is numerical analysis by finite elements.

#### 4. LIST OF PUBLICATIONS

1. Z.Hashin - Analysis of stiffness reduction of cracked cross-ply laminates - Engng.Fracture Mech.,25, 771-778, (1986)
2. Z.Hashin - Analysis of orthogonally cracked laminates under tension - J.Appl.Mech., 54, 872-879, (1987)
3. Z.Hashin - Thermal expansion coefficients of cracked laminates - Composites Science & Technology, in press.
4. Z.Hashin - Analysis of damage in composite materials - Proc.IUTAM Symp. on Yielding, Damage and Failure of Anisotropic Solids, Villard de Lans, France, to appear.
5. Z.Hashin - The differential scheme and its application to cracked materials - J.Mech.Phys.Solids, to appear.
6. Z.Hashin - Thermal stresses in orthogonally cracked laminates - in preparation.

## 5. PROFESSIONAL PERSONNEL

Dr. Zvi Hashin - Principal Investigator

## 6. INTERACTIONS

- (a) Analysis of Cracked Laminates - invited lecture, Gordon Research Conference on Composites, Santa Barbara, CA. January 1986
- (b) Analysis of Damaged Laminates - seminar lecture, Center for Composite Materials, RPI, Troy, NY August 1986; NASA Program for Composite Materials, VPI, Blacksburg, VA, February 1987.
- (c) Analysis of damage in composite materials - invited general lecture, IUTAM Symposium on Yielding, Damage and Failure of Anisotropic Materials, Villard de Lans, France, August 1987.

## ANALYSIS OF STIFFNESS REDUCTION OF CRACKED CROSS-PLY LAMINATES

Z. HASHIN

Department of Solid Mechanics, Materials and Structures, Tel-Aviv University, Tel-Aviv, Israel

**Abstract**—Stiffness reduction of cracked  $[0^\circ/90^\circ]$  laminates is analyzed by variational methods on the basis of the principle of minimum complementary energy. For this purpose admissible stress systems are constructed which satisfy equilibrium and all boundary and interface conditions. The optimal stress field is then determined by minimization of complementary energy. The analysis allows for crack interaction and random crack distribution. Results are given for Young's modulus, shear modulus and Poisson's ratio. Young's modulus results are in excellent agreement with experimental data for  $[0^\circ/90^\circ]$  glass/epoxy laminate.

### 1. INTRODUCTION

DURING static or cyclic loading, fiber composite laminates in which the matrix is polymeric develop distributions of *intralaminar* cracks which extend along the fibers, traverse the plies through their thickness and are essentially perpendicular to the planes of the plies. Other kinds of cracks are *interlaminar*, i.e. plane cracks within the interfaces between plies. Such cracks may be initiated at the intersection of intralaminar cracks as well as at laminate edges due to high interlaminar stresses which develop at such locations. Such cracks are the major *damage* which occurs in a laminate during the process of loading.

The main macroscopic effect of such cracks on laminate properties is reduction of stiffness. Since a laminate is a thin plane structural element, the effect of interlaminar cracks on stiffness reduction is in general negligible. Indeed the only effect of stiffness reduction of such cracks appears in the case of bending stiffness at regions of high transverse shear. Here we shall only be concerned with in-plane stiffness and in this case only the intralaminar cracks produce stiffness reduction. Thus the problem to be considered is the effect of distributions of intralaminar cracks on laminate in-plane stiffness.

There has been much interest in this problem in recent years. We cite the works of Reifsneider[1] and Highsmith and Reifsneider[2], who treated the problem in terms of shear lag analysis, Laws and Dvorak[3], who employed the self-consistent scheme approximation to assess the stiffness reduction of a cracked lamina in a laminate, and Talreja[4], who employed continuous damage theory.

The various approaches cited well-illustrate the dilemmas with which one is faced in the general problem of analysis of the effects of damage on stiffness reduction. It is certainly desirable to recognize and incorporate the microstructural details of damage (cracks in the present case) but this leads to severe mathematical difficulties, primarily because of the zero traction conditions which have to be satisfied on crack surfaces. Such treatment must of necessity be approximate, thus the simple shear lag analysis. It is thus tempting to describe damage in terms of some continuous fields, as was done in [4], but the precise mathematical nature of such a description is not clear, must be assumed, and involves parameters which must be experimentally determined with the hope that they are indeed material constants. Here we present a microstructural approach based on variational methods which is more realistic and accurate than the simple shear lag analysis. The analysis involves construction of admissible stress fields which satisfy equilibrium, all boundary conditions on laminate and crack surfaces and all interlaminar traction continuity conditions. These admissible fields deviate from the exact stress fields only in terms of a single approximation as will be explained below. The stress energies associated with these fields define lower bounds on stiffness which are optimized by variational methods.

### 2. ANALYSIS OF CRACKED CROSS-PLY UNDER TENSION

We first consider a cracked cross-ply laminate which is subjected to simple tension (Fig. 1). In the absence of cracks the stresses in the plies are plane and constant in each lamina and are readily found by elementary conventional laminate analysis. We denote such stresses as  $\sigma_{xx}^{0(m)}$ ,  $\sigma_{yy}^{0(m)}$  and  $\sigma_{xy}^{0(m)}$

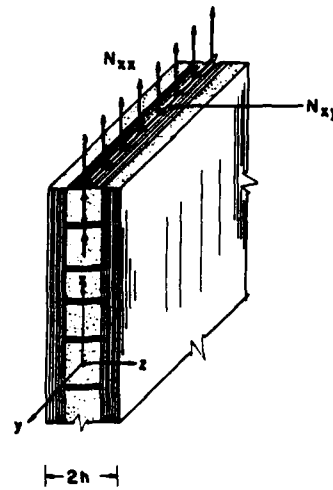


Fig. 1. Cracked cross-ply loaded by tension and shear.

where  $m = 1, 2$  is the ply index. In particular we shall use the notation

$$\sigma_{xx}^{0(1)} = \sigma_1, \quad \sigma_{xx}^{0(2)} = \sigma_2$$

where from now on 1 indicates the  $90^\circ$  ply and 2 indicates the  $0^\circ$  plies.

The presence of cracks will produce a different space variable stress system which is  $xz$  plane. We denote the stress perturbations produced by the cracks in the different plies by  $\sigma_{ij}^{(m)}$ ;  $i, j = x, z$ . We introduce the basic approximation that  $\sigma_{xx}^{(1)}$  and  $\sigma_{xx}^{(2)}$  are not functions of  $z$ . We thus denote these stresses as

$$\sigma_{xx}^{(1)} = -\sigma_1 \phi_1(x), \quad \sigma_{xx}^{(2)} = -\sigma_2 \phi_2(x) \quad (2.1)$$

where  $\phi_1$  and  $\phi_2$  are unknown functions. We seek stress systems  $\sigma_{ij}^{(1)}$  and  $\sigma_{ij}^{(2)}$  which satisfy the equilibrium equations and all boundary and interface conditions of the laminate. It may be shown (see [5] for details) that such stress systems are

$$\begin{aligned} \sigma_{xx}^{(1)} &= -\sigma_1 \phi(x) \\ \sigma_{xz}^{(1)} &= \sigma_1 \phi'(x)z \\ \sigma_{zz}^{(1)} &= \sigma_1 \phi''(x) \frac{1}{2} (ht_1 - z^2) \\ \sigma_{xx}^{(2)} &= \sigma_1 \frac{t_1}{t_2} \phi(x) \end{aligned} \quad (2.2)$$

$$\sigma_{xz}^{(2)} = \sigma_1 \frac{t_1}{t_2} \phi'(x)(h - z)$$

$$\sigma_{zz}^{(2)} = \sigma_1 \frac{t_1}{t_2} \phi''(x) \frac{1}{2} (h - z)^2$$

with the crack boundary conditions

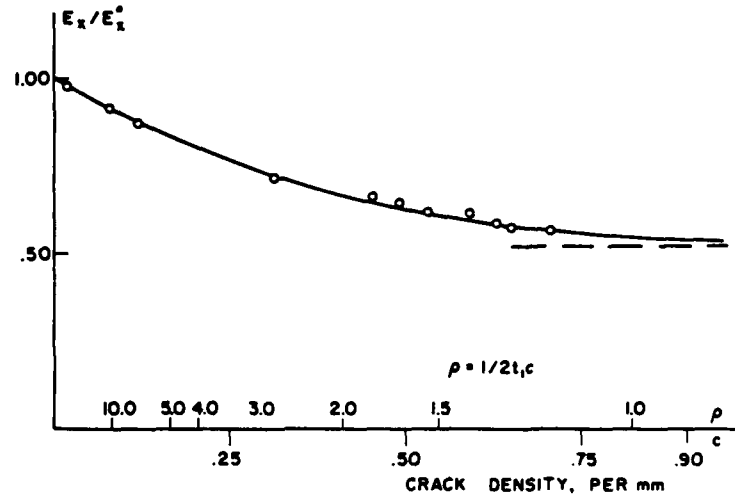
$$\phi(\pm a) = 1, \quad \phi'(\pm a) = 0 \quad (2.3)$$

where  $t_1$  and  $t_2$  are ply thicknesses,  $\phi = \phi_1$  and primes on  $\phi$  denote  $x$  derivatives. The stresses are defined for any region of length  $2a$  between adjacent cracks (Fig. 1) and these distances may be different. The admissible stresses  $\tilde{\sigma}_{ij}$  of the laminate are then

$$\tilde{\sigma}_{ij}^{(m)} = \sigma_{ij}^{0(m)} + \sigma_{ij}^{(m)}. \quad (2.4)$$

STIFFNESS REDUCTION OF  $[0^\circ/90^\circ]$ ,  
GLASS/EPOXY LAMINATE

$E_x^0$  YOUNG'S MODULUS OF UNDAMAGED LAMINATE  
 $E_x$  YOUNG'S MODULUS OF CRACKED LAMINATE  
 ○ EXPERIMENTAL

Fig. 2. Stiffness reduction of  $[0^\circ/90^\circ]$ , glass/epoxy laminate.

The stresses (2.4) satisfy equilibrium, traction continuity at ply interfaces  $z = \pm t_1$ , vanishing of tractions on laminate free surfaces  $z = \pm h$  and on crack surfaces  $x = \pm a$  and the loading conditions on the laminate in the  $x$  direction.

Let the average stress in the  $x$  direction on the laminate be denoted by  $\sigma_0$  thus,

$$\sigma_0 = N_{xx}/2h. \quad (2.5)$$

It is then rigorously true that the stress energy stored in the laminate is given by

$$U_c = \frac{\sigma_0^2}{2E_x} V \quad (2.6)$$

where  $E_x$  is the Young's modulus in the  $x$  direction of the cracked laminate. The complementary energy functional  $\bar{U}_c$  of the cracked laminate is given by

$$\bar{U}_c = \frac{1}{2} \int S_{ijkl} \bar{\sigma}_{ij} \bar{\sigma}_{kl} dV \quad (2.7)$$

where  $S_{ijkl}$  are the local compliances of the plies. It has been shown [5] that in the present case this can be expressed as

$$\bar{U}_c = \frac{\sigma_0^2}{2E_x^0} V + \frac{1}{2} \sum_m \int_{V_m} S_{ijkl}^{(m)} \sigma_{ij}^{(m)} \sigma_{kl}^{(m)} dV \quad (2.8)$$

where  $\sigma_{ij}^{(m)}$  are given by (2.2) and  $E_x^0$  is the Young's modulus of the undamaged laminate. Introducing (2.2) into (2.8) and performing  $z$  integrations we have

$$\bar{U}_c = \frac{\sigma_0^2}{2E_x^0} V + \frac{1}{2} \sigma_0^2 t_1^2 \sum_n J_n \quad (2.9)$$

$$J_n = \int_{-\rho_n}^{\rho_n} \left[ C_{00} \phi_n^2 + C_{02} \phi_n \frac{d^2 \phi_n}{d\xi^2} + C_{22} \left( \frac{d^2 \phi_n}{d\xi^2} \right)^2 + C_{11} \left( \frac{d \phi_n}{d\xi} \right)^2 \right] d\xi \quad (2.10)$$

where

$$\xi = x/t_1, \quad \rho_n = a_n/t_1$$

$$C_{00} = 1/E_T + 1/\lambda E_A$$

$$C_{02} = (v_T/E_T)(\lambda + 2/3) - v_A \lambda / 3 E_A$$

$$C_{22} = (\lambda + 1)(3\lambda^2 + 12\lambda + 8)/60E_T$$

$$C_{11} = \frac{1}{2}(1/G_T + \lambda/G_A)$$

$$\lambda = t_2/t_1$$

where  $a_n$  are the distances between adjacent cracks and  $E_A$ ,  $E_T$ ,  $v_A$ ,  $v_T$ ,  $G_T$  and  $G_A$  are, respectively, axial and transverse Young's moduli, Poisson's ratios and shear moduli.

It follows from the principle of minimum complementary energy that

$$U_c \leq \bar{U}_c \quad (2.11)$$

or in terms of (2.6) and (2.9)

$$\frac{1}{E_x} \leq \frac{1}{E_x^0} + \frac{\sigma_1^2 t_1^2}{\sigma_0^2 V} \sum_n J_n. \quad (2.12)$$

This provides a lower bound on  $E_x$  for any  $\phi_n$  which satisfy the conditions (2.3) on the cracks. To obtain the best lower bound the right side of (2.12) is minimized using techniques of the calculus of variations. This procedure establishes differential equations for the functions  $\phi_n$  which all have the form

$$\frac{d^4 \phi_n}{d\xi^4} + p \frac{d^2 \phi_n}{d\xi^2} + q \phi_n = 0 \quad (2.13)$$

$$p = (C_{02} - C_{11})C_{22}, \quad q = C_{00}/C_{22}$$

with the boundary conditions

$$\phi_n(\pm \rho_n) = 1, \quad \frac{d\phi}{d\xi}(\pm \rho_n) = 0 \quad (2.14)$$

$$\rho_n = a_n/t_1.$$

The solution of (2.13) subject to (2.14) is

$$\phi_n(\xi) = A_n^{(1)} C \alpha \xi \cos \beta \xi + A_n^{(2)} S \alpha \xi \sin \beta \xi$$

$$\alpha = q^{1/4} \cos(\theta/2), \quad \beta = q^{1/4} \sin(\theta/2) \quad (2.15)$$

$$\tan \theta = \sqrt{(4q/p^2 - 1)}$$

where  $A_n^{(1)}$  and  $A_n^{(2)}$  are easily determined from the boundary conditions (2.14). The solution is different when  $4q/p^2 < 1$ .

Introducing these functions into (2.10) and (2.12) we find

$$\frac{1}{E_x} \leq \frac{1}{E_x^0} + \frac{1}{E_T} k_1^2 \eta(\lambda) \frac{\langle \chi(\rho) \rangle}{\langle \rho \rangle} \quad (2.16)$$

where

$$\begin{aligned} k_1 &= \sigma_1/\sigma_0 = \sigma_{xx}^{0(1)}/\sigma^0 \\ \eta(\lambda) &= (3\lambda^2 + 12\lambda + 8)/60, \quad \lambda = t_2/t_1 \\ \chi(\rho_n) &= 2\alpha\beta(\alpha^2 + \beta^2) \frac{Ch2\alpha\rho_n - \cos 2\beta\rho_n}{\alpha \sin 2\beta\rho_n + \beta Sh2\alpha\rho_n} \end{aligned} \quad (2.17)$$

and the brackets  $\langle \rangle$  denote average with respect to the random variable  $\rho_n$ . In the case when the distances between cracks are equal and given by  $2a$

$$\begin{aligned} \langle \rho \rangle &= \rho = a/t_1 \\ \langle \chi(\rho) \rangle &= \chi(\rho). \end{aligned} \quad (2.18)$$

When the cracks are far apart (all  $\rho_n$  are large) and do not interact, the results reduce to

$$\frac{1}{E_x} \leq \frac{1}{E_x^0} + \frac{4}{E_T} k_1^2 \eta(\lambda) \alpha(\alpha^2 + \beta^2) t_1 c \quad (2.19)$$

where  $c$  is the crack density, i.e. the number of cracks per unit length.

When distances between cracks are small, thus all  $\rho_n \rightarrow 0$ , we have

$$\frac{1}{E_x} \leq \frac{1}{E_x^0} + \frac{k_1^2}{\lambda + 1} \left( \frac{1}{E_T} + \frac{1}{\lambda E_A} \right). \quad (2.20)$$

Determination of the Poisson's ratio  $\nu_{xy}$  (tension in the  $x$  direction, strain in the  $y$  direction) needs special additional analysis. We shall consider this problem in approximate fashion. Tension in the  $y$  direction (Fig. 1) will primarily produce stress  $\sigma_{yy}$  in the plies and very small stresses  $\sigma_{xx}$ . If the latter are neglected it follows that the cracks in the  $90^\circ$  ply have no effect on the stress distribution and therefore  $E_y$  and  $\nu_{xy}$  are not affected by the cracks. Thus

$$\begin{aligned} E_y &\approx E_y^0 \\ \nu_{xy} &\approx \nu_{xy}^0. \end{aligned} \quad (2.21)$$

It follows from the usual elastic symmetry of compliances that

$$\frac{\nu_{xy}}{E_x} = \frac{\nu_{yy}}{E_y}. \quad (2.22)$$

Therefore

$$\nu_{xy} \approx \frac{E_x}{E_y^0} \nu_{yy}^0 = \frac{E_x}{E_y^0} \nu_{xy}^0. \quad (2.23)$$

Experiments to determine stiffness reduction of glass/epoxy cross-ply laminates have been performed by Highsmith and Reifsnider and have been reported in [2]. The elastic properties of the single unidirectionally reinforced ply are

$$\begin{aligned} E_A &= 41.7 \text{ GPa}, & E_T &= 13.0 \text{ GPa}, & G_A &= 3.40 \text{ GPa} \\ G_T &= 4.58 \text{ GPa}, & \nu_A &= 0.30, & \nu_T &= 0.42 \end{aligned}$$

where  $G_T$  and  $\nu_T$  have been computed and the others are experimental values. For the  $[0^\circ 90^\circ]$  laminate it follows from elementary laminate analysis that

$$\begin{aligned} E_x^0 &= 20.30 \text{ GPa} \\ k_1 &= \sigma_1/\sigma^0 = 0.636 \quad (90^\circ \text{ ply}). \end{aligned}$$

Figure 2 shows the comparison of the result (2.16)–(2.18) with the experimental data for a  $[0^\circ/90^\circ]$ , laminate and it is seen that the agreement is excellent. The agreement is not quite as good for the  $[0^\circ/90^\circ]$ , laminate but it should be noted that in this case there is an unusual discrepancy between measured  $E_x^0$  (22.7 GPa) and calculated  $E_x^0$  (27.57 GPa) which needs explanation.

### 3. ANALYSIS OF CRACKED CROSS-PLY UNDER SHEAR

The cracked cross-ply (Fig. 1) is now assumed to be loaded by a shear membrane force  $N_{xy}$ . This is equivalent to average shear stress loading  $\bar{\sigma}_{xy}$ , given by

$$\bar{\sigma}_{xy} = N_{xy}/2h = \tau_0. \quad (3.1)$$

When there are no cracks in the laminate the only surviving internal stress is

$$\sigma_{xy}^0 = \tau_0 \quad (3.2)$$

in both plies.

When the  $90^\circ$  ply is cracked as in Fig. 1, the state of stress in the plies is antiplane, thus the only surviving stresses are  $\sigma_{xy}$  and  $\sigma_{yz}$ . We proceed as in Section 2 and construct an admissible stress system on the basis of the assumption that  $\bar{\sigma}_{xy}$  is a function of  $x$  only. Thus

$$\begin{aligned} \bar{\sigma}_{xy}^{(1)} &= \tau_0[1 - \psi_1(x)] \\ \bar{\sigma}_{xy}^{(2)} &= \tau_0[1 - \psi_2(x)]. \end{aligned} \quad (3.3)$$

The functions  $\psi_1(x)$  and  $\psi_2(x)$  are related in terms of the equilibrium condition

$$\bar{\sigma}_{xy}^{(1)}t_1 + \bar{\sigma}_{xy}^{(2)}t_2 = \tau_0h. \quad (3.4)$$

Satisfaction of stress equilibrium, interface traction continuity and boundary conditions leads to the admissible stresses

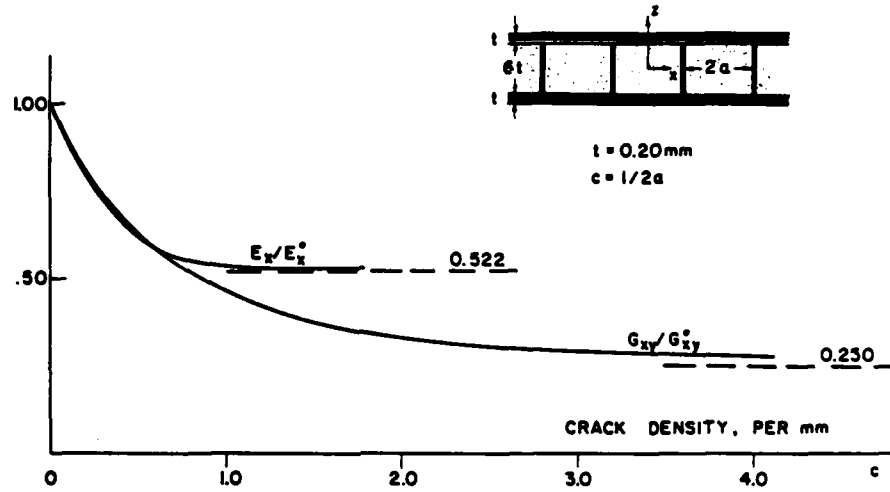
$$\begin{aligned} \bar{\sigma}_{xy}^{(1)} &= \tau_0[1 - \psi(x)] \\ \bar{\sigma}_{xy}^{(2)} &= \tau_0 \left[ 1 + \frac{t_1}{t_2} \psi(x) \right] \\ \bar{\sigma}_{yz}^{(1)} &= \tau_0 \psi'(x)z \\ \bar{\sigma}_{yz}^{(2)} &= \tau_0 \frac{t_1}{t_2} \psi'(x)(h - z). \end{aligned} \quad (3.5)$$

Proceeding as in Section 2, in terms of the principle of minimum complementary energy we arrive at the result

$$\begin{aligned} G_{xy} &\geq \frac{G_A}{1 + \langle Th\mu\rho \rangle / \lambda\mu\langle\rho\rangle} \\ \mu^2 &= \frac{3(1 + 1/\lambda)}{1 + \lambda G_A/G_T}, \quad \lambda = t_2/t_1. \end{aligned} \quad (3.6)$$

Again when the cracks are equidistant,  $2a$  apart,

$$\begin{aligned} \langle\rho\rangle &= \rho = a/t_1 \\ \langle Th\mu\rho\rangle &= Th\mu\rho. \end{aligned} \quad (3.7)$$

YOUNG'S AND SHEAR MODULUS REDUCTION  
OF  $[0^\circ/90^\circ_s]$  GLASS/EPOXY LAMINATEFig. 3. Young's and shear modulus reduction of  $[0^\circ/90^\circ_s]$ , glass/epoxy laminate.

When the distances between cracks are large

$$G_{xy} \geq \frac{G_A}{1 + 1/\lambda\mu\rho} \quad (3.8)$$

and when the distances are small

$$G_{xy} \geq \frac{G_A}{1 + 1/\lambda} = G_A \frac{t_2}{h}. \quad (3.9)$$

The last result has a very simple interpretation. It is the shear modulus of the cross-ply when the shear stiffness of the  $90^\circ$  ply has reduced to zero. Figure 3 shows the reduction of shear modulus due to crack distribution as a function of crack density. The reduction as a function of Young's modulus given in Fig. 2 is also shown by comparison.

## 4. DISCUSSION AND CONCLUSIONS

The variational method developed permits the evaluation of stiffness reduction of any  $[0_m/90_n]$  laminate. Of particular interest is the limiting value of stiffness when the cracks become very close to one another. Table 1 shows such results for glass/epoxy and graphite (T300)/epoxy quoting the ratio  $E_x(\rho \rightarrow 0)/E_x^0$ .

It is seen that because of the much larger ratio  $E_A/E_T$  for the graphite/epoxy the stiffness reduction is much smaller since the undamaged  $0^\circ$  plies are the major contribution to stiffness. The situation is different for shear modulus where the limiting ratio is defined in all cases by the simple expression (3.9) which is purely geometrical. The analysis also easily permits evaluation of approximate stresses. These have been given in detail in [5] and their significance for the damage to failure process of the laminate has also been discussed.

Table 1

	Glass/epoxy	Graphite/epoxy
$[0^\circ/90^\circ]$	0.770	0.970
$[0^\circ/90^\circ_s]$	0.522	0.914

When the position of the 90° and 0° plies is reversed, i.e. the 0° is in between the 90°, the cracked laminate is of course easily analyzed by the same method and it may be shown that the results are the same as for the 90° inside and the 0° outside provided that total thickness of plies of each kind is preserved. It should be noted that the laminates analyzed are of limited practical significance. It would be desirable to evaluate stiffness reduction in cracked [ $\pm 45^\circ$ ], [ $0^\circ/\pm 45^\circ$ ], and [ $0^\circ/90^\circ/\pm 45^\circ$ ] laminates. For such cases a minimal requirement is to analyze the [ $\pm 45^\circ$ ], laminate which is cracked in both layers, thus forming an orthogonal crack net. This is of course much more difficult than the present case and such work is now in progress.

*Acknowledgement*—Support of the Air Force Office of Scientific Research under Contract 84-0251 is gratefully acknowledged.

#### REFERENCES

- [1] K. L. Reifsnider, Some fundamental aspects of the fatigue and fracture response of composite materials. *Proc. 14th Annual Meeting of Society of Engineering Science*, Bethlehem, Pennsylvania, pp. 343-384 (1977).
- [2] A. L. Highsmith and K. L. Reifsnider, Stiffness-reduction mechanisms in composite laminates. *Damage in Composite Materials* (Edited by K. L. Reifsnider), *ASTM STP 115*, 103-117 (1982).
- [3] N. Laws and G. J. Dvorak, The loss of stiffness of cracked laminates. *Fundamentals of Deformation and Fracture, Proc. IUTAM Eshelby Memorial Symp.*, pp. 119-128. Cambridge University Press (1985).
- [4] R. Talreja, Transverse cracking and stiffness reduction in composite laminates. *J. compos. Mater.* **19**, 355-375 (1985).
- [5] Z. Hashin, Analysis of cracked laminates: A variational approach. *Mech. Mater.* **4**, 121-136 (1985).

## Z. Hashin

Dept. of Solid Mechanics,  
Materials and Structures,  
Faculty of Engineering,  
Tel-Aviv University,  
Tel-Aviv, Israel 69978  
Fellow ASME

# Analysis of Orthogonally Cracked Laminates Under Tension

*The problems of stiffness reduction and stress analysis of cross-ply fiber composite laminates, where all plies are cracked in fiber directions, are treated by a variational method on the basis of the principle of minimum complementary energy. The Young's modulus obtained is a strict lower bound but is expected to be close to the true value on the basis of experience with a previous analysis. Approximate values of Poisson's ratio and internal stresses have been obtained. The latter reveal important tendencies of continued failure by delamination.*

## Introduction

The major damage which develops in laminates under static or cyclic loading is in the form of interlaminar and intralaminar cracks. The former develop gradually and slowly in between plies. The latter appear suddenly and in large numbers in plies in which the stresses reach critical values, perhaps defined by the first failure criteria of the plies. They are families of parallel cracks in fiber direction and their macroscopic effect is reduction of the inplane stiffness of the laminate.

The subject of the analysis of stiffness reduction of cracked laminates has received repeated attention but has mainly been concerned with cross-ply laminates, i.e.,  $[0^\circ/90^\circ]$ , configurations in which only the  $90^\circ$  plies are cracked. The main methods of analysis employed are: a simple shear-lag method (Reifsnider and Talug, 1980; Reifsnider and Jamison, 1982), self-consistent approximation to assess ply stiffness reduction in conjunction with classical laminate analysis (Laws et al., 1983, 1985), and a variational method (Hashin, 1985). All of these methods give results which are in good to excellent agreement with experimental data. The last method, unlike the others, also provides useful estimates of the internal stresses in the cracked laminate.

In many cases of damage in laminates, several plies will be cracked and in particular adjacent plies. As a typical and relatively simple case we shall consider the problem of a  $[0^\circ/90^\circ]$ , laminate in which all plies have intralaminar cracks and which is thus orthogonally cracked. Because of the complicated interaction of the orthogonal cracks this problem is much more difficult than the one with plies cracked in only one direction. We are aware of only one publication in the literature (Highsmith and Reifsnider, 1986) on this subject, which is concerned with evaluation of stresses in a typical repeating cracked laminate element by numerical analysis.

Contributed by the Applied Mechanics Division for publication in the JOURNAL OF APPLIED MECHANICS.

Discussion on this paper should be addressed to the Editorial Department, ASME, United Engineering Center, 345 East 47th Street, New York, N.Y. 10017, and will be accepted until two months after final publication of the paper itself in the JOURNAL OF APPLIED MECHANICS. Manuscript received by ASME Applied Mechanics Division, January 2, 1987.

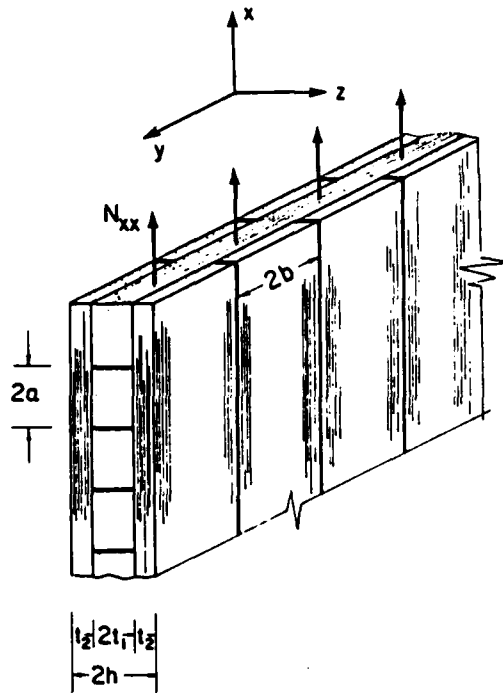


Fig. 1 Orthogonally cracked laminate

The present problem is closely related to that of a cracked  $\pm 45^\circ$  symmetric laminate which is indeed merely a rotated  $0^\circ/90^\circ$ . It is easily seen that uniaxial tension of a  $[+45^\circ/-45^\circ]$ , in bisector direction can be analyzed in terms equibiaxial tension and shear of a  $[0^\circ/90^\circ]$ , laminate. Indeed a typical case of orthogonal cracking is encountered for cyclic loading of a  $\pm 45^\circ$  laminate. The problem of shearing of a cross-ply will be considered elsewhere. Here we are concerned with uniaxial tensile loading of an orthogonally cracked cross-ply. Our purpose is to evaluate stiffness reduction due to cracks and approximate local stresses. We shall do this by generalization of the variational method which has been developed in Hashin (1985).

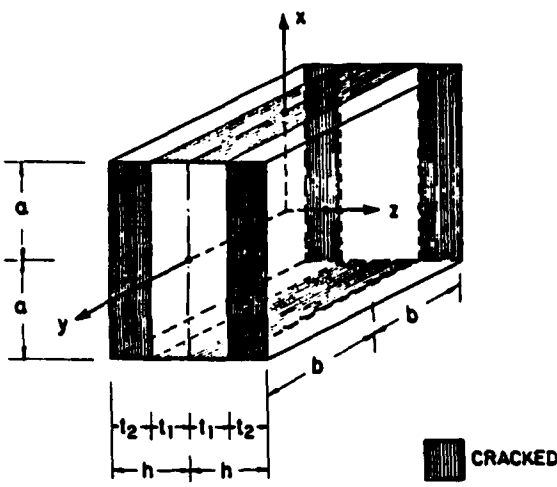


Fig. 2 Repeating element

### Admissible Field Construction

Consider an orthogonally cracked laminate, Fig. 1, and a typical laminate element defined by intersecting crack pairs, Fig. 2. Let the laminate be subjected to constant membrane force

$$N_{xx} = 2\sigma^0 h \quad (1)$$

and no other loads. Thus  $\sigma^0$  is the average stress  $\delta_{xx}$  over the laminate and also over the thickness  $2h$ .

In the event that longitudinal and transverse crack families are each equidistant, the stresses and strains in each element (Fig. 2) are the same, the boundary and interface conditions of the repeating element can be formulated and the problem can be treated numerically in terms of finite elements, if desired. The problems associated with such an approach will be discussed at the end of the paper. Here we shall proceed differently; it is our purpose to construct admissible stress fields which satisfy equilibrium and all traction, boundary and interface conditions. These admissible fields will then be optimized in the context of the principle of minimum complementary energy to yield approximate stresses and lower bounds on stiffness.

The stresses in the undamaged laminate under the loading considered are

$$\begin{aligned} \sigma_{xx}^{(1)} &= \sigma_x^{(1)} = k_x^{(1)} \sigma^0 & \sigma_{yy}^{(1)} &= \sigma_y^{(1)} = k_y^{(1)} \sigma^0 \\ \sigma_{xx}^{(2)} &= \sigma_x^{(2)} = k_x^{(2)} \sigma^0 & \sigma_{yy}^{(2)} &= \sigma_y^{(2)} = k_y^{(2)} \sigma^0 \\ \sigma_{xy}^{(1)} &= \sigma_{xy}^{(2)} = 0 \end{aligned} \quad (2)$$

where the  $k$  coefficients are easily found from conventional laminate analysis.

Let  $\delta_y$  be a three-dimensional admissible stress field within the cracked laminate. By definition such a stress field must satisfy equilibrium, traction continuity, and traction boundary conditions. For reasons of symmetry it is sufficient to consider one half of the element of Fig. 2 defined by  $-a \leq x \leq a$ ,  $-b \leq y \leq b$ ,  $0 \leq z \leq h$ , as will be understood from now on. We list required boundary and interface conditions

$$\delta_{xx}^{(1)}(x, y, 0) = 0 \quad \delta_{yz}^{(1)}(x, y, 0) = 0 \quad (3)$$

$$\delta_{xx}^{(2)}(x, y, h) = 0 \quad \delta_{yz}^{(2)}(x, y, h) = 0 \quad (4)$$

$$\delta_{yz}^{(2)}(x, y, h) = 0$$

$$\delta_{xx}^{(1)}(x, y, t_1) = \delta_{xx}^{(2)}(x, y, t_1)$$

$$\delta_{yz}^{(1)}(x, y, t_1) = \delta_{yz}^{(2)}(x, y, t_1)$$

$$\delta_{zz}^{(1)}(x, y, t_1) = \delta_{zz}^{(2)}(x, y, t_1)$$

$$\delta_{xx}^{(1)}(\pm a, y, z) = \delta_{yy}^{(1)}(\pm a, y, z) = \delta_{zz}^{(1)}(\pm a, y, z) = 0$$

(6)

$$\delta_{xy}^{(2)}(x, \pm b, z) = \delta_{yy}^{(2)}(x, \pm b, z) = \delta_{xz}^{(2)}(x, \pm b, z) = 0$$

Here and from now on superscripts 1, 2 indicate the plies, equations (3) are symmetry conditions, equations (4) are free surface conditions, equations (5) express traction interface continuity, and equations (6) are zero traction conditions on the crack surface. There are still needed traction conditions on the faces  $x = \pm a$ ,  $t_1 \leq z \leq h$  and  $y = \pm b$ ,  $0 \leq z \leq t_1$ , which shall be considered further below.

The  $xy$  in-plane parts of the admissible stress fields are chosen in the form

$$\delta_{xx}^{(1)} = \sigma_x^{(1)}[1 - \phi_1(x)] \quad \delta_{xx}^{(2)} = \sigma_x^{(2)}[1 - \phi_2(x)] \quad (7a)$$

$$\delta_{yy}^{(1)} = \sigma_y^{(1)}[1 - \psi_1(y)] \quad \delta_{yy}^{(2)} = \sigma_y^{(2)}[1 - \psi_2(y)] \quad (7b)$$

$$\delta_{xy}^{(1)} = \delta_{xy}^{(2)} = 0 \quad (7c)$$

where  $\phi$  and  $\psi$  are unknown functions. The physical significance of these assumptions will be discussed further below.

Force equilibrium of the undamaged laminate in the  $x$  and  $y$  directions requires

$$\sigma_x^{(1)} t_1 + \sigma_x^{(2)} t_2 = \sigma^0 h$$

$$\sigma_y^{(1)} t_1 + \sigma_y^{(2)} t_2 = 0 \quad (8)$$

Examining force equilibrium in the same directions in the cracked laminate, in terms of the admissible stresses (7), we find

$$\sigma_x^{(1)} t_1 \phi_1(x) + \sigma_x^{(2)} t_2 \phi_2(x) = 0$$

$$\sigma_y^{(1)} t_1 \psi_1(y) + \sigma_y^{(2)} t_2 \psi_2(y) = 0 \quad (9)$$

This reduces the number of unknown functions from four to two.

In view of equation (7c), the equilibrium equations for the admissible ply stresses assume the form

$$\delta_{xx,x} + \delta_{zz,x} = 0$$

$$\delta_{yy,y} + \delta_{zz,y} = 0 \quad (10)$$

$$\delta_{xz,x} + \delta_{yz,y} + \delta_{zz,z} = 0$$

where commas denote partial differentiation.

We now define perturbation stresses  $\delta_y^{(m)}$  for the plies,  $m = 1, 2$ , by

$$\delta_y^{(m)} = \sigma_y^{(m)} + \sigma_y^{(m)} \quad (11)$$

where  $\sigma_y^{(m)}$  are given by the undamaged laminate stresses (2).

Insertion of equations (7) into (10) for each ply and systematic integration, with elimination of unknown residual functions by use of equations (3)–(5), and utilization of equations (9), leads to the results

$$\delta_{xx}^{(1)} = -\sigma_x^{(1)} \phi(x) \quad (12a)$$

$$\delta_{xx}^{(2)} = \frac{1}{\lambda} \sigma_x^{(1)} \phi(x) \quad (12b)$$

$$\delta_{xx}^{(1)} = \sigma_x^{(1)} \phi'(x) z \quad (12c)$$

$$\delta_{xx}^{(2)} = \frac{1}{\lambda} \sigma_x^{(1)} \phi'(x) (h-z) \quad (12d)$$

$$\delta_{yz}^{(1)} = \sigma_y^{(1)} \psi(y) z \quad (12e)$$

$$\delta_{yz}^{(2)} = \frac{1}{\lambda} \sigma_y^{(1)} \psi(y) (h-z) \quad (12f)$$

$$\sigma_{xx}^{(1)} = [\sigma_x^{(1)} \phi''(x) + \sigma_y^{(1)} \psi''(y)] \frac{1}{2} (ht_1 - z^2) \quad (12e)$$

$$\sigma_{xx}^{(2)} = \frac{1}{\lambda} [\sigma_x^{(1)} \phi''(x) + \sigma_y^{(1)} \psi''(y)] \frac{1}{2} (h - z)^2 \quad (12f)$$

where prime and dot indicate  $x$  and  $y$  derivative, respectively, and

$$\begin{aligned} \phi &= \phi_1 & \psi &= \psi_1 \\ \lambda &= t_2/t_1 \end{aligned} \quad (13)$$

It follows from equations (6) and (9) that  $\phi$  and  $\psi$  must satisfy the boundary conditions

$$\begin{aligned} \phi(\pm a) &= 1 & \phi'(\pm a) &= 0 \\ \psi(\pm a) &= 1 & \psi'(\pm a) &= 0 \end{aligned} \quad (14)$$

The above formulation determines the traction components on the faces  $x = \pm a$ ,  $t_1 \leq z \leq h$  and  $y = \pm b$ ,  $0 \leq z \leq t_1$ . It is seen that the only nonvanishing traction component is

$$\delta_{xx}^{(2)}(\pm a) = \sigma_x^{(1)}(1 + t_1/t_2) \quad (15)$$

Thus the admissible tractions are continuous across all common faces of adjacent elements, regardless of their  $a, b$  dimensions. Therefore, the stresses (11)–(12) rigorously satisfy all conditions of admissibility.

### Variational Formulation

Next we evaluate the complementary energy functional  $\bar{U}_c$  associated with the admissible stresses. In the present case where tractions are prescribed everywhere

$$\bar{U}_c = \frac{1}{2} \int_V S_{ijkl} \delta_{ij} \delta_{kl} dV \quad (16)$$

where  $V$  is laminate volume and  $S_{ijkl}$  are local compliances. It has been shown in Hashin (1985) that for any cracked body

$$\bar{U}_c = U_c^0 + \bar{U}'_c \quad (17)$$

where

$$U_c^0 = \frac{1}{2} \int S_{ijkl} \sigma_{ij}^0 \sigma_{kl}^0 dV \quad (18a)$$

$$\bar{U}'_c = \frac{1}{2} \int S_{ijkl} \sigma_{ij}' \sigma_{kl}' dV \quad (18b)$$

$$\delta_{ij} = \sigma_{ij}^0 + \sigma_{ij}' \quad (18c)$$

Here  $\sigma_{ij}^0$  are the actual stresses in the uncracked body, i.e., in the undamaged laminate; thus  $U_c^0$  is the actual stress energy of the undamaged laminate. In the present case it is rigorously true that

$$U_c^0 = \frac{\sigma^0}{2E_x^0} V \quad (19)$$

where  $E_x^0$  is the Young's modulus in the  $x$  direction of the undamaged laminate. Furthermore, the stress energy  $U_c$  of the cracked laminate can be rigorously expressed in the form

$$U_c = \frac{\sigma^0}{2E_x} V \quad (20)$$

where  $E_x$  is the effective Young's modulus of the cracked laminate. Also from the principle of minimum complementary energy

$$U_c \leq \bar{U}_c \quad (21)$$

Combining equations (17) and (19)–(21) we have

$$\frac{1}{E_x} \leq \frac{1}{E_x^0} + \frac{2\bar{U}'_c}{V\sigma^0} \quad (22)$$

which provides a lower bound on  $E_x$ .

In the present case the stresses (12) are identified with the  $\sigma_{ij}'$  in equation (18c). In order to evaluate equation (18b) we list the local stress energy densities in the plies as referred to the common  $x, y, z$  system of the laminate

$$\begin{aligned} 2W^{(1)} &= \sigma_{yy}^{(1)} / E_A + (\sigma_{xx}^{(1)} + \sigma_{yy}^{(1)})^2 / E_T - \sigma_{yy}^{(1)} (\sigma_{xx}^{(1)} \\ &+ \sigma_{yy}^{(1)}) 2\nu_A / E_A - \sigma_{xx}^{(1)} \sigma_{yy}^{(1)} 2\nu_T / E_T \\ &+ (\sigma_{xy}^{(1)} + \sigma_{yx}^{(1)})^2 / G_A + \sigma_{xx}^{(1)}^2 / G_T \end{aligned} \quad (23)$$

$$\begin{aligned} 2W^{(2)} &= \sigma_{xx}^{(2)} / E_A + (\sigma_{yy}^{(2)} + \sigma_{xx}^{(2)})^2 / E_T - \sigma_{xx}^{(2)} (\sigma_{yy}^{(2)} \\ &+ \sigma_{xx}^{(2)}) 2\nu_A / E_A - \sigma_{yy}^{(2)} \sigma_{xx}^{(2)} 2\nu_T / E_T \\ &+ (\sigma_{xy}^{(2)} + \sigma_{yx}^{(2)})^2 / G_A + \sigma_{yy}^{(2)} / G_T \end{aligned}$$

where the coefficients are in terms of the following properties of the unidirectional ply material

$E_A$  = Axial Young's modulus (fiber direction)

$\nu_A$  = Axial Poisson's ratio

$E_T$  = Transverse Young's modulus

$\nu_T$  = Transverse Poisson's ratio

$G_A$  = Axial shear modulus

$G_T$  = Transverse shear modulus

Suppose a typical element, Fig. 2, has in-plane dimensions  $2a_m$  and  $2b_n$ . Then for half the laminate  $0 \leq z \leq h$

$$\begin{aligned} \bar{U}'_{cn} &= \int_{-a_m}^{a_m} \int_{-b_n}^{b_n} \int_0^{t_1} W^{(1)} dx dy dz \\ &+ \int_{-a_m}^{a_m} \int_{-b_n}^{b_n} \int_{t_1}^h W^{(2)} dx dy dz \end{aligned} \quad (24a)$$

$$\bar{U}'_c = \Sigma \bar{U}'_{cn} \quad (24b)$$

which can now be evaluated in terms of equations (12). For simplicity in writing we shall perform detailed analysis for the case when  $a_m = a$ ,  $b_n = b$  and give results for the more general case of unequal intercrack distances at the end. When  $a_m$  and  $b_n$  are constant we can, without loss of generality, interpret all preceding energies as those stored in an element with dimensions  $2a$ ,  $2b$ ,  $h$ . Introducing equations (12) into (24a), performing all  $z$  integrations and using the nondimensional variables

$$\xi = x/t_1 \quad \eta = y/t_1 \quad (25)$$

we have

$$\begin{aligned} 2\bar{U}'_c &= \sigma^0 t_1^2 \int_{-p_1}^{p_1} \int_{-p_2}^{p_2} [k_x^2 A_0 \phi^2 + 2k_x k_y B_0 \phi \psi \\ &+ k_y^2 C_0 \psi^2 + A_1 k_x^2 \phi'^2 + B_1 k_y^2 \psi'^2 \\ &+ A_2 k_x \phi(k_x \phi'' + k_y \psi) + B_2 k_y \psi(k_x \phi'' + k_y \psi) \\ &+ C(k_x \phi'' + k_y \psi)^2] d\xi d\eta \end{aligned} \quad (26)$$

where prime and dot now denote  $\xi$  and  $\eta$  derivative, respectively, and

$$\begin{aligned} \phi &= \phi(\xi) & \psi &= \psi(\eta) \\ p_1 &= a/t_1 & p_2 &= b/t_1 \\ k_x &= k_x^{(1)} & k_y &= k_y^{(1)} \end{aligned} \quad (27)$$

$$\begin{aligned}
A_0 &= 1/\lambda E_A + 1/E_T & B_0 &= -(1 + 1/\lambda) \nu_A/E_A \\
C_0 &= 1/E_A + 1/\lambda E_T \\
A_1 &= (\lambda/G_A + 1/G_T)/3 & B_1 &= (1/G_A + \lambda/G_T)/3 \\
A_2 &= [(3\lambda + 2)\nu_T/E_T - \lambda\nu_A/E_A]/3 \\
B_2 &= [(3\lambda + 2)\nu_A/E_A - \lambda\nu_T/E_T]/3 \\
C &= (\lambda + 1)(3\lambda^2 + 12\lambda + 8)/60E_T
\end{aligned} \tag{28}$$

and the boundary conditions (14) now assume the form

$$\begin{aligned}
\phi(\pm p_1) &= 1 & \phi'(\pm p_1) &= 0 \\
\psi(\pm p_2) &= 1 & \psi'(\pm p_2) &= 0
\end{aligned} \tag{29}$$

In view of (22) any functions  $\phi$  and  $\psi$  which satisfy equations (29) will, when introduced into equations (24) and (22), provide an upper bound for  $1/E_x$ . To obtain the best bound  $\bar{U}'_c$  should be minimized. Using techniques of the calculus of variations we find that the minimum conditions of the integral (26) are the integro-differential equations

$$\frac{d^4\phi}{d\xi^4} + p_1 \frac{d^2\phi}{d\xi^2} + q_1 \phi + \frac{k_x}{k_y} \frac{B_0}{C} \frac{1}{2p_2} \int_{-p_2}^{p_2} \psi d\eta = 0 \tag{30a}$$

$$\frac{d^4\psi}{d\eta^4} + p_2 \frac{d^2\psi}{d\eta^2} + q_2 \psi + \frac{k_y}{k_x} \frac{B_0}{C} \frac{1}{2p_1} \int_{-p_1}^{p_1} \phi d\xi = 0 \tag{30b}$$

where

$$\begin{aligned}
p_1 &= \frac{A_2 - A_1}{C} & q_1 &= \frac{A_0}{C} \\
p_2 &= \frac{B_2 - B_1}{C} & q_2 &= \frac{C_0}{C}
\end{aligned} \tag{31}$$

### Solution of the Integro-Differential Equations

Obviously the solution of equations (30) with (29) is insensitive to change of sign of independent variables. Therefore,

$$\phi(\xi) = \phi(-\xi) \quad \psi(\eta) = \psi(-\eta) \tag{32}$$

Now define the mean values

$$\frac{1}{2p_1} \int_{-p_1}^{p_1} \phi d\xi = \bar{\phi} \quad \frac{1}{2p_2} \int_{-p_2}^{p_2} \psi d\eta = \bar{\psi} \tag{33}$$

Then the general solutions of equations (30) can be written in the form

$$\phi = \phi_0(\xi) - m_1 \bar{\psi} \tag{34a}$$

$$\psi = \psi_0(\eta) - m_2 \bar{\phi} \tag{34b}$$

$$m_1 = \frac{k_y}{k_x} \frac{B_0}{A_0} \quad m_2 = \frac{k_x}{k_y} \frac{B_0}{C_0} \tag{34c}$$

where the terms with subscripts zero are general solutions of the homogeneous versions of equations (30) and the remaining terms are particular solutions. A homogeneous differential equation of type (30) has four independent solutions which may be arranged into two symmetric and two antisymmetric ones. In view of equations (32) only symmetric solutions need be retained. These are:

when  $4q > p^2$

$$\begin{aligned}
f(v) &= Ch\alpha v & g(v) &= Ch\beta v \\
\alpha &= q^{1/4} \cos(\theta/2) & \beta &= q^{1/4} \sin(\theta/2)
\end{aligned} \tag{35}$$

$$\tan \theta = \sqrt{4q/p^2 - 1}$$

when  $4q < p^2$   $p < 0$

$$f(v) = Ch\alpha v \quad g(v) = Ch\beta v \tag{36}$$

$$\alpha, \beta = \sqrt{(-1 \pm \sqrt{1 - 4q/p^2})p/2}$$

where  $v$  is either  $\xi$  or  $\eta$ , and  $p$  and  $q$  are either of  $p_1, p_2$  or  $q_1, q_2$ .

The case  $p > 0$  is unlikely for the usual stiff fiber composites.

To solve the problem (29) and (30) let equations (34) be expressed in the form

$$\begin{aligned}
\phi(\xi) &= D_1 f_1(\xi) + F_1 g_1(\xi) - m_1 \bar{\psi} \\
\psi(\eta) &= D_2 f_2(\eta) + F_2 g_2(\eta) - m_2 \bar{\phi}
\end{aligned} \tag{37}$$

where  $f_1, g_1$  indicate solutions in terms of  $p_1, q_1$  and  $f_2, g_2$ —in terms of  $p_2, q_2$ . Introducing equations (37) into (29) we obtain sets of linear equations for the constants  $D, F$  with solutions

$$\begin{aligned}
D_1 &= \frac{(1 + m_1 \bar{\psi}) g_1(p_1)}{f_1(p_1) g_1'(p_1) - f_1'(p_1) g_1(p_1)} \\
F_1 &= - \frac{(1 + m_1 \bar{\psi}) f_1'(p_1)}{f_1(p_1) g_1'(p_1) - f_1'(p_1) g_1(p_1)} \\
D_2 &= \frac{(1 + m_2 \bar{\phi}) g_2(p_2)}{f_2(p_2) g_2'(p_2) - f_2'(p_2) g_2(p_2)} \\
F_2 &= - \frac{(1 + m_2 \bar{\phi}) f_2'(p_2)}{f_2(p_2) g_2'(p_2) - f_2'(p_2) g_2(p_2)}
\end{aligned} \tag{38}$$

Now average both sides of equations (37) as in (33). The result can be written in the form

$$\begin{aligned}
\bar{\phi} + m_1 \bar{\psi} &= D_1 \bar{f}_1 + F_1 \bar{g}_1 = (1 + m_1 \bar{\psi}) \omega_1 \\
\bar{\psi} + m_2 \bar{\phi} &= D_2 \bar{f}_2 + F_2 \bar{g}_2 = (1 + m_2 \bar{\phi}) \omega_2
\end{aligned} \tag{40}$$

where

$$\begin{aligned}
\omega_1 &= \frac{f_1 g_1'(p_1) - f_1'(p_1) g_1}{f_1(p_1) g_1'(p_1) - f_1'(p_1) g_1(p_1)} \\
\omega_2 &= \frac{f_2 g_2'(p_2) - f_2'(p_2) g_2}{f_2(p_2) g_2'(p_2) - f_2'(p_2) g_2(p_2)}
\end{aligned} \tag{41}$$

Since expressions (41) are known, equations (40) can be solved for  $\bar{\phi}$  and  $\bar{\psi}$ . Thus

$$\begin{aligned}
\bar{\phi} &= \frac{\omega_1 - m_1(1 - \omega_1)\omega_2}{1 - m_1 m_2(1 - \omega_1)(1 - \omega_2)} \\
\bar{\psi} &= \frac{\omega_2 - m_2(1 - \omega_2)\omega_1}{1 - m_1 m_2(1 - \omega_1)(1 - \omega_2)}
\end{aligned} \tag{42}$$

These results together with equations (30)–(39) determine the solution (37) of equations (29) and (30). Specific results for the two cases (35) and (36) are given in the Appendix.

The perturbation stresses (12) now assume the form

$$\begin{aligned}
\sigma_{xx}^{(1)} &= -\sigma_x^{(1)} \phi(\xi) & \sigma_{xx}^{(2)} &= \frac{1}{\lambda} \sigma_x^{(1)} \phi(\xi) \\
\sigma_{xx}^{(1)} &= \sigma_x^{(1)} \frac{d\phi}{d\xi} z/l_1 & \sigma_{xx}^{(2)} &= \frac{1}{\lambda} \sigma_x^{(1)} \frac{d\phi}{d\xi} (h-z)/l_1 \\
\sigma_{yy}^{(1)} &= -\sigma_y^{(1)} \psi(\eta) & \sigma_{yy}^{(2)} &= \frac{1}{\lambda} \sigma_y^{(1)} \psi(\eta) \\
\sigma_{yy}^{(1)} &= \sigma_y^{(1)} \frac{d\psi}{d\eta} z/l_1 & \sigma_{yy}^{(2)} &= \frac{1}{\lambda} \sigma_y^{(1)} \frac{d\psi}{d\eta} (h-z)/l_1
\end{aligned} \tag{43}$$

$$\sigma_{xx}^{(2)} = \left( \sigma_x^{(1)} \frac{d^2\phi}{d\xi^2} + \sigma_y^{(1)} \frac{d^2\psi}{d\eta^2} \right) (ht_1 - z^2)/2t_1^2$$

$$\sigma_{yy}^{(2)} = \left( \sigma_x^{(1)} \frac{d^2\phi}{d\xi^2} + \sigma_y^{(1)} \frac{d^2\psi}{d\eta^2} \right) (h - z^2)/2t_1^2$$

### Effective Young's Modulus $E_x$ and Poisson's Ratio $\nu_{xy}$

It is first necessary to evaluate the minimum value of the integral (26) and to introduce it into (22). Direct evaluation of the integral (26) in terms of the functions  $\phi$  and  $\psi$  which have been determined above is a formidable undertaking which can fortunately be avoided. The best way to proceed is to integrate equation (30a) multiplied by  $\phi$  from  $-\rho_1$  to  $\rho_1$  and, similarly, equation (30b) multiplied by  $\psi$  from  $-\rho_2$  to  $\rho_2$ . These integrals obviously vanish and when transformed by integration by part with use of the boundary conditions (29) they can be identified with substantial parts of the integral (26). As a result of this procedure we find the simple result

$$U'_{\min} = -2t_1^2 \sigma^2 C [k_x^2 \rho_2 \phi''(\rho_1) + k_y^2 \rho_1 \psi''(\rho_2)] \quad (44)$$

To evaluate the third derivatives in equation (44) we evaluate the mean of equation (30a) with respect to  $\xi$  within  $[-\rho_1, \rho_1]$  and of equation (30b) with respect to  $\eta$  within  $[-\rho_2, \rho_2]$ . Noting that the means of the second derivatives vanish because of equations (29) and taking into account equations (31) we obtain

$$\begin{aligned} -C \frac{\phi''(\rho_1)}{\rho_1} &= A_0 \dot{\phi} + \frac{k_y}{k_x} B_0 \dot{\psi} \\ -C \frac{\psi''(\rho_2)}{\rho_2} &= C_0 \dot{\psi} + \frac{k_x}{k_y} B_0 \dot{\phi} \end{aligned} \quad (45)$$

Substituting equations (45) into (44) and (27) we have

$$U'_{\min} = 2t_1 ab \sigma^2 [(k_x A_0 + k_y B_0) k_x \dot{\phi} + (k_x B_0 + k_y C_0) k_y \dot{\psi}] \quad (46)$$

Thus the minimum energy has been expressed in terms of  $\dot{\phi}$  and  $\dot{\psi}$  which are explicitly determined by equations (42). Since the reference volume in the present case is

$$V = 4abh = 4ab(t_1 + t_2) \quad (47)$$

we have from equations (46), (47), and (22)

$$\frac{1}{E_x} \leq \frac{1}{E_x^0} + \frac{1}{1+\lambda} (K_x \dot{\phi} + K_y \dot{\psi}) \quad (48)$$

$$K_x = (k_x A_0 + k_y B_0) k_x \quad K_y = (k_x B_0 + k_y C_0) k_y$$

This provides a rigorous lower bound on  $E_x$  in the event that all cracks are equidistant. If this is not the case let inter-crack distances be  $2a_m$  in  $x$  direction and  $2b_n$  in  $y$  direction, respectively. Then the admissible stress fields employed are still valid in each laminate element of dimensions  $2a_m, 2b_n, h$ . The complementary energy functional is now equations (24) and each term in the summation is expressed in terms of functions  $\phi_m$  and  $\psi_n$ , in the form equation (26), leading to extremum conditions of form (30) for each of these functions, subject to boundary condition of type (29)

$$\phi_m(\pm \rho_{1m}) = 1 \quad \phi'_m(\pm \rho_{1m}) = 0 \quad (49)$$

$$\psi_n(\pm \rho_{2n}) = 1 \quad \psi'_n(\pm \rho_{2n}) = 0$$

where

$$\rho_{1m} = a_m/t_1 \quad \rho_{2n} = b_n/t_1 \quad (50)$$

This defines means  $\bar{\phi}_m$  and  $\bar{\psi}_n$  which are precisely  $\dot{\phi}$  and  $\dot{\psi}$  expressed in terms of (50). Thus

$$U'_{\min} = -2t_1 a_m^2 \sum_m \sum_n a_m b_n (K_x \bar{\phi}_m + K_y \bar{\psi}_n) \quad (51)$$

and the relevant laminate volume is now

$$V = 4h \sum_m \sum_n a_m b_n \quad (52)$$

Introducing equations (51) and (52) into (22) we obtain again a lower bound for  $E_x$ :

This result can be put into more compact form if the inter-crack distances are random variables  $a, b$ , assuming values  $a_m, b_n$ . Then (50) are the values of associated random variables  $\rho_1$  and  $\rho_2$  with joint probability density function  $P(\rho_1, \rho_2)$ . In this event (22) will assume the form

$$\frac{1}{E_x} \leq \frac{1}{E_x^0} + \frac{K_x \langle \rho_1 \rho_2 \phi(\rho_1) \rangle + K_y \langle \rho_1 \rho_2 \psi(\rho_2) \rangle}{(1+\lambda) \langle \rho_1 \rho_2 \rangle} \quad (53)$$

where  $\langle \cdot \rangle$  indicates probability average. It can probably be assumed that  $\rho_1$  and  $\rho_2$  are independent random variables. In this event

$$P(\rho_1, \rho_2) = P_1(\rho_1)P_2(\rho_2) \quad (54)$$

and (53) assumes the form

$$\frac{1}{E_x} \leq \frac{1}{E_x^0} + \frac{1}{1+\lambda} \left[ K_x \frac{\langle \phi(\rho_1) \rangle}{\langle \rho_1 \rangle} + K_y \frac{\langle \psi(\rho_2) \rangle}{\langle \rho_2 \rangle} \right] \quad (55)$$

where

$$\langle \rho_1 \rangle = \int_{-\infty}^{\infty} P_1(\rho_1) \rho_1 d\rho_1 \quad \langle \rho_2 \rangle = \int_{-\infty}^{\infty} P_2(\rho_2) \rho_2 d\rho_2 \quad (56)$$

and also

$$\langle \rho_1 \rangle = \langle a \rangle / t_1 \quad \langle \rho_2 \rangle = \langle b \rangle / t_2$$

The effective Poisson's ratio  $\nu_{xy}$  is defined by

$$\nu_{xy} = -\frac{\epsilon_{yy}}{\epsilon_{xx}} \quad \epsilon_{xx} = \frac{\sigma^0}{E_x} \quad (57)$$

Since  $\nu_{xy}$  cannot be bounded by variational methods we evaluate it in terms of the approximate stresses resulting from our variational treatment. For the case of equidistant cracks in the  $x$  and  $y$  direction

$$\epsilon_{yy} = \frac{1}{4ab} \left\{ \int_{-a}^a \int_{-b}^b \int_0^{t_1} \epsilon_{yy}^{(1)} dx dy dz + \int_{-a}^a \int_{-b}^b \int_{t_1}^h \epsilon_{yy}^{(2)} dx dy dz \right\} \quad (58)$$

It follows from the ply orientations and the stress-strain relations of the ply material that

$$\begin{aligned} \epsilon_{yy}^{(1)} &= -\sigma_{xx}^{(1)} \nu_A / E_A + \sigma_{yy}^{(1)} / E_A - \sigma_{xx}^{(1)} \nu_A / E_A \\ \epsilon_{yy}^{(2)} &= -\sigma_{xx}^{(2)} \nu_A / E_A + \sigma_{yy}^{(2)} / E_T - \sigma_{xx}^{(2)} \nu_T / E_T \end{aligned} \quad (59)$$

Next we introduce the stresses (11) and (12) into equations (59) and the resulting expressions into equation (58). We observe that: (1) The stresses  $\sigma_{yy}^{(0,m)}$  produce the Poisson's ratio  $\nu_{xy}^0$  of the undamaged laminate; (2) The contribution of  $\sigma_{xx}$  to equation (58) vanishes since

$$\int_{-a}^a \int_{-b}^b \phi''(x) dx dy = 2b \int_{-a}^a \phi''(x) dx = 2b[\phi'(x)]_{-a}^a$$

and this vanishes because of equations (14). A similar result is true for the integral of  $\psi$  over the rectangle. An easy calculation then yields the result

Table 1 Properties of unidirectional material. Moduli in GPa.

	$E_A$	$E_T$	$G_A$	$G_T$	$\nu_A$	$\nu_T$
Glass/Epoxy	41.7	13.0	3.40	4.58	0.300	0.420
Graphite/Epoxy	208.3	6.5	1.65	2.30	0.255	0.413

$$\nu_{xy} = \nu_{xy}^0 - \frac{E_x^0}{E_x} \frac{K^{(1)} \downarrow}{1+\lambda} \left( \frac{E_x}{E_T} - \frac{E_x}{E_A} \right) \quad (60)$$

where  $\downarrow$  is defined by equations (33). Evaluation of  $\nu_{xy}$  is of course entirely analogous.

### Results, Discussion and Conclusions

The approximate nature of the analysis which has been developed here is contained in the assumed form of the stresses (7) which certainly cannot be correct. Indeed from experience with crack field solutions one would expect local singularities at the crack tips, which are absent from equations (7). But it should be remembered that in the usual structural laminates we are dealing with very thin plies of thickness of order 0.2–0.4 mm. Typical glass and carbon fiber diameters are 0.01 mm. Assuming for the sake of argument that fibers are arranged in regular hexagonal arrays, we find that at the usual 0.60 fiber volume fraction the ply thickness can accommodate about 16–32 fibers. Now the basic assumption in laminate theory is that plies are homogeneous anisotropic with elastic properties equal to the effective elastic properties of the unidirectionally reinforced ply material. But it should be remembered that the concept of effective modulus is based on stress and strain averages over representative volume elements (RVE) which by definition must contain many fibers. It follows that a ply can accommodate perhaps 2–3 RVE sizes across its thickness. Therefore, a severe gradient of local average stress or strain through the thickness is impossible. This does not present a problem for the simple cases of undamaged laminates when the stresses are constant or linear across ply thickness, but the situation is very different in the case of an intralaminar crack. If it is assumed that the fields of the homogeneous ply model are averages over RVE, then the crack tip singularities of fracture mechanics and their associated large stress gradient cannot exist. If this assumption is not made, there remains the choice between two difficult alternatives: (a) The crack tip is in the matrix and recognizes the adjacent fibers as distinct heterogeneities, thus creating an intractable problem in crack mechanics; (b) The crack tip vicinity is governed by a nonlocal elasticity theory of unknown nature or with many unknown elastic constants. None of these alternatives is useful or practical and it would therefore appear that the simple assumptions (7), with their resultant gentle through-the-thickness variations of the stresses, are less severe than would perhaps appear at first sight.

All of these considerations apply also to finite element analysis. The number of finite elements allowable through the thickness must be severely limited and singular elements raise the same problems as the crack tip singularities discussed above.

Highsmith and Reifsnider (1986) have treated the problem of orthogonally cracked cross-plies in terms of a refined laminate theory advanced by Pagano (1978) in which stress variation through ply thickness is restricted to be linear. The treatment is of necessity restricted to equidistant cracks and requires extensive numerical analysis. Their results, Highsmith and Reifsnider (1986) show that the stress  $\sigma_{xx}$  depends only weakly on  $y$ , the stress  $\sigma_{yy}$  depends only weakly on  $x$ , and  $\sigma_{xy}$  is negligible. This is in accordance with our basic assumptions (7). Furthermore, the shear stress  $\sigma_{xy}$  practically does not depend on  $y$  and  $\sigma_{xy}$  practically does not depend on  $x$  and this agrees with (12 b,d,g,i).

Table 2 The effect of cracks on Young's modulus  $E_x$  and Poisson's ratio  $\nu_{xy}$

Glass/Epoxy		$\iota_1 = 3\iota_2$		Glass/Epoxy		$\iota_1 = \iota_2$		Graphite/Epoxy		$\iota_1 = \iota_2$	
$\rho_1 = \rho$	$\rho_2 = \infty$	$\rho_1 = \rho_2 = \rho$	$\rho_1 = \rho$	$\rho_2 = \infty$	$\rho_1 = \rho_2 = \rho$	$\rho_1 = \rho$	$\rho_2 = \infty$	$\rho_1 = \rho_2 = \rho$			
$\rho$	$E_x/E_x^0$	$\nu_{xy}^0$	$E_x/E_x^0$	$\nu_{xy}^0$	$E_x/E_x^0$	$\nu_{xy}^0$	$E_x/E_x^0$	$\nu_{xy}^0$	$E_x/E_x^0$	$\nu_{xy}^0$	$E_x/E_x^0$
50	.299	.111	.980	.110	.990	.141	.990	.142	.999	.0154	.999
20	.951	.108	.951	.106	.976	.139	.975	.140	.997	.0154	.997
10	.907	.102	.906	.100	.953	.134	.951	.139	.994	.0153	.994
5	.830	.094	.829	.091	.910	.129	.907	.138	.989	.0152	.988
3	.745	.084	.743	.082	.859	.122	.853	.140	.982	.0151	.981
2	.661	.074	.658	.073	.813	.115	.804	.144	.975	.0150	.974
1	.548	.061	.542	.073	.773	.109	.762	.149	.971	.0149	.969
.50	.524	.058	.516	.075	.770	.108	.757	.150	.970	.0149	.968
no cracks	$E_x^0 = 20.30 \text{ GPa}$	$\nu_{xy}^0 = .113$	$E_x^0 = 27.57 \text{ GPa}$	$\nu_{xy}^0 = .143$		$E_x^0 = 107.6 \text{ GPa}$		$\nu_{xy}^0 = .0154$			

For purpose of numerical evaluation we have used glass/epoxy and graphite/epoxy laminates with unidirectional ply properties as in Hashin (1985). These are given in Table 1.

Table 2 shows Young's modulus reduction and also Poisson's ratio for various laminates with equidistant cracks in both directions. Also shown by comparison are results of Hashin (1985) for the case when there are cracks only in the 90° ply. It is seen that the effect of the cracks in the 0° plies is quite small, no doubt because of the small value of transverse  $\sigma_{yy}$  stress in the 0° plies due to tension in 0°, i.e.,  $x$  direction. This is also in agreement with the results of Highsmith and Reifsnider (1986). The situation is quite different for the Poisson's ratio. It is seen that cracks have significant effects

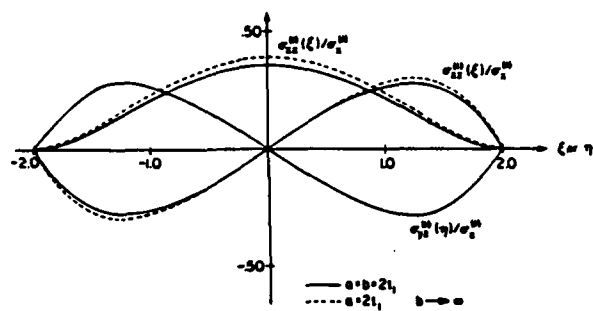


Fig. 3  $\sigma_{zz}^{(1)}, \sigma_{zz}^{(2)},$  and  $\sigma_{yz}^{(1)}$  variation

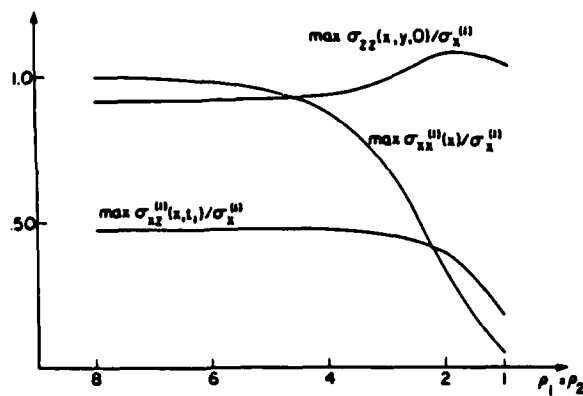


Fig. 4 Variation of maximum  $\sigma_{zz}$ ,  $\tau$ , and  $\sigma_{yz}$  with  $\rho$

on the value of this quantity and that the effect of orthogonal cracks can be very substantial as is evidenced in particular by the Graphite/Epoxy cross ply.

For the loading case of uniaxial tension considered here the stresses of major interest are:  $\sigma_{zz}^{(1)}$  and  $\sigma_{zz}^{(2)}$  which are transverse to the fibers in their respective layers and may thus produce intralaminar cracks; the interlaminar shear stresses  $\sigma_{yz}$  and  $\sigma_{xz}$ ; the stress  $\sigma_{zz}$  normal to the plane of the laminate which is called peeling stresses when tensile. It is seen from the form of equations (12) and (43) that the shear stresses assume their maximum values at the interface of the plies and that  $\sigma_{zz}$  assumes its maximum value on the midplane  $z = 0$ . However, the value of  $\sigma_{zz}$  at the interface is also of importance, for the stress which produces interlaminar separation may be smaller than the one producing midplane transverse cracking.

We have evaluated stress distributions for  $[0^\circ/90^\circ]$ , graphite/epoxy laminates assuming equidistant cracks  $a = b$ , for various crack densities defined by different ratios  $\rho = a/t_1$ . We have observed the following significant phenomena:

(1) The tensile stress  $\sigma_{yy}^{(2)}$  is much smaller than the tensile stress  $\sigma_{zz}^{(1)}$  in the load direction. It can, therefore, be assumed that during loading no new intralaminar cracks will develop in the  $0^\circ$  plies in the  $y$  direction.

(2) The stresses  $\sigma_{zz}^{(1)}$  and  $\sigma_{zz}^{(2)}$  are close in value to the same stresses produced in the same laminate when only the  $90^\circ$  plies are cracked (Hashin, 1985). A comparison is shown in Fig. 3 for the case  $a/t_1 = 2$ .

(3) The maximum value of tensile transverse stress  $\sigma_{yz}^{(1)}$  is midway between cracks, is equal to the corresponding stress  $\sigma_y^{(1)}$  in the undamaged laminate when distances between cracks are large, and decreases monotonically with increasing crack density (decreasing  $\rho$ ) (Fig. 4).

(4) The intralaminar shear stress  $\sigma_{yz}$  has significant values (Fig. 3) and therefore the important interlaminar shear stress is  $\tau = \sqrt{\sigma_{yz}^2 + \sigma_{xz}^2}$ . Figure 4 shows the value of  $\tau_{\max}$  as a function of crack density. It is seen that this stress starts out with a

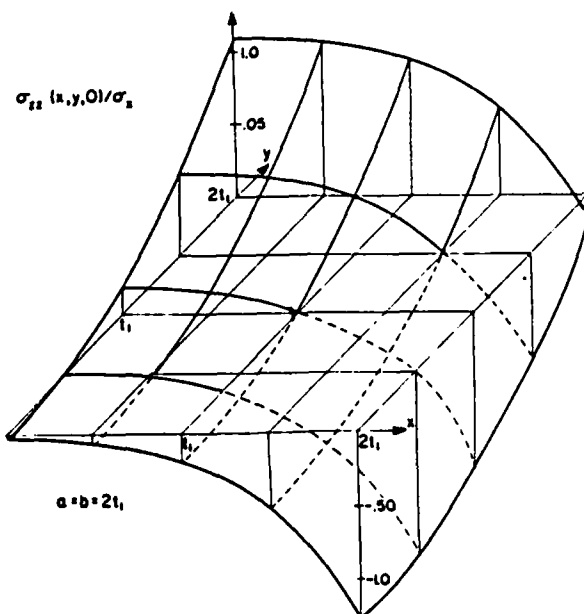


Fig. 5 Variation of  $\sigma_{zz}$  over midplane

value of  $0.48\sigma_x^{(1)}$  which is certainly significant. When the value of  $\sigma_x^{(1)}$  is large enough to cause cracking,  $\tau$  may be large enough to produce shear delamination. It is interesting to note that increasing crack density decreases this shear stress.

(5) The peeling stress  $\sigma_{zz}$  assumes significant values. Figure 5 shows the variation of midplane  $\sigma_{zz}$  over one quarter of the square defined by the intersection of two pairs of cracks. Observe the large tensile stress  $1.08\sigma_x^{(1)}$  in the middle of the  $y = a$  edge. When  $\sigma_x^{(1)}$  is large enough to crack the  $90^\circ$  ply transversely, this stress is certain to produce a crack in the  $xy$  plane. Note that for the present laminate  $\sigma_{zz}$  at the ply interface is one half of the midplane value. Depending on interface strength such a stress may also produce interface separation. The largest value of  $\sigma_{zz}$  is always located on the edges  $y = \pm a$ . For small crack density the maximum is close to the cracks  $x = \pm a$  and its location moves to the center of the edge with increasing crack density. Figure 4 shows the variation of  $\max \sigma_{zz}$  with intercrack distance. It would be of interest to analyze various other cases and also biaxial loading, which is easily carried out by superposing the results of two uniaxial loads in the  $x$  and  $y$  directions.

#### Acknowledgment

Support of the Air Force Office of Scientific Research under Contract 85-0342 is gratefully acknowledged.

#### References

- Hashin, Z., 1985, "Analysis of Cracked Laminates: A Variational Approach," *Mechanics of Materials*, Vol. 4, pp. 121-136.
- Highsmith, A. L., and Reifsnider, K. L., 1986, "Internal Load Distribution Effects During Fatigue Loading of Composite Laminates," *ASTM, STP 907*, pp. 233-251.
- Laws, N., Dvorak, G. J., and Hejazi, M., 1983, "Stiffness Changes in Unidirectional Composites Caused by Crack Systems," *Mechanics of Materials*, Vol. 2, pp. 123-137.
- Laws, N., Dvorak, G. J., and Hejazi, M., 1985, "The Loss of Stiffness in Cracked Laminates," *Fundamentals of Deformation and Fracture, Proc. IUTAM Eshelby Memorial Symposium*, Cambridge University Press, pp. 119-128.
- Pagano, N. J., 1978, "Stress Fields in Composite Laminates," *International Journal of Solids and Structures*, Vol. 14, pp. 385-400.
- Reifsnider, K. L., and Jamison, R., 1982, "Fracture of Fatigue-loaded Composite Laminates," *International Journal of Fatigue*, pp. 187-197.
- Reifsnider, K. L., and Talug, A., 1980, "Analysis of Fatigue Damage in Composite Laminates," *International Journal of Fatigue*, pp. 3-11.

## APPENDIX

Denote for convenience

$$\dot{\phi} = \Phi_1 \quad \dot{\psi} = \Phi_2$$

For case (35)

$$D_1 = 2(1 + m_1 \Phi_2) [\alpha_1 Ch(\alpha_1 \rho_1) \sin(\beta_1 \rho_1) + \beta_1 Sh(\alpha_1 \rho_1) \cos(\beta_1 \rho_1)] / M_1$$

$$F_1 = 2(1 + m_1 \Phi_2) [\beta_1 Ch(\alpha_1 \rho_1) \sin(\beta_1 \rho_1) - \alpha_1 Sh(\alpha_1 \rho_1) \cos(\beta_1 \rho_1)] / M_1$$

$$M_1 = \alpha_1 \sin(2\beta_1 \rho_1) + \beta_1 Sh(2\alpha_1 \rho_1)$$

$$\omega_1 = \frac{2[Ch(2\alpha_1 \rho_1) - \cos(2\beta_1 \rho_1)]}{\rho_1 (\alpha_1 / \beta_1 + \beta_1 / \alpha_1) M_1}$$

To obtain  $D_2$ ,  $F_2$ , and  $\omega_2$ , simply replace 1 by 2 in the above equations. Then

$$\phi(\xi) = D_1 Ch(\alpha_1 \xi) \cos(\beta_1 \xi) + F_1 Sh(\alpha_1 \xi) \sin(\beta_1 \xi) - m_1 \dot{\psi}$$

$$\psi(\eta) = D_2 Ch(\alpha_2 \eta) \cos(\beta_2 \eta) + F_2 Sh(\alpha_2 \eta) \sin(\beta_2 \eta) - m_2 \dot{\phi}$$

For case (36)

$$D_1 = (1 + m_1 \Phi_2) \beta_1 Sh(\beta_1 \rho_1) / N_1$$

$$F_1 = -(1 + m_1 \Phi_2) \alpha_1 Sh(\alpha_1 \rho_1) / N_1$$

$$N_1 = \beta_1 Ch(\alpha_1 \rho_1) Sh(\beta_1 \rho_1) - \alpha_1 Sh(\alpha_1 \rho_1) Ch(\beta_1 \rho_1)$$

$$\omega_1 = (\beta_1 / \alpha_1 - \alpha_1 / \beta_1) Sh(\alpha_1 \rho_1) Sh(\beta_1 \rho_1) / \rho_1 N_1$$

To obtain  $D_2$ ,  $F_2$ , and  $\omega_2$ , replace 1 by 2 in the above equations. Then

$$\phi(\xi) = D_1 Ch(\alpha_1 \xi) + F_1 Sh(\beta_1 \xi) - m_1 \dot{\psi}$$

$$\psi(\eta) = D_2 Ch(\alpha_2 \eta) + F_2 Sh(\beta_2 \eta) - m_2 \dot{\phi}$$

## ANALYSIS OF DAMAGE IN COMPOSITE MATERIALS

Zvi Hashin

Dept. of Solid Mechanics, Materials and Structures  
Faculty of Engineering  
Tel-Aviv University  
Tel-Aviv, Israel

**Abstract.**— The various damage phenomena in statically or cyclically loaded unidirectional fiber composites and their laminates are described and classified. Existing analytical methods to evaluate the effect of damage in laminates on their thermoelastic properties are described and discussed. Fundamental problems arising in application of classical mechanics methods to very thin cracked plies are pointed out. Existing work on damage prediction and failure analysis is described.

### 1. Introduction

The word Damage has different connotations in different areas of science and technology, not to speak of everyday life. In the present context we shall define damage as an accumulation of many small internal defects inside a solid body. Defect implies an internal discontinuity such as void, crack or dislocation. It is assumed that the damaged body can be described on a suitable scale of magnitude by an effective continuum with stress-strain relations defined as the relations between average stress and average strain where averages are taken over the usual representative volume elements (RVE) which are small compared to body dimensions yet contain a large number of defects:

The mechanics of a damaged body will be called Damage Mechanics. We shall distinguish between micro-damage mechanics (MIDM) and macro-damage mechanics (MADM). The former implies evaluation of the detailed micro-fields of stress and strain in the vicinity of defects which may then be utilized to evaluate average stress and strain, thus the effective or macro stress-strain relations, and also to obtain some information concerning local failures. Within this frame the defects are explicitly recognized by shape and spatial distribution. By contrast the latter approach, often also called continuum theory of damage, describes damage in terms of abstract fields of scalar, vectorial or tensorial nature which also contain unknown parameters to be determined by fit to experimental data. Such description of damage is by no means unique and the appropriate choice may at this time be regarded as an open question. Evidently MADM cannot be expected to provide information beyond the dependence of macro-material parameters or effective stress-strain relations of the damaged body on the chosen "damage" field.

It would appear therefore that MIDM should be preferred since it is more closely tied to physical reality and because it provides more relevant information. It is unfortunately also very difficult to carry out since it requires the determination of detailed fields produced by many interacting defects and this can be done only for relatively simple geometries or on the basis of simplifying assumptions. It is therefore our view that MIDM and MADM should be viewed as complementary approaches. Whenever MIDM is possible it should be pursued; otherwise we should resort to MADM. It is of primary importance that MIDM and MADM should communicate efficiently and share their results. A recent IUTAM Symposium on Mechanics of Damage and Fatigue [3] has been concerned with damage mechanics from both those points of view.

Damage in the composite materials which are used in engineering practice occurs primarily in the form of micro-cracks. There exists a considerable body of literature on stiffness reduction of homogeneous elastic bodies by crack distributions most of which is based on what has been here called MIDM and well illustrates the difficulty of the problems involved. Such difficulties are magnified in composites because of the presence of a reinforcing phase in the form of inclusions or fibers and consequently cracks do not only interact with one another but also with the inhomogeneities.

We shall here focus our attention on unidirectional fiber composites (UFC) and laminates which are made of UFC plies with analytical emphasis of the latter. From the engineering point of view there are two main reasons to study damage in fiber composite laminates. Firstly the state of damage is a prelude to the event of failure. Several attempts to predict laminate failure in simple fashion, without consideration of damage, can be found in the older literature and these undertakings have not been very successful. It would therefore appear that analysis of damage is prerequisite to analysis of failure.

Secondly, it is necessary to have an estimate of the remaining fatigue life and residual strength of a damaged laminate and to characterize the state of damage by observable parameters. In metal structures this is done in terms of the present and (predicted) future of a dominant crack. But in laminates damage develops as a collection of many interior microcracks and therefore different methods are needed. It might be hoped that stiffness reduction, measured and analyzed, could serve as such parameters; hence the fundamental importance of analytical relation of stiffness to crack distribution or density.

## 2. Classification of Damage

A UFC is made of stiff and strong parallel continuous fibers (glass, graphite, carbon) which are embedded in a relatively compliant matrix (polymer, aluminum). We are here primarily concerned with the case of polymeric matrix. When such a UFC is loaded by tension in fiber direction, whether static or cyclic, fibers will rupture at different random locations, Fig. 1. These fiber ruptures are micro-cracks which may be regarded as damage in the sense defined in the introduction above. At each rupture there must develop a significant shear interfacial stress as may be easily shown just from equilibrium considerations, Rosen [27]. This shear stress may produce interfacial deterioration or separation in the form of interfacial cracks which is another kind of, subsequent, damage. A statistical analysis of strength based on this kind of damage has been pioneered in [27] and has been refined and extended in subsequent works, e.g. [21].

If on the other hand the usual thin specimen of UFC is loaded transversely, normal to the fibers, the specimen fails abruptly by a single crack along the fibers without prior discernible development of internal damage. There are thus two major modes of failure in tension: The fiber mode which involves prior development of damage and the matrix mode which does not, [7].

It is of considerable interest to evaluate the stiffness reduction of a UFC which has been damaged by tension in fiber direction. Steif [28] has given an approximate analysis of reduction of Young's modulus  $E_A$  in fiber direction, on the basis of a simple shear lag model. Reduction of transverse modulus  $E_T$  and axial shear modulus  $G_A$  by cracks along fibers has been analyzed, approximately, on the basis of so-called self-consistent estimates in [6] and [17]. All of these treatments fall within the MIDM category.

Since the strength and stiffness of UFC are very high in fiber direction but low transversely to the fibers it is necessary in most engineering applications to use these materials in the form of laminates as is shown schematically in Fig. 2. We consider for the sake of simplicity only laminates which are symmetric with respect to their midplanes and are subjected to constant midplane membrane loads. Then, as is well known, the state of stress in any ply of the laminate is constant and plane except for edge boundary layers where the state of stress is three dimensional and complex.

Static or cyclic loading may lead to the following events:

- (a) If there is high stress in fiber direction a ply will develop fiber damage as has been described above. This will be called: intralaminar fiber damage.
- (b) At some level of transverse tensile stress a fiber mode crack will be triggered by some micro-defect. Such an intralaminar crack propagates along the fibers and generally reaches the edges of the laminate. The formation of such a crack is a random event and the probability of its occurrence increases with increasing magnitude of tensile transverse stress. It follows that, initially, only a small number of isolated intralaminar cracks will appear in the ply. Isolated implies that there is no mutual crack interaction and therefore the transverse tensile stress builds up from zero on the crack to its initial magnitude when there are no cracks. This is unavoidably accompanied by interlaminar shear stress, Fig. 3, a phenomenon similar to that of interfacial shear stress near a fiber rupture. As the ply tensile stress increases because of increase of external load more and more intralaminar cracks will appear. Fig. 4 redrawn from X-radiographs given in [30] shows the increase of crack density in the 90° ply of a graphite/epoxy cross-ply laminate, with load increase.

As cracks become closer the in-between tensile stresses diminish and can no longer build up as before and therefore ever increasing rate of loading is required to produce new cracks. This is well illustrated by plots of crack density versus load as shown in [13]. Experimental evidence shows that crack densities in plies reach asymptotic saturation values at which they form roughly regular patterns [24,25]. This has been called Characteristic Damage State (CDS), Reifsnider [24].

We shall call the type of damage described intralaminar matrix damage.

(c) With intralaminar saturation the interlaminar stresses produced near the cracks, and in particular at locations where intralaminar cracks in neighboring plies cross, may produce local interfacial debonding between plies [26] which may be described as a collection of small interlaminar cracks or disbonds. This will be called interlaminar damage.

Note that a laminate may have initial interlaminar damage, before loading, in the form of interlaminar disbonds, due, for example, to faulty manufacturing. This damage, by itself, has no effect in the case of in-plane loading of a laminate and only little effect in the case of bending. The reason is that in the former case the plies are in states of plane stress; therefore the ply interfaces are traction free and thus an interlaminar disbond, sufficiently far removed from the edges, has no effect. In the latter case there are also interlaminar shear stresses due to bending which are, in principle, affected by such a disbond but are in general very small compared to in-plane stresses.

In the case of in-plane compressive load a disbond whose dimensions are much larger than the smaller distance from its plane to laminate free surface may be the source of local buckling and propagation of an interlaminar crack. This is an isolated damage phenomenon and is therefore not within our present

scope.

(d) It has been observed [15,16] that intralaminar cracks trigger the development of fiber ruptures in adjacent plies, which are distributed in bands along the cracks.

(e) Independently of the damage modes described, the high interlaminar stress concentration at laminate free edge may be the source of initiation and growth of an interlaminar edge crack which may propagate into the laminate with increasing load or number of load cycles. The analysis of such a crack is within the scope of fracture mechanics and since it is an isolated damage event, such as the disbond buckling mentioned above, it is not within the scope of our discussion of damage.

Most of the analytical discussion to follow will be concerned with intralaminar matrix damage. It is seen from our description of damage that it is the central damage mode, as it is the source of others. It is the primary cause of stiffness reduction of a laminate and most of the analytical investigations of laminate damage have been concerned with this damage mode.

### 3. Damage Mechanics of Laminates

#### 3.1. Stiffness reduction and stress analysis

According to the description and discussion of the various forms of damage in laminates given above the primary problem is to evaluate the effect of distributions of many intralaminar cracks in the plies. The major problems are: (a) Analysis of stiffness reduction. (b) Analysis of internal stresses and consequent implications for the internal failure process.

All of laminate analysis in the literature is based on the assumption that the plies are homogeneous anisotropic with the effective properties of the UFC. This is a valid assumption for undamaged laminates for the usual cases of membrane force and moment loading when the variation of the primary,

in-plane, laminate stresses through ply thickness is constant or linear. But the presence of intralaminar cracks may invalidate this assumption because it would lead to very large stress gradients through very thin plies. The implications of this difficulty will be discussed further below. Even the classical version of the problem is exceedingly difficult for it requires three dimensional analysis of the effects of many interacting cracks within different plies inside a laminate.

We shall first summarize various simple approaches which have been developed. Within the context of an old and somewhat primitive attempt to estimate laminate failure it has been assumed that ply failure is governed by some semi-empirical failure criterion, e.g. a quadratic polynomial of stress, thus determining first ply failure which mostly occurs in the matrix mode. Since, as has been explained above, the failed ply will develop many intralaminar cracks, it is assumed that the transverse Young's modulus  $E_T$  and the axial shear modulus  $G_A$  of the "failed" ply reduce to zero. A new stress analysis of the laminate is then performed on the basis of stiffness reduction of the failed ply and the next ply to fail is identified and its stiffnesses are then similarly reduced. This procedure which has sometimes been called the Ply Discount Method is continued until the occurrence of fiber failure in the  $0^\circ$  ply, i.e. the one with fiber orientation in load direction. This simple method is based on a crude estimate of the effect of intralaminar damage and not surprisingly such analysis of failure is mostly unreliable.

Reifsnider [24] and Reifsnider et al. [25,26] have advanced beyond this simple approach by recognizing that when a ply develops intralaminar cracks the load transfer must take place through interlaminar shear stresses in the vicinity of the crack, Fig. 3. They have accordingly devised a simple "strength-of-materials" type shear lag analysis which recognizes only two

kinds of stress: load carrying ply stresses which are constant through ply thickness and variable in load direction, and interlaminar shear stresses which are confined to a narrow layer of arbitrarily assumed thickness in-between plies. While the local stresses predicted by such simple analysis can hardly be reliable the stiffness reduction thus determined is often from fair to good agreement with experimental data.

Another approach has been taken by Laws and Dvorak [5]. They have used the approximate method known as the Self Consistent Scheme (SCS) to estimate the stiffness reduction of a cracked ply [17] and then proceeded on that basis to evaluate stiffness reduction of cracked laminates. The SCS has first been employed to evaluate stiffness reduction of a homogeneous body containing many cracks by Budiansky and O'Connell [4]. It is based on the drastic assumption that any crack is embedded in the effective medium whose properties are to be determined. The results thus obtained are not always acceptable. Thus for randomly oriented penny-shaped cracks the stiffness vanishes at some definite crack density which is unreasonable for stiffness must vanish asymptotically with indefinitely increasing crack density.

The difficulties are compounded in the case of a cracked ply. Fig. 5a shows the Crack Opening Displacements (COD) of intralaminar cracks which are of necessity restrained by the neighboring plies. The SCS cannot cope with this situation. It needs to assume that ply thickness is infinitely larger than typical crack length as is shown in Fig. 5b. It follows that (a) crack density of Fig. 5a has to be somehow translated into a crack density parameter appropriate to Fig. 5b. (b) Crack lengths are now of the order of fiber diameters and in spite of this it is assumed that cracks are embedded in a material with the effective properties of the UFC.

With all of these drastic assumptions the SCS stiffness predictions are in fair to good agreement with some available experimental data [5]. Obviously the SCS cannot provide any information regarding microstresses and local failure.

The methods described so far may be regarded as approximate MIDM approaches. A MADM approach has been proposed by Talreja [29]. He has described interlaminar and intralaminar damage in terms of general vector fields and has reduced them to more specific forms on the basis of symmetry arguments. The final forms involve undetermined constants to be determined by fitting to experiment. The basic question which arises is: are the constants so determined material constants? i.e. independent of laminate internal geometry. To examine this the prediction of stiffness reduction due to intralaminar damage in terms of such continuum damage fields was compared to experimental data thus obtaining a set of constants for glass epoxy. These constants were then used to compare analytical to other experimental results, obtaining fair to good agreement [29]. However, the analysis of interlaminar damage is unacceptable for it predicts in-plane stiffness reduction due to interlaminar cracks alone and as has been pointed out in part 2 cracks have no effect on in-plane stiffness (this is an exact elasticity theory conclusion).

It should be realized that stiffness reduction analysis is much less sensitive to simplifying assumptions than stress analysis, for effective stiffness is defined as a relation between stress and strain averages and an average is not necessarily sensitive to local errors. This may explain why such simple methods often yield effective elastic properties which are in reasonable agreement with experimental results.

More accurate methods are clearly required. Bearing in mind that analytical rigorous solutions can not be constructed there remain two avenues

of approach: More accurate analytical approximations and numerical analysis in terms of finite elements (or finite differences). All existing work of this nature is based on the classical description of a laminate in terms of homogeneous anisotropic plies. Before proceeding we must examine the implications of the homogeneous ply assumption within the present context.

A typical ply thickness may be of the order of .2 mm while typical fiber diameter (glass, carbon, graphite) is of the order of .01 mm. At typical fiber volume fraction .60 such ply thickness can accommodate about 15 fibers. Now the concept of effective media is based on scaling involving three orders of magnitude, [8], the microscale, the miniscale and the macroscale. In a composite material micro is the size of heterogeneities (e.g. fiber diameter). Mini (also called Meso) is the size of a typical Representative Volume Element (RVE) which is the smallest element of the composite to exhibit the effective properties with sufficient accuracy and must contain many heterogeneities (fibers). Macro is the size of the composite material body. To apply elasticity theory in terms of effective elastic moduli to a composite material body there must be fulfilled the necessary requirement Micro << Mini << Macro. Note that in the classical theory of elasticity there is no microscale: the differential element is the miniscale while the body dimensions are the macroscale.

Furthermore, in classical elasticity there are only surface forces and no surface moments on the faces of a differential element. Such assumption can be transferred to RVE faces in terms of local surface averages only if gradients of local average stress are sufficiently small, otherwise non-classical elasticity theory - such as multipolar or non-local - would have to be invoked for the continuum description of the composite.

All of this has significant implications for crack mechanics of composites. Consider as a pertinent example a transverse crack through a UFC. It must be our primary goal to avoid the intractable problem of a crack which "can distinguish" between fibers and matrix and therefore the UFC must be viewed as a homogeneous material with the effective properties. A typical plane RVE for random fiber locations is a square of about 10x10 fibers. The crack length is the macro dimension which must be by order of magnitude larger than the RVE dimension. If we view this crack in the classical crack mechanics sense then the usual stress "at a point" is now replaced by local average stress and this stress variable will become singular at the crack tip. This really implies that local average stress at this location has some large unknown value and therefore a criterion for crack criticality has been formulated in terms of surface energy, this being regarded as a material property. The contribution of the crack to the energy balance is evaluated in terms of the stress field or the COD in spite of the crack tip state of uncertainty; obviously, such evaluation can be reliable only when the crack tip uncertainty regions are small relative to total crack length and not when they are substantial parts of crack length.

In the case of an intralaminar crack the crack length is equal to the ply thickness which is of the order of about two RVE sizes. Since this is the macro dimension the necessary condition  $\text{Min} \ll \text{Macro}$  is thus violated. Or to put it differently, the crack consists entirely of crack tip regions and is too short to develop COD and stress which can be reliably predicted by classical crack mechanics in terms of effective elastic UFC properties.

This is a severe problem which goes to the fundaments of mechanics of solids. It implies that very accurate numerical solutions involving of necessity many finite elements through the thickness are not necessarily

correct and singular finite crack tip elements are not necessarily applicable for it is unlikely that there are crack tip singularities of local RVE average stress. There is of course the microfield alternative to recognize fibers and matrix at the crack tip but this is an intractable problem, even from the point of view of numerical analysis, not to mention its futility.

We shall refer to the problem discussed above as the thin ply problem and we believe that it is unresolved at the present time and should be pursued. In the meanwhile there is no choice but to continue with damage analysis based on classically homogeneous plies, allowing however certain flexibility in result interpretation in view of the thin ply problem.

The most basic problems concern a cracked laminate which is subjected to constant membrane forces  $N_{ij}$  which produce the average stresses

$$\bar{\sigma}_{ij} = N_{ij}/2h \quad i,j = 1,2 \quad (1)$$

where  $2h$  is the laminate thickness.

It is assumed that the laminate is symmetric before and after cracking. Then the effective elastic stress strain relations are

$$\bar{\epsilon}_{ij} = S_{ijkl}^* \bar{\sigma}_{kl} \quad (2)$$

where  $\bar{\epsilon}_{ij}$  is average strain and  $S_{ijkl}^*$  is the effective compliance tensor.

Assuming furthermore that the laminate is orthotropic in all stages we write (2) with abbreviated property notation

$$\bar{\epsilon}_{22} = S_{12}^* \bar{\sigma}_{11} + S_{22}^* \bar{\sigma}_{22}$$

$$S_{11}^* = \frac{1}{E_1} \quad S_{12}^* = -\frac{v_{12}}{E_1} = -\frac{v_{21}}{E_2}$$

$$S_{22}^* = \frac{1}{E_2} \quad S_{16}^* = \frac{1}{4G_{12}}$$

Here  $E_1$ ,  $E_2$ , are Young's moduli,  $v_{12}$ ,  $v_{21}$  are Poisson's ratios, and  $G_{12}$  is the shear modulus - all for the cracked laminate. For the uncracked laminate (2-3) retain their forms and we shall distinguish the properties in this case by superscript 0, e.g.  $E_1^0$ .

It is seen from (2) that to determine the effective thermoelastic properties of a cracked laminate it is necessary to evaluate the average strains for specified load. This requires in general a detailed internal field solution, satisfying zero traction conditions on crack surfaces and other boundary and continuity conditions.

The effective elastic compliances may also be expressed in terms of the crack opening displacements (COD), [8]. Thus for applied  $\bar{\sigma}_{1j}$

$$S_{ijkl}^* \bar{\sigma}_{kl} = S_{ijkl}^0 \bar{\sigma}_{kl} + \gamma_{ij} \quad (4)$$

$$\gamma_{ij} = \frac{1}{2V} \sum \int_{S_C} ([u_i]n_j + [u_j]n_i) dS$$

Here  $S_{ijkl}^0$  are the compliances of the uncracked laminate,  $[u_i]$  is the

the displacement jump across a crack - thus the COD,  $n_i$  is the normal to the crack surface, the summation is over all cracks and  $V$  is the laminate volume.

An important alternative definition of  $S_{ijkl}^*$  is in terms of stress energy since the stress energy of the laminate is rigorously given by

$$U^0 = \frac{1}{2} S_{ijkl}^* \bar{\sigma}_{ij} \bar{\sigma}_{kl} V \quad (5)$$

which may be decomposed into

$$\begin{aligned} U^0 &= U_0^0 + U' \\ U_0^0 &= \frac{1}{2} S_{ijkl}^0 \bar{\sigma}_{ij} \bar{\sigma}_{kl} V \\ U' &= \frac{1}{2} \sum_{S_C} T_i^0 [u_i] dS \end{aligned} \quad (6)$$

where the surface integral is again over all cracks and  $T_i^0$  is the traction at crack surface location in the uncracked laminate.

All the relations listed so far are exact and may be used to obtain the compliances of a cracked laminate on the basis of exact analytical or accurate numerical solutions.

An important and more flexible alternative is the variational formulation, primarily in terms of the principle of minimum complementary energy, which has been initiated for cracked laminates in [9]. Let  $\bar{\sigma}_{ij}$  be an admissible stress field. Such stress field must satisfy (a) Equilibrium everywhere. (b) Traction continuity at ply interfaces. (c) Laminate load boundary conditions and crack surface zero traction conditions. In this case the complementary energy functional  $\bar{U}^0$  is defined as

$$\tilde{U}^{\sigma} = \frac{1}{2} \int_V S_{ijkl} \tilde{\sigma}_{ij} \tilde{\sigma}_{kl} dV \quad (7)$$

where  $S_{ijkl}$  is the local compliance and  $\tilde{\sigma}_{ij}$  is in general three dimensional. In the common event that  $\tilde{\sigma}_{ij}$  are linear functions of  $\tilde{\sigma}_{ij}$ , (7) will have the form

$$\tilde{U}^{\sigma} = \frac{1}{2} \tilde{S}_{ijkl}^* \tilde{\sigma}_{ij} \tilde{\sigma}_{kl} V \quad (8)$$

where  $\tilde{S}_{ijkl}^*$  are coefficients which result from the integration. Now the principle of minimum complementary energy states that

$$\tilde{U}^{\sigma} \geq U^{\sigma} \quad (9)$$

Introducing (7-8) into (9) we find the condition

$$\tilde{S}_{ijkl}^* - S_{ijkl}^* \rightarrow \text{positive semi-definite} \quad (10)$$

which by suitable manipulation leads to upper bounds on some of the compliance components and thus to lower bounds on Young's and shear moduli.

For example: if the laminate is loaded by  $\tilde{\sigma}_{11} = N_{11}/2h$  only, then

$$U^{\sigma} = \frac{\tilde{\sigma}_{11}^2}{2E_1} V \quad \tilde{U}^{\sigma} = \frac{\tilde{\sigma}_{11}^2}{2\tilde{E}_1} \quad \tilde{E}_1 \leq E_1 \quad (11)$$

All of the variational work and, to the best of our knowledge, all of the numerical work has been concerned with the relatively simple case of cracked  $[0_m^{\circ}, 90_n^{\circ}]_s$  laminates, also called cross-ply laminates. Initially the case when only the  $90^{\circ}$  ply is cracked, Fig. 6, has been considered and more recently also the case when all plies are cracked, Fig. 7. These will be referred to as singly and orthogonally cracked, respectively. The first case occurs when a cross-ply is loaded monotonically or cyclically in simple tension, the second - when a  $[45_m^{\circ}/45_n^{\circ}]_s$ , which is merely a rotated cross-ply, is loaded in simple tension and also when a cross-ply is subjected to cyclic temperature change.

Basic to all analytical work is the identification of a typical or repeating element of the cracked laminate. Such an element is indicated in Fig. 7 and is shown enlarged in Fig. 8. In the event that in each crack family the cracks are equidistant the element shown is a repeating element in which case stress and strain fields are periodic with periods  $2a$  and  $2b$ . Such periodicity is essential for numerical work. If the cracks are not equidistant the element is called typical and it is then a typical building block of the cracked laminate.

An admissible stress field for an orthogonally cracked laminate, Fig. 7, under tension, has been constructed in [10] starting out from the premise that  $\bar{\sigma}_{xx}$  is only a function of  $x$ ,  $\bar{\sigma}_{yy}$  is only a function of  $y$  and  $\bar{\sigma}_{xy} = 0$ . Then systematic integration of the equations of equilibrium, taking into account traction continuity and boundary conditions defines an admissible stress field in terms of two unknown functions  $\phi(x), \psi(y)$ , as follows:

$$\bar{\sigma}_{xx}^{(1)} = \sigma_x^{(1)} [1 - \phi(x)] \quad \bar{\sigma}_{xx}^{(2)} = \sigma_x^{(2)} + \frac{1}{\lambda} \sigma_x^{(1)} \phi(x)$$

$$\bar{\sigma}_{xz}^{(1)} = \sigma_x^{(1)} \phi'(x) z \quad \bar{\sigma}_{xz}^{(2)} = \frac{1}{\lambda} \sigma_x^{(1)} \phi'(x) (h-z)$$

$$\bar{\sigma}_{yy}^{(1)} = \sigma_y^{(1)} [1 - \psi(y)] \quad \bar{\sigma}_{yy}^{(2)} = \sigma_y^{(2)} + \frac{1}{\lambda} \sigma_y^{(1)} \psi(y)$$

(12)

$$\bar{\sigma}_{yz}^{(1)} = \sigma_y^{(1)} \psi(y) z \quad \bar{\sigma}_{yz}^{(2)} = \frac{1}{\lambda} \sigma_y^{(1)} \psi(y) (h-z)$$

$$\bar{\sigma}_{zz}^{(1)} = [\sigma_x^{(1)} \phi''(x) + \sigma_y^{(1)} \psi(y)] \frac{1}{2} (ht_1 - z^2)$$

$$\bar{\sigma}_{zz}^{(2)} = \frac{1}{\lambda} [\sigma_x^{(1)} \phi''(x) + \sigma_y^{(1)} \psi(y)] \frac{1}{2} (h - z)^2$$

$$\lambda = t_2/t_1$$

where superscripts 1 and 2 identify the plies as labeled in Figs. 7, 8,  $\sigma_x^{(1)}$ ,  $\sigma_y^{(1)}$ ,  $\sigma_x^{(2)}$ , and  $\sigma_y^{(2)}$  are ply stresses in the uncracked laminate, prime and dot indicate x and y derivative, respectively, and the functions  $\phi$  and  $\psi$  must satisfy the following boundary conditions

$$\phi(\pm a_m) = 1 \quad \phi'(\pm a_m) = 0$$

(13)

$$\psi(\pm b_n) = 1 \quad \psi'(\pm b_n) = 0$$

Note that the stress fields thus defined satisfy traction continuity where the typical elements are joined, thus satisfying admissibility for the entire

cracked laminate. It is seen that in-plane stresses are constant, shear stresses linear and  $\tilde{\sigma}_{zz}$  is quadratic through ply thickness, thus exhibiting none of the classical crack tip singularities. In view of the discussion of the thin ply problem given above such gentle through-ply thickness variation does not seem unreasonable.

To employ the variational formulation, (12) is introduced into (7). Note in this respect that the plies are transversely isotropic unidirectional fiber composites and therefore the integrand in (7) for a ply has the form

$$\frac{1}{2} S_{ijkl} \tilde{\sigma}_{ij} \tilde{\sigma}_{kl} = \frac{1}{2} [\tilde{\sigma}_{11}^2/E_A + (\tilde{\sigma}_{22}^2 + \tilde{\sigma}_{33}^2)/E_T - 2\tilde{\sigma}_{11}(\tilde{\sigma}_{22} + \tilde{\sigma}_{33}) v_A/E_A - 2\tilde{\sigma}_{22}\tilde{\sigma}_{33} v_T/E_T + \tilde{\sigma}_{23}^2/G_T + (\tilde{\sigma}_{12}^2 + \tilde{\sigma}_{13}^2)/G_A]$$

where 1 indicates fiber direction and 2,3 are transverse directions. These material axes change orientation from ply to ply. Subscript A indicates property in fiber direction and T in direction transverse to fibers. Carrying out the z integration in (7) we obtain a double integral in x,y which must be minimized to obtain an optimum bound. This results in linear integro-differential equations for the function  $\phi$  and  $\psi$  subject to the boundary conditions (13). These equations have been solved analytically and then (9) or (11) define optimum lower bounds on Young's modulus. Furthermore the optimizing function  $\phi$  and  $\psi$  now determine approximate stresses. Details are given in [10]. Note that Poisson's ratios cannot be bounded directly, but they may be evaluated approximately by averaging of the strains associated with the approximate stresses.

The case when only the 90° ply is cracked is of course a special case of orthogonal cracking when the intercrack distances b, say, become very large.

A detailed solution has been given in [9] which also includes results for shear modulus. Note that results for shear modulus of orthogonally cracked crossplies are not available in the literature.

Fig. 9 shows analytical results for reduction of Young's modulus of singly cracked  $[0^\circ/90^\circ]$ <sub>s</sub> glass/epoxy, [9], and experimental results for this case from [13], demonstrating excellent agreement. Fig. 10 shows stresses near an isolated crack in 90° ply for  $[0^\circ/90^\circ]$ <sub>s</sub> T300/epoxy and Fig. 11 for the same material when the cracks are close enough to interact significantly. It is seen that in the first case the tensile stress  $\sigma_{xx}$  builds up to its initial value in the uncracked laminate. But in the second case it cannot do so because of crack proximity. Therefore a significant portion of ply tensile force must now be carried by interlaminar shear stress and this will ultimately result in delamination. Also note the tensile interlaminar stress at mid-distance between cracks which may also produce delamination.

Young's moduli of orthogonally cracked laminates are only insignificantly affected by the crack family in load direction. Thus to all practical purposes they are the same as in the previous case when only the 90° ply is cracked. The Poisson's ratios, however, are significantly different in the two cases of one or two crack families as is shown in Fig. 12. Fig. 13 shows maximum values of in-plane tensile stress  $\sigma_{xx}$ , principal interlaminar shear stress and of tensile  $\sigma_{zz}$  on  $[0^\circ/90^\circ]$ <sub>s</sub> laminate midplane as function of crack density. It is assumed that all cracks are equidistant and that crack density is the same in both plies. The ply material is T300/epoxy and stress values are normalized by the tensile  $\sigma_{xx}$  ply stress of the uncracked laminate. Note the large value attained by  $\sigma_{zz}$  which is bound to produce cracking on the laminate midplane. Such cracks are similar to interlaminar damage discussed in Section 2.

Analysis of singly cracked cross-plies [9] has shown that elastic properties approach asymptotic limits with increasing crack density. Such limits indicated by superscripts  $\ell$  are shown below

Material	Glass/Epoxy		Graphite/Epoxy	
Configuration	$[0/90]_s$	$[0/90_s]_s$	$[0/90]_s$	$[0/90_s]_s$
$E_x^\ell / E_{xy}^0$	.770	.522	.970	.914
$G_{xy}^\ell / G_{xy}^0$	.500	.250	.500	.250

Note that Young's modulus reduction of graphite/epoxy cannot be large. This is due to the large ratio between axial and transverse Young's moduli for this material. Results for orthogonal cracking are practically the same. The situation is very different for the shear modulus. Results for orthogonal cracking are unfortunately not available in this case.

We now turn to numerical methods for cracked laminate analysis. It is evidently impractical to consider the case when cracks are not equidistant for this would require an enormous computer program. It is for this reason that all numerical methods for composites are based on idealized periodic models. For example, unidirectional fiber composites have been modeled as periodic hexagonal arrays of identical circular fibers. The central task is then to formulate the boundary conditions on the surface of the repeating element and this can only be done from symmetry considerations.

Consider for example the orthogonally cracked laminate of Fig. 7. In the event that the two crack families are equidistant the repeating element is as

shown in Fig. 8. When such a laminate is loaded by constant biaxial membrane forces all the faces of the repeating element and also its midplanes are planes of symmetry. It is convenient for our purpose to choose as repeating element the region  $0 \leq x \leq a$ ;  $0 \leq y \leq b$ ;  $0 \leq z \leq h$ . It follows that the shear stresses must vanish on all faces, providing two boundary conditions on each face. The third condition for each face is as follows: planes  $x,y,z=0$ , normal displacement component vanishes; plane  $z=h$ , normal stress vanishes; planes  $x=a$ ,  $y=b$ , normal stress vanishes on cracked part, normal components of displacement constant, equal  $\delta_1$ ,  $\delta_2$ , say, on uncracked parts.

Now define the two boundary problems

$$u_x(a,y,z) = 1 \quad t \leq z \leq h \quad u_x(a,y,z) = 0 \quad t \leq z \leq h \quad (14)$$

$$u_y(x,b,z) = 0 \quad 0 \leq z \leq t \quad u_y(x,b,z) = 1 \quad 0 \leq z \leq h$$

while all other listed boundary conditions remain the same. The elasticity solutions of these problems, satisfying all required traction and displacement continuity conditions on the interface  $z=t$ , may be found numerically and are labeled by superscripts I and II. It follows from linearity that the fields in the repeating element are given by

$$\underline{u} = \delta_1 \underline{u}^I + \delta_2 \underline{u}^{II} \quad \underline{\sigma} = \delta_1 \underline{\sigma}^I + \delta_2 \underline{\sigma}^{II} \quad (15)$$

In order to determine the quantities  $\delta_1, \delta_2$  consider the loading  $\bar{\sigma}_{xx}$ ,  $\bar{\sigma}_{yy}$  on the laminate edges. Then it is easily shown that

$$\delta_1 \bar{\sigma}_{xx}^I + \delta_2 \bar{\sigma}_{xx}^{II} = \bar{\sigma}_{xx}$$

(16)

$$\delta_1 \bar{\sigma}_{yy}^I + \delta_2 \bar{\sigma}_{yy}^{II} = \bar{\sigma}_{yy}$$

where overbars on the right side denote averages over the repeating element which are known from the numerical solution. This completes the field solution and effective properties can now be determined by relation of stress to strain averages of repeating element.

Note that this procedure is by no means restricted to cross-ply. Fig. 14 shows a repeating element for a  $[0_m^0/n^0/-0_n^0]$  laminate which is biaxially loaded and which has symmetric interlaminar crack distributions within the  $\pm 0^\circ$  plies. This can be formulated by similar symmetry arguments and the basic solutions I and II must now satisfy zero traction boundary conditions on internal crack surfaces. But the problem posed is very complex even from a numerical point of view since the material axes of the plies and the cracks are now at different non-orthogonal directions. Note that the finite elements must be suitable to model the edges and the cracks and in addition must have congruent faces across ply interfaces because of required satisfaction of continuity conditions at these locations.

Numerical work which has appeared in the literature has been restricted to singly and orthogonally cracked cross-ply. Altus and Ishai [2] have presented a finite difference analysis of singly cracked cross-ply and have given results for in plane - normal stress only. Similar analysis and results have been obtained by Wang [31] by use of finite elements. Highsmith and Reifsnider [14] have performed a numerical analysis of orthogonally cracked cross-ply under tension on the basis of a higher order laminate theory which is due to Pagano [20], which assumes linear variation of stress through ply

thickness. This is not unlike the variational method which is also based on gentle through-thickness stress variation, which in view of the two methods are in many respects similar, but the computational effort required by the numerical work is higher by order of magnitude.

### 3.2. Thermal Effects

Temperature changes are a major cause of interlaminar damage. Consider for example the case of temperature change of a  $[0^\circ/90^\circ]_s$  laminate. Cooling of the laminate produces compressive stresses in fiber direction and tensile stresses transverse to the fibers, of equal magnitude, in the plies. Since transverse tensile strength is much lower than axial compressive strength the first damage to appear is intralaminar cracking of all plies, thus orthogonal cracking. We note in passing that all laminates which are thermally isotropic, thus  $[0^\circ/90^\circ]_s$ ,  $[0^\circ/90^\circ/45^\circ/-45^\circ]_s$ ,  $[0^\circ/60^\circ/-60^\circ]_s$ , develop the same thermal stresses and therefore the same interlaminar cracking of all plies. It is important to realize that when a laminate is heated the signs of ply stresses reverse; the fiber direction stress is tensile and the transverse stress is compressive. Therefore heating does not produce interlaminar cracking.

The effective thermal expansion coefficients (ETEC)  $\alpha_{ij}^*$  of any heterogeneous body are defined by the relation

$$\bar{\epsilon}_{ij} = \alpha_{ij}^* \theta \quad (17)$$

where  $\bar{\epsilon}_{ij}$  are the average strains produced by the temperature change  $\theta$ . Note that (17) merely states that the average strains are proportional to the temperature change. It follows at once that the ETEC of a cracked laminate may be determined by evaluation of the average strains due to temperature

change in such a laminate. This is a very difficult problem of thermoelasticity and it can fortunately be avoided.

To see this consider a cracked laminate which is subjected to constant membrane load and to temperature change. In this case the average strains are the sum of (1) and (17). Denoting the internal stresses due to load alone as  $\sigma_{ij}^s$  and the stresses due to unit temperature change alone by  $\sigma_{ij}^t$  we have from superposition

$$\sigma_{ij} = \sigma_{ij}^s + \theta \sigma_{ij}^t \quad (18)$$

Levin [18] has proved a remarkable theorem which states

$$\int_V a_{ij}(x) \sigma_{ij}^s(x) dV = a_{ij}^* \bar{\sigma}_{ij} V \quad (19)$$

It is seen that the ETEC are determined in terms of the known constituent thermal expansion coefficients and the stresses due to mechanical load. The remarkable aspect of the theorem is in that the thermal stresses do not enter. Now the mechanical stresses have been discussed before and it is thus seen that stress analysis of a loaded cracked laminate, whether analytical or numerical, also provides the ETEC.

The relation (19) has been exploited in [11] to obtain in simple fashion the ETEC of an orthogonally cracked cross-ply, using for  $\sigma_{ij}^s$  the approximate variational stresses obtained in [10]. Fig. 15 shows the variation of ETEC with crack density for T300/Epoxy plies, assuming equal crack density in all plies. Also shown are results when only one kind of plies is cracked. It is

seen that ETEC diminish substantially with increasing crack density and that they approach asymptotically, the fiber direction TEC of the ply. This last result has been proved analytically [11] and its physical interpretation is as follows: for large crack density the plies lose their transverse stiffness ( $E_T=0$ ) and therefore the  $90^\circ$  plies no longer affect the axial expansion of the  $0^\circ$  plies.

Loading and/or temperature change produce either tensile or compressive transverse stresses in the plies. The former open cracks while the latter close existing cracks. This produces complex thermo-elastic behavior since there are several possibilities: all cracks open, some cracks open and all cracks closed. In the last case the ETEC are simply those of the uncracked laminate. Fig. 16 shows schematically possible values of ETEC for combination of uniaxial load (tension or compression) and temperature change (heating or cooling), [11].

Adams and Herakovich [1] and Herakovich and Hyer [12] have performed numerical analysis based on finite elements to obtain ETEC of cross-ply in which the  $90^\circ$  plies are cracked. They also obtained significant reduction of ETEC with increasing crack density.

### 3.3. Damage Prediction. Failure Analysis.

So far we have considered the problem of the relation of properties to damage in the form of crack density. Since crack density is not easily measured it is natural to inquire if it can be analytically predicted. Initial attempts to do this [24,25] were based on the assumption that cracks will form saturation patterns (characteristic damage state) at intercrack distances which are large enough to neglect crack interaction. But later analytical and experimental evidence does not seem to support this assumption. The analysis given in [9] for the singly cracked cross-ply, while approximate, is certainly

much more accurate than the simple shear lag approach. According to this analysis crack interaction effects can be disregarded when the ratio of crack interdistance to 90° ply thickness,  $\rho$  say, is larger than 4. But according to experiments reported in [13] for glass/epoxy cross-ply  $[0^\circ/90^\circ]_s$  and  $[0^\circ/90^\circ]_s$  the value of  $\rho$  is as low as 1.1 and is between the values 1.1 and 1.6 for substantial ranges of the intralaminar cracking process. But at such low values of  $\rho$  interaction between cracks is very significant.

Very simple analytical considerations show that the highest in-plane stress  $\sigma_{xx}$  in load direction in the cracked 90° ply is midway between cracks. It would thus be tempting to create a very simple model of crack-density to load relation according to which, with the help of the analysis of [9], formation of new cracks would occur when the load is large enough for the mid-crack stress to attain the transverse tensile failure stress of the ply. But the realism of such a procedure is doubtful since the failure stress is generally not some definite number but a random variable the reason for that being that formation of a crack is due to a local micro-defect and is thus a random event whose probability increases with increasing stress. Therefore probability of occurrence of a new crack in the region between two existing ones depends not only on the value of maximum stress but also on its variation in the interval. Analysis requires assumption of some form of probability function. An example of such work is given in [2] which also cites previous work on this subject.

Everything discussed so far is based on the simplification of constant through-thickness in-plane stress or in other words: the important quantity in a thin ply is the in-plane force. If the ply is thick, stress variation through the thickness can become important and a more refined approach may be needed. Wang [30] has considered this problem in terms of critical flaws in the form

of transverse micro-cracks whose lengths may be much smaller than ply thickness. This approach requires intricate numerical analysis combining crack criticality and probability concepts. Monte Carlo simulation of intralaminar crack density in singly cracked graphite/epoxy cross-ply, produced by static load was found to be in very good to reasonable agreement with experimentally determined crack density. But we should remember the thin ply problem difficulties discussed above. The implication for the present subject is that a transverse crack length must be much larger than UFC RVE in order to be amenable to fracture mechanics treatment and it would therefore seem that this approach should be confined to plies which are sufficiently thick.

It is at present an open question whether damage prediction methods can be carried beyond the simple case of single ply cracking and whether they can develop into an engineering tool.

The problem of damage prediction becomes even more difficult with crack saturation and the development of interlaminar damage. If one adopts the point of view that the opening of interlaminar cracks is a problem which is governed by the laws of classical fracture mechanics, then it becomes necessary to formulate a criterion for interlaminar crack criticality and to employ it to predict branching of intralaminar cracks into the interface. If there are intralaminar cracks in neighboring plies, e.g. orthogonal cracks in a cross ply, the crossing points of cracks in the different plies become sources of intralaminar damage. A numerical finite element procedure for such delamination problems has been reported in [31].

We should remember, that as discussed above, finite elements can not be as small as "we please; they must be large enough to represent the ply properties and this is a problematic limitation on such numerical analyses.

Given the severe complexities of damage and failure prediction in terms of micro-analysis and adding the fundamental difficulty of finite element size limitation it would appear to us that an engineering tool for damage and failure prediction could hardly be formulated on the basis of MIDM alone and, as we have said in the beginning, a complementary combined MIDM - MADM is needed. A simple example of such an approach is provided by the work of Poursartip et al. [22] who have developed a method to evaluate the fatigue life of a laminate by description of damage evolution as a continuum damage process, thus MADM, where the necessary ingredient to perform the analysis is the stiffness reduction of the laminate, which can be obtained by MIDM methods. Further interesting developments in such directions, within the context of fatigue of laminates, can be found in [19,23].

#### 4. Conclusion

Most of our discussion has been concerned with damage mechanics of fiber composite laminates, a subject of significant engineering importance. Most of the work discussed has been of MIDM nature since most of the literature on laminate damage has been based on this approach. It may be mentioned that, in contrast, most of the work on metal damage has followed the MADM or continuum approach. The reason, we believe, is in that the internal damage geometry of laminates is very much simpler than in metals, where one has to deal with irregular grain boundaries.

Even so the micro-analysis problems which must be solved are very complex, and assume increasing complexity with advancing stage of damage and with engineering realism of loading patterns and laminate stacking sequence. It is therefore not surprising that most of the literature has been concerned with analysis of symmetric cross-ply, the simplest laminates in existence.

Apart from the mathematical difficulties arising in problems which involve many interacting cracks there are difficulties of even more fundamental nature. These have been brought out in our discussion of the thin ply problem and the associated difficulty of smallest permissible size of finite elements representing a heterogeneous medium. And there is also the question to what extent are micro-cracks in a composite amenable to treatment by classical fracture mechanics methods in terms of the effective elastic properties of same composite.

We would, in conclusion, venture the opinion that MIDM for damaged laminates should be pursued to the best of our ability, that MADM should be developed in concert with MIDM in order to deal with those cases which are too complicated for MIDM treatment and that efforts should be made to develop methods to deal with the fundamental difficulties outlined above.

#### Acknowledgement

Support by the Air Force Office of Scientific Research under contract 85-0342, Major George Haritos - contract monitor, is gratefully acknowledged.

## References

- 1 ADAMS D.S. and C.T. HERAKOVICH. - "Influence of damage on the thermal response of graphite-epoxy laminates", J. Thermal Stresses, 7 (1984) : 91-103.
- 2 ALTUS E. and O. ISHAI. - "Transverse cracking and delamination interaction in the failure process of composite materials", Composites Science & Technology, 26 (1986) : 59-77.
- 3 BODNER R.S. and Z. HASHIN, eds. - Mechanics of Damage and Fatigue, Proc. IUTAM Symposium, Haifa and Tel-Aviv, Israel, 1985. Pergamon Press, Engng. Fract. Mech., 25 (1986) : 603-67.
- 4 BUDIANSKY G.J. and R.J. O'CONNELL. - "Elastic moduli of a cracked solid", Int. J. Solids & Structures, 12 (1976) : 81-97.
- 5 DVORAK G.J. and N. LAWS. - "Analysis of matrix cracking in composite laminates: theory and experiment". in U. YUCEOGLU and R. HESSER, eds., Structures, Materials, Dynamics and Space Station Propulsion - AD-08, ASME (1984) : 69-78.
- 6 GOTTESMAN T., Z. HASHIN and M.A. BRULL. - "Effective elastic moduli of cracked fiber composites", in BUNSELL / et al. eds., Advances in Composite Materials, Proc. ICCM 3, Pergamon Press (1980) : 749-758.
- 7 HASHIN Z. - "Failure criteria for unidirectional fiber composites", J. Appl. Mech., 47 (1980) : 329-334.
- 8 HASHIN Z. - "Analysis of composite materials - a survey", J. Appl. Mech., 50 (1983) : 481-505.

- 9 HASHIN Z. - "Analysis of cracked laminates: a variational approach", Mechanics of Materials, 4 (1985) : 121-136.
- 10 HASHIN Z. - "Analysis of orthogonally cracked laminates under tension", J. Appl. Mech., (in press).
- 11 HASHIN Z. - "Thermal expansion coefficients of cracked laminates", Composites Science & Technology, (to appear).
- 12 HERAKOVICH C.T. and M.W. HYER. - "Damage induced property changes in composites subjected to cyclic thermal loading", in S.R. BODNER and Z. HASHIN, eds. Mechanics of Damage and Fatigue, Pergamon Press, Engng. Fract. Mech., 25 (1986) : 779-791.
- 13 HIGHSMITH A.L. and K.L. REIFSNIDER. - "Stiffness-reduction mechanisms in composite laminates", in K.L. REIFSNIDER, ed., Damage in Composite Materials, ASTM STP 775, ASTM, (1982) : 103-117.
- 14 HIGHSMITH A.L. and K.L. REIFSNIDER. - "Internal load distribution effects during fatigue loading of composite laminates", in H.T. HAHN ed. Composite Materials: Fatigue and Fracture, ASTM STP 907, ASTM 9 (1986) : 233-251.
- 15 JAMISON R.D. - "The role of microdamage in tensile failure of graphite/epoxy laminates", Composites Science and Technology, 24 (1985): 83-100.
- 16 JAMISON R.D., K. SCHULTE, K.L. REIFSNIDER and W.W. STINCHCOMB. - "Characterization and analysis of damage mechanisms in tension-tension fatigue of graphite/epoxy laminates", in D.J. WILKINS, ed. Effects of Defects in Composite Materials, ASTM STP 836, ASTM (1984) : 21-55.
- 17 LAWS N., G.J. DVORAK and M. HEJAZI. - "Stiffness changes in unidirectional

composites caused by crack systems",, Mechanics of Materials, 2 (1983) : 123-137.

18 LEVIN V.M. - "On the coefficients of thermal expansion of heterogeneous materials", Mekhanika Tverdogo Tela, 1 (1967) 88-94. English translation, Mechanics of Solids, 2 (1967) : 58-61.

19 OGIN S.L., P.A. SMITH and P.W.R. BEAUMONT. - "Matrix cracking and stiffness reduction during the fatigue of a [0/90]<sub>s</sub> GFRP laminate", Composites Science and Technology, 22 (1985) : 23-32.

20 PAGANO N.J. - "Stress fields in composite laminates", Int. J. Solids & Structures, 14 (1978) : 385-400.

21 PHOENIX S.L. - "Statistical aspects of failure of fibrous materials", in S.W. TSAI, ed., Composite Materials: Testing and Design, ASTM STP 674, ASTM, (1979) : 455-483.

22 POURSARTOU A., M.F. ASHBY and P.W.R. BEAUMONT. - "Damage accumulation in composites during fatigue", in H. LILHOLT and R. TALREJA, eds., Fatigue and Creep of Composite Materials, RISO Nat. Lab., Roskilde, Denmark, (1982) : 279-284.

23 POURSARTIP A., M.F. ASHBY and P.W.R. BEAUMONT. - "The fatigue damage mechanics of a carbon fiber composite laminate", Pts.I & II, Composites Science and Technology, (1986) : 193-218, 283-300.

24 REIFSNIDER, K.L. - "Some fundamental aspects of the fatigue and fracture response of composite materials", in Proc. 14th Ann. Meeting Soc. Engng. Science, Lehigh University, (1977).

25 REIFSNIDER, K.L. - "Analysis of fatigue damage in composite laminates", Int. J. Fatigue, 3 (1980) : 3-11.

- 26 REIFSNIDER, K.L. and R. JAMISON. - "Fracture of fatigue loaded composite laminates", Int. J. Fatigue, 5 (1982) : 187-197.
- 27 ROSEN, B.W. - "Tensile failure of fibrous composites", AIAA J., 2 (1964) 1985-1991.
- 28 STEIF P.S. - "Stiffness reduction due to fiber breakage", J. Composite Materials, 18 (1984) : 153-172.
- 29 TALREJA R. - "Stiffness properties of composite laminates with matrix cracking and interior delamination", in S.R. BODNER and Z. HASHIN eds., Mechanics of Damage and Fatigue, Pergamon Press, Engng. Fract. Mech., 25 (1986) : 751-762.
- 30 WANG, A.S.D. - "Fracture mechanics of sublamine cracks", Composite Technology Review, 6 (1984) : 45-62.
- 31 WANG A.S.D., N.N. KISHORE and C.A. LI. - "Crack development in graphite/epoxy cross-ply laminates under uniaxial tension", Composites Science and Technology, 24 (1985) : 1-31.

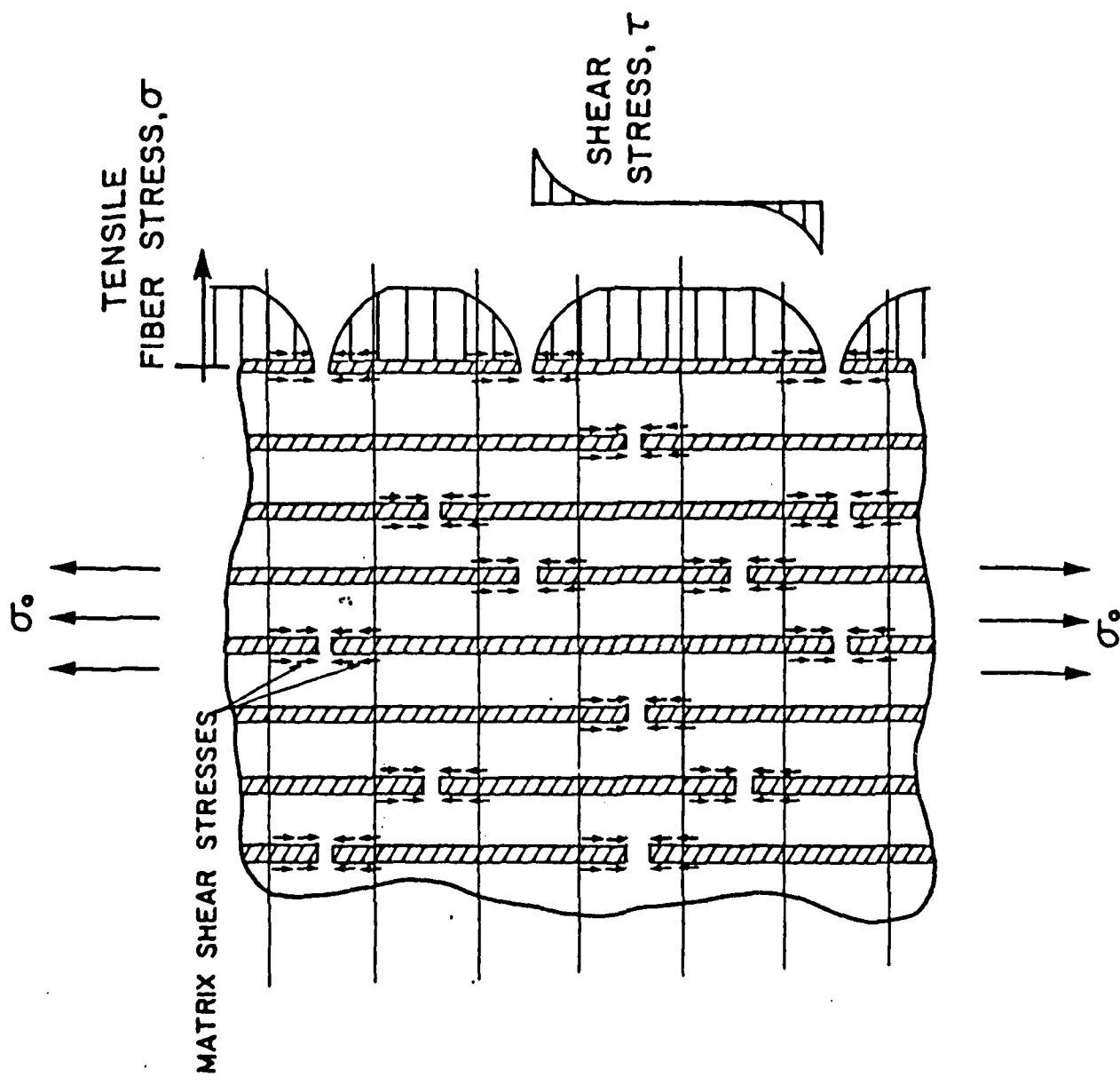


Fig. 1 - Fiber ruptures accumulation and shear stress concentrations

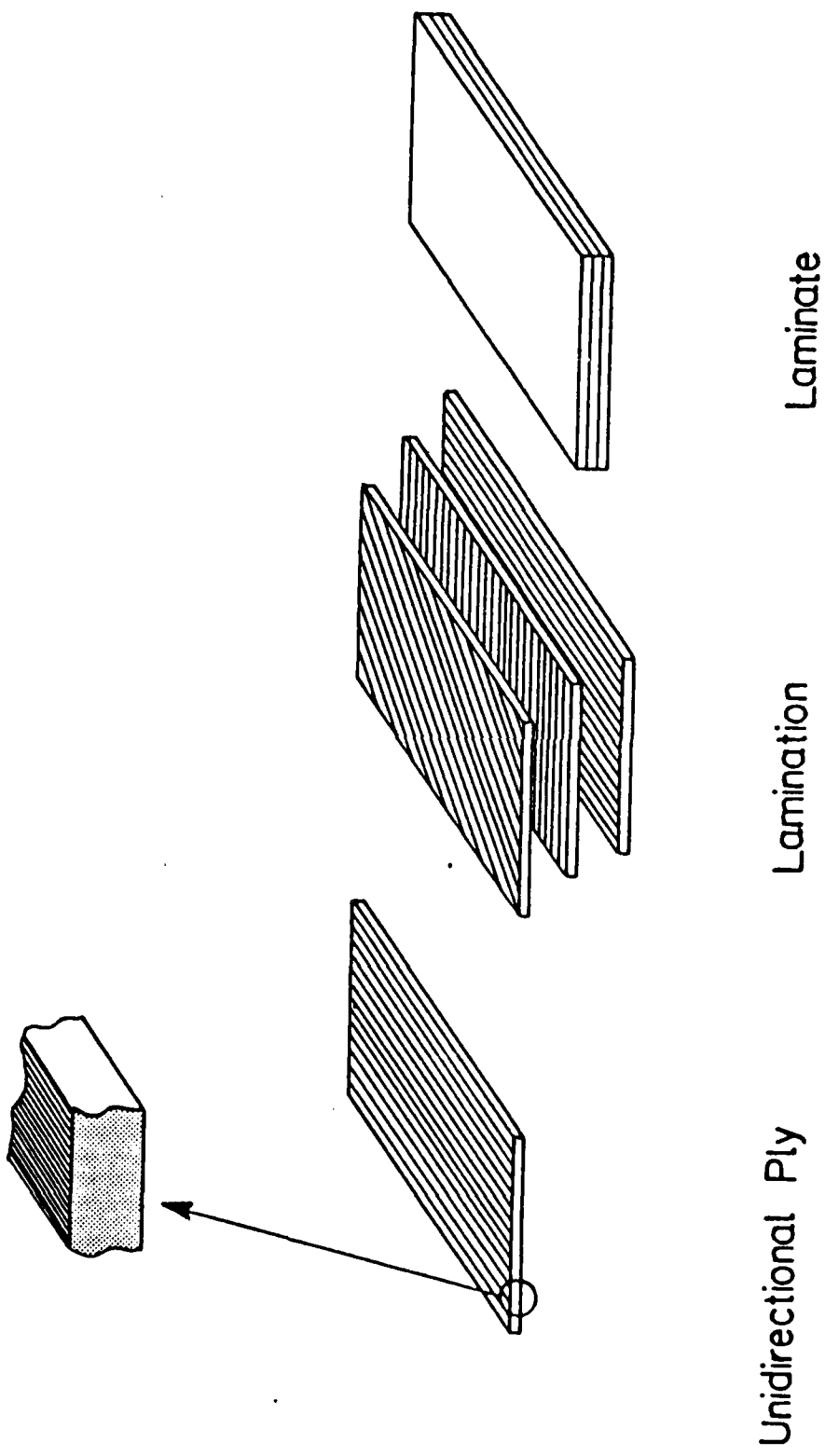


Fig. 2 - Laminate

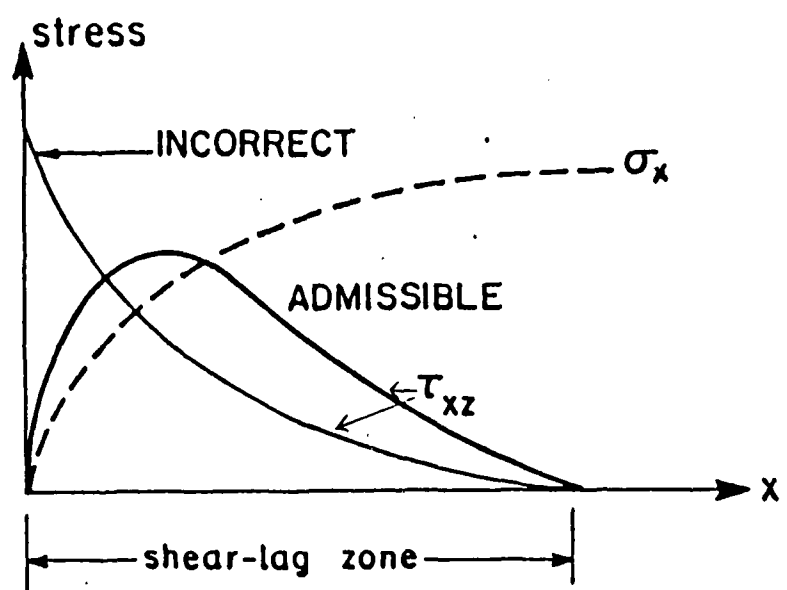
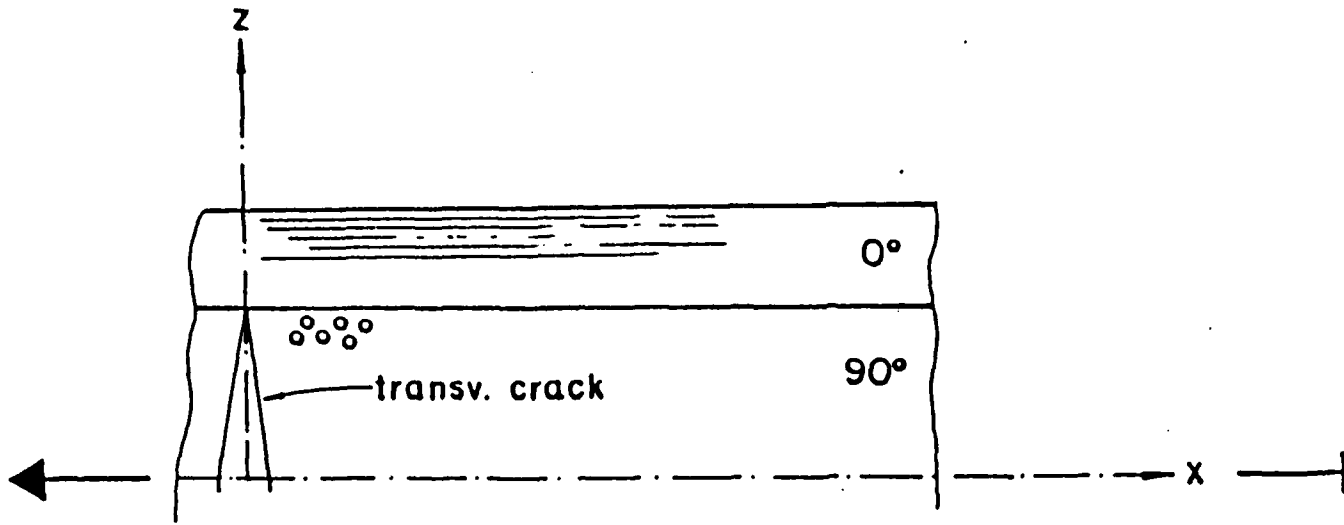


Fig. 3 - Stress variation near interlaminar crack

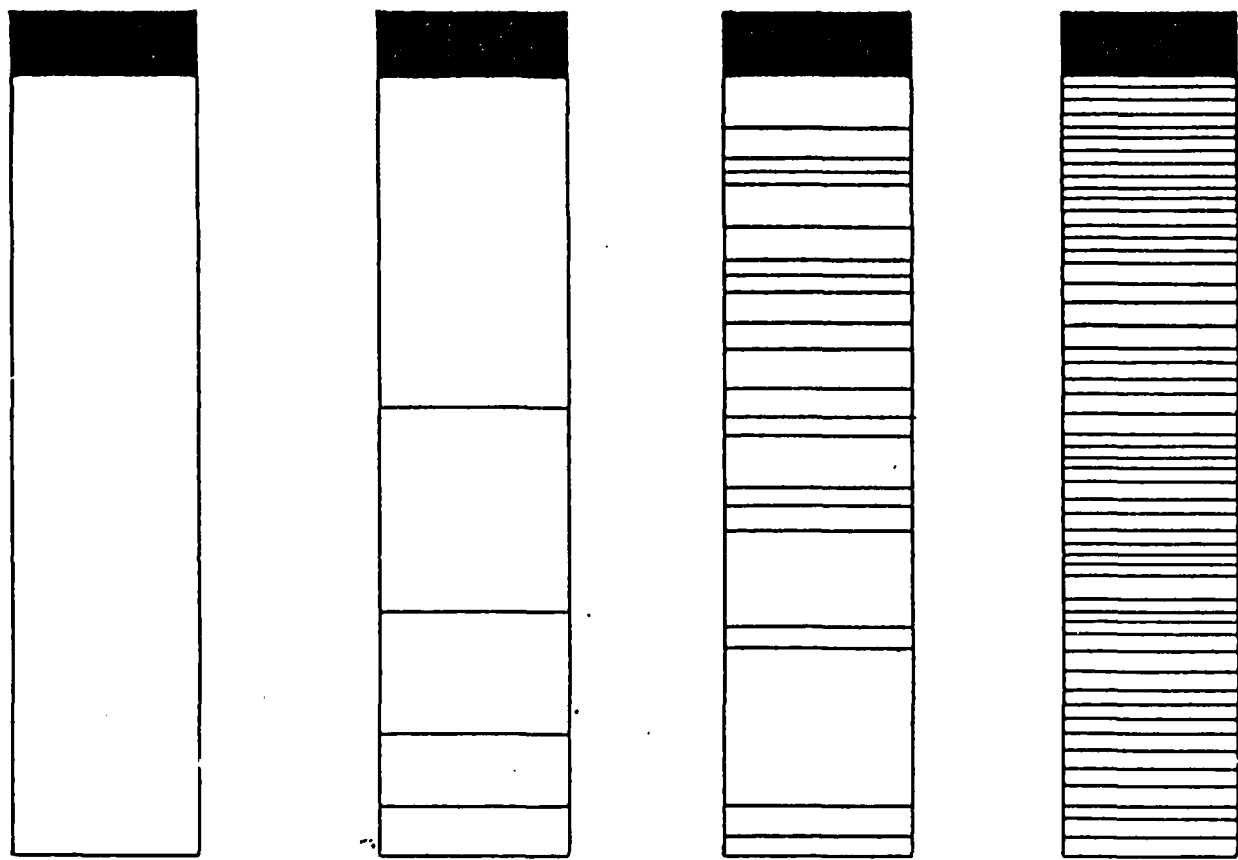


Fig. 4 - Interlaminar crack accumulation under tension (after Wang [30])

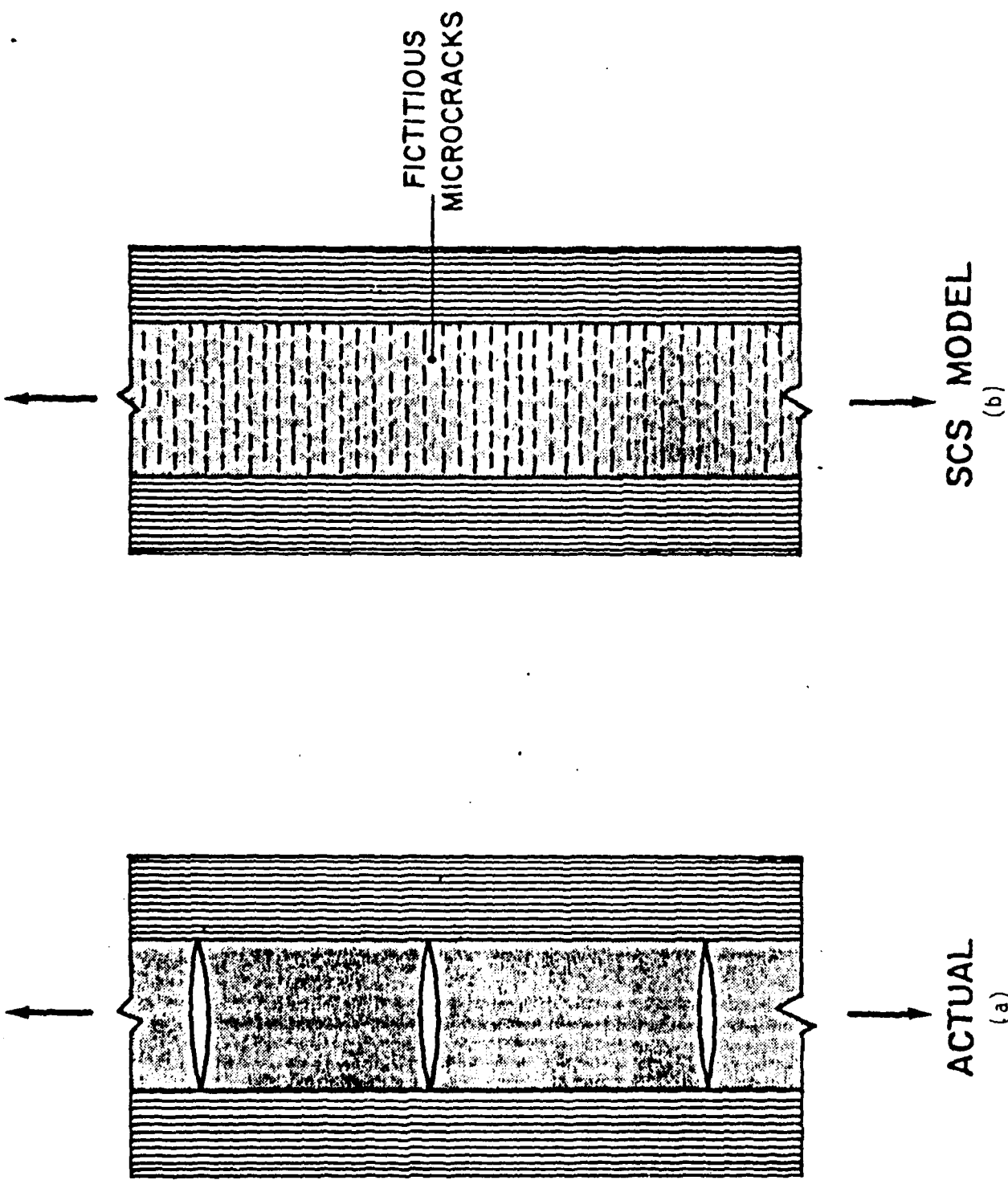


Fig. 5 - Interlaminar cracks: reality and SCS modeling

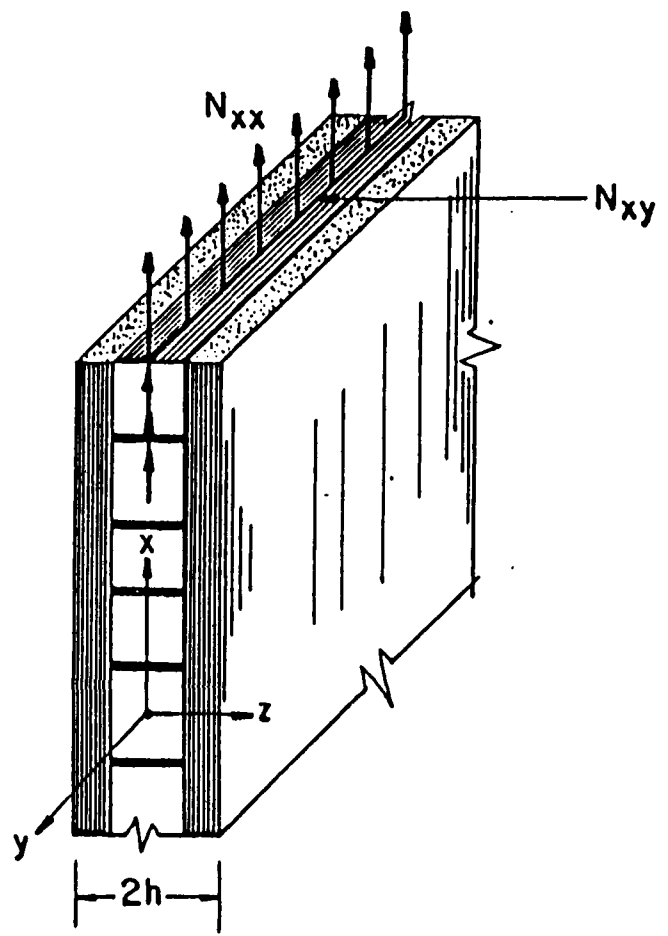


Fig. 6 - Singly cracked cross-ply

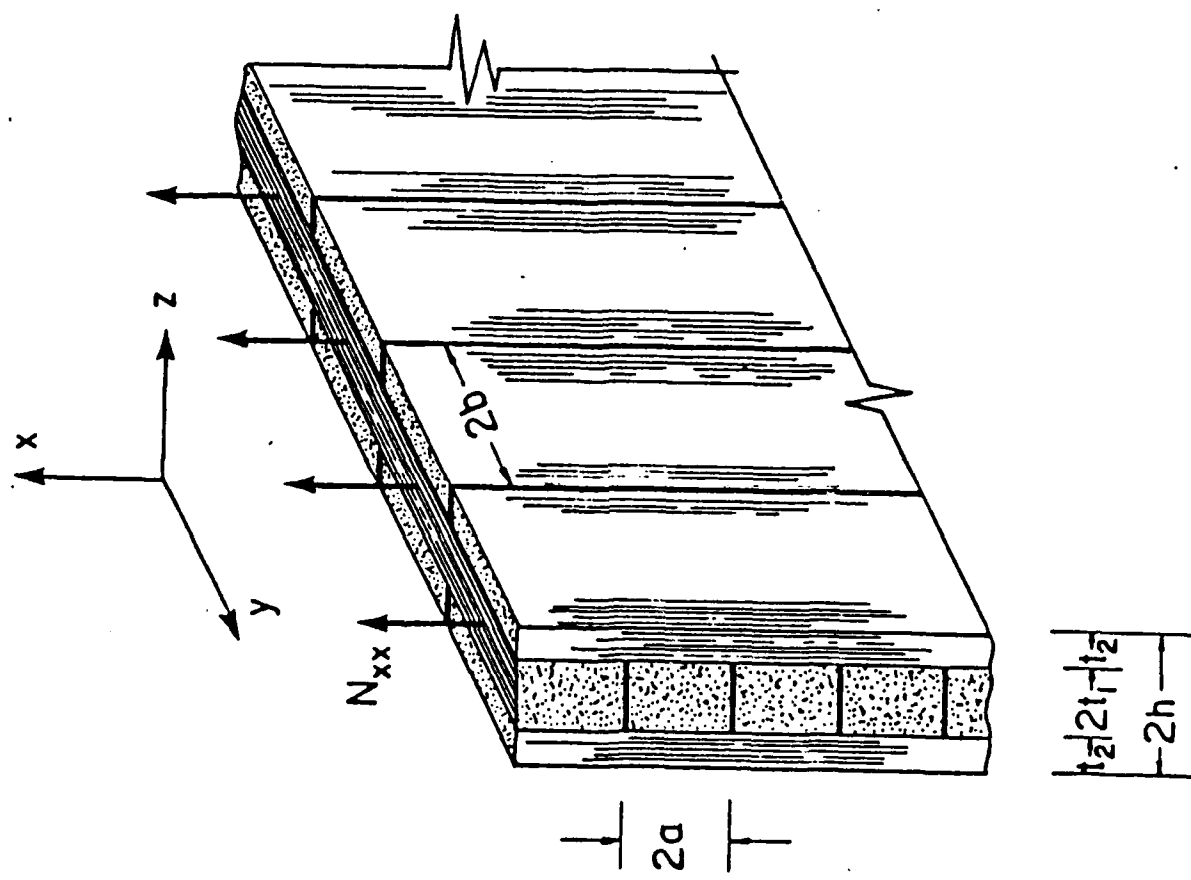


Fig. 7 - Orthogonally cracked cross-ply

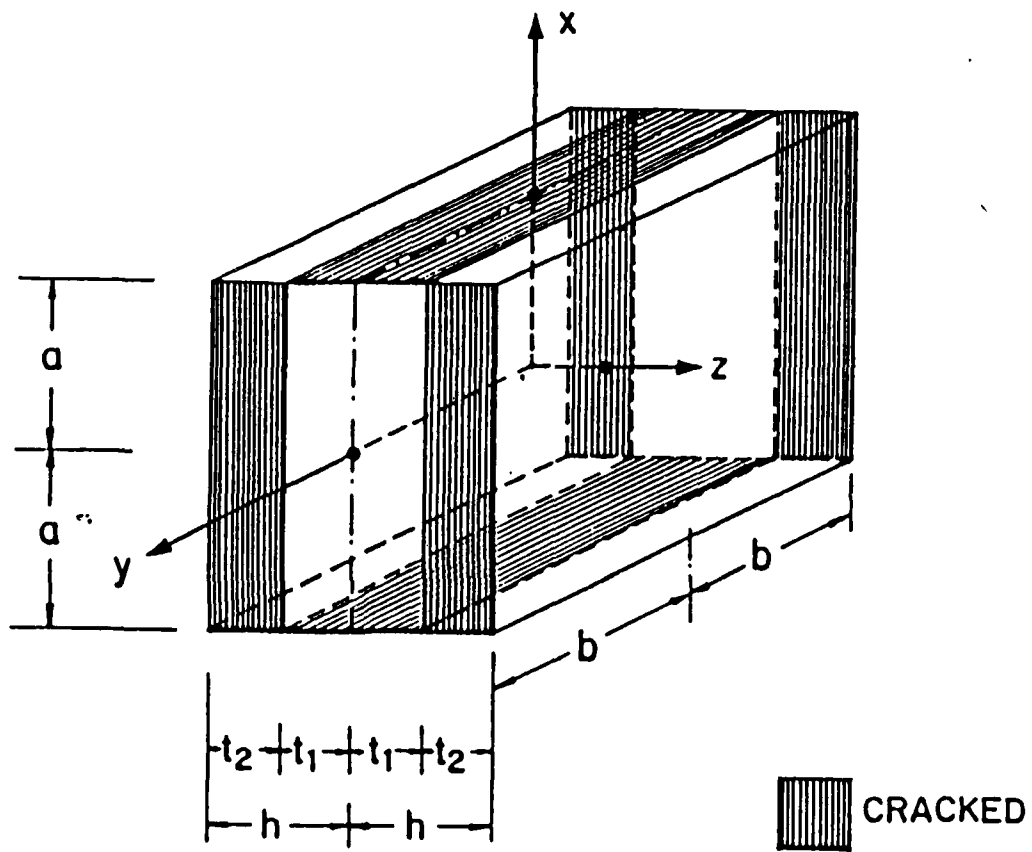


Fig. 8 - Typical or repeating element

STIFFNESS REDUCTION OF  $[0^\circ/90^\circ]$ <sub>s</sub>  
 GLASS/EPOXY LAMINATE ONLY 90° CRACKED

$E_x^\circ$  YOUNG'S MODULUS OF UNDAMAGED LAMINATE

$E_x$  YOUNG'S MODULUS OF CRACKED LAMINATE

○ EXPERIMENTAL, HIGHSMITH & REIFSNIDER [13]

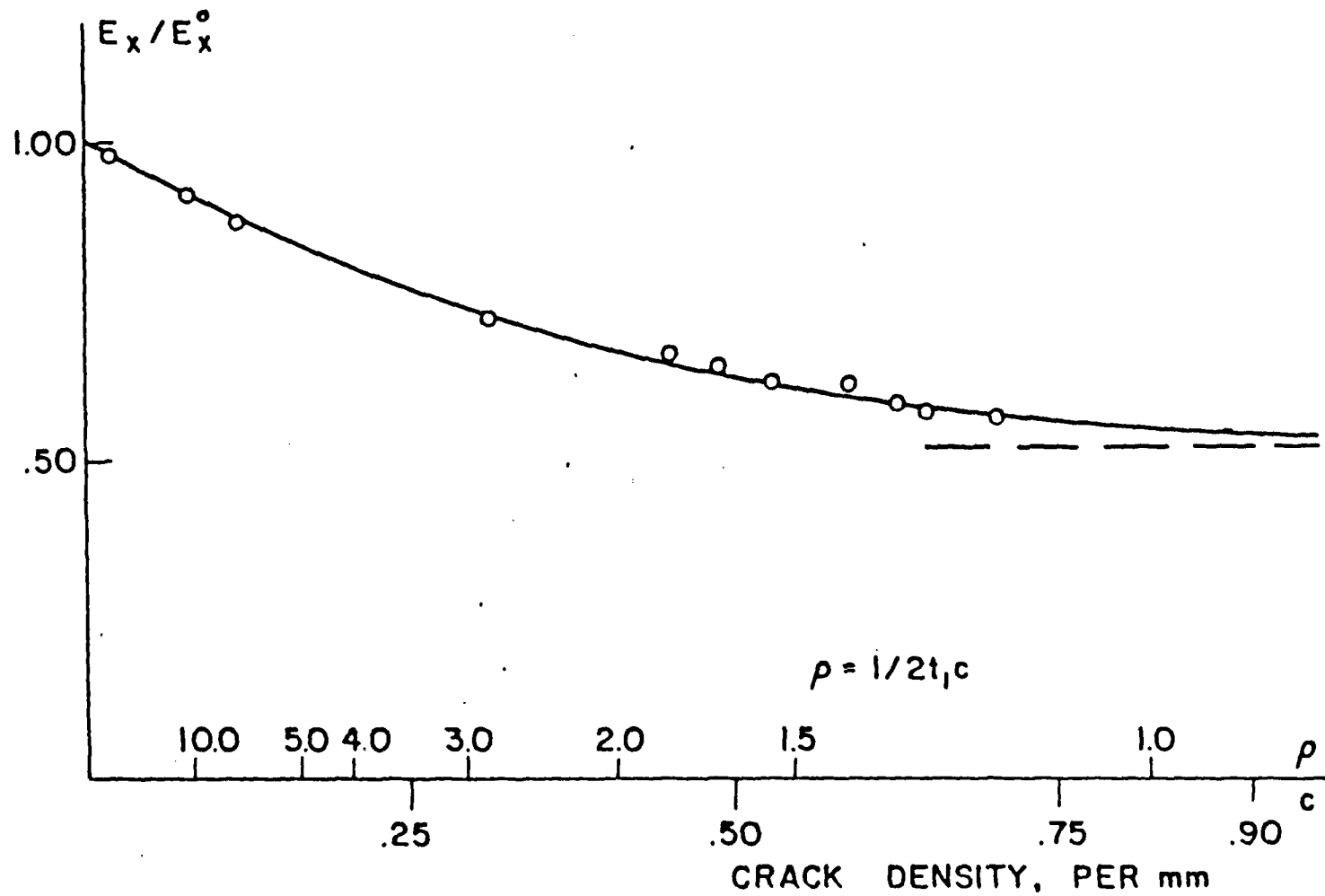


Fig. 9 - Stiffness reduction of  $[0^\circ/90^\circ]$ <sub>s</sub> glass/epoxy laminate: theory and experiment

STRESSES AT INTERACTING CRACKS  
 $[0^\circ/90^\circ]_s$  GRAPHITE / EPOXY LAMINATE - UNIAXIAL TENSION

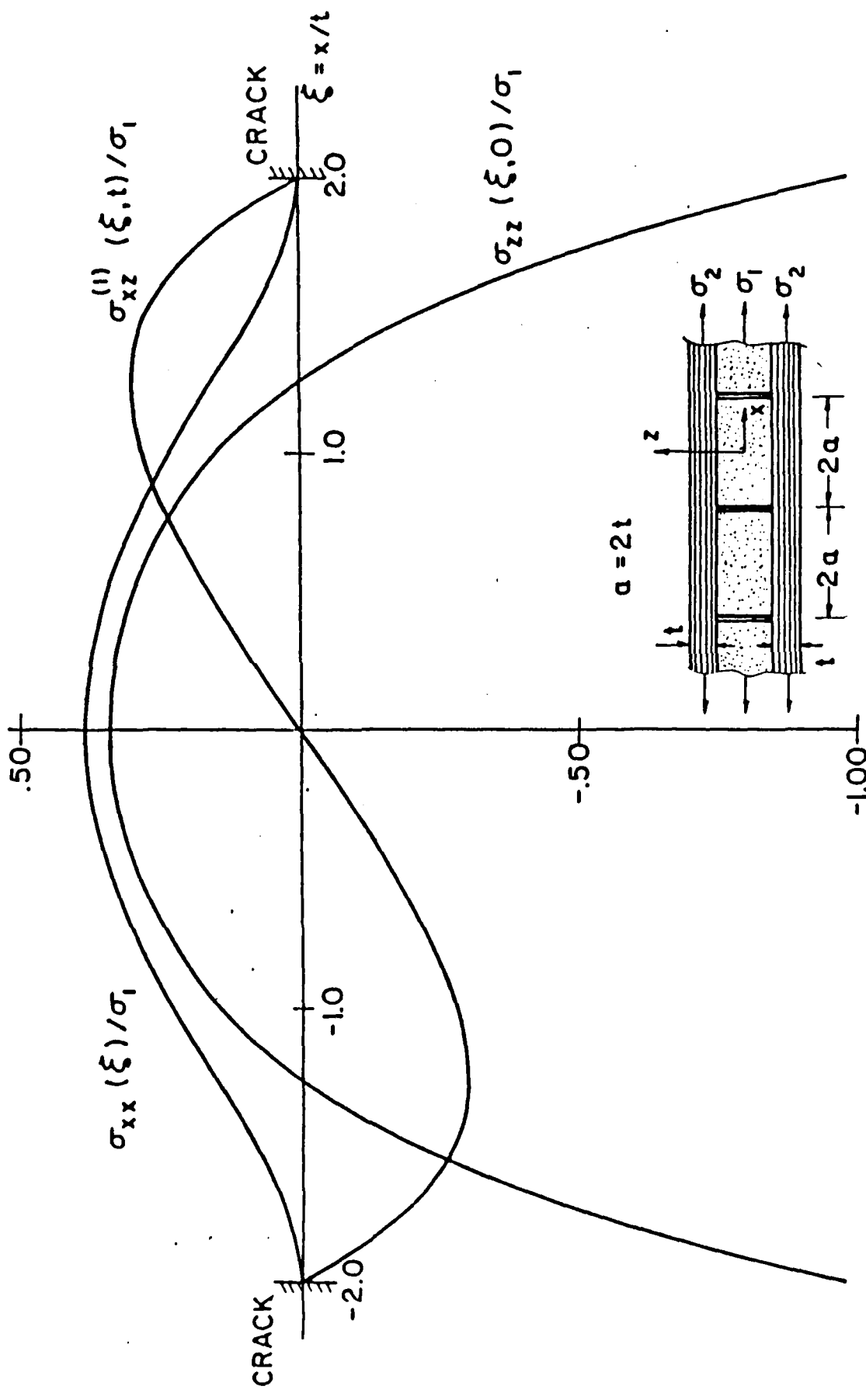


Fig. 11 - Stresses near interacting interlaminar cracks; graphite/epoxy  $[0^\circ/90^\circ]_s$

POISSON'S RATIO  $\nu_{xy}$   
 GRAPHITE/EPOXY  $[0^\circ/90^\circ]_s$

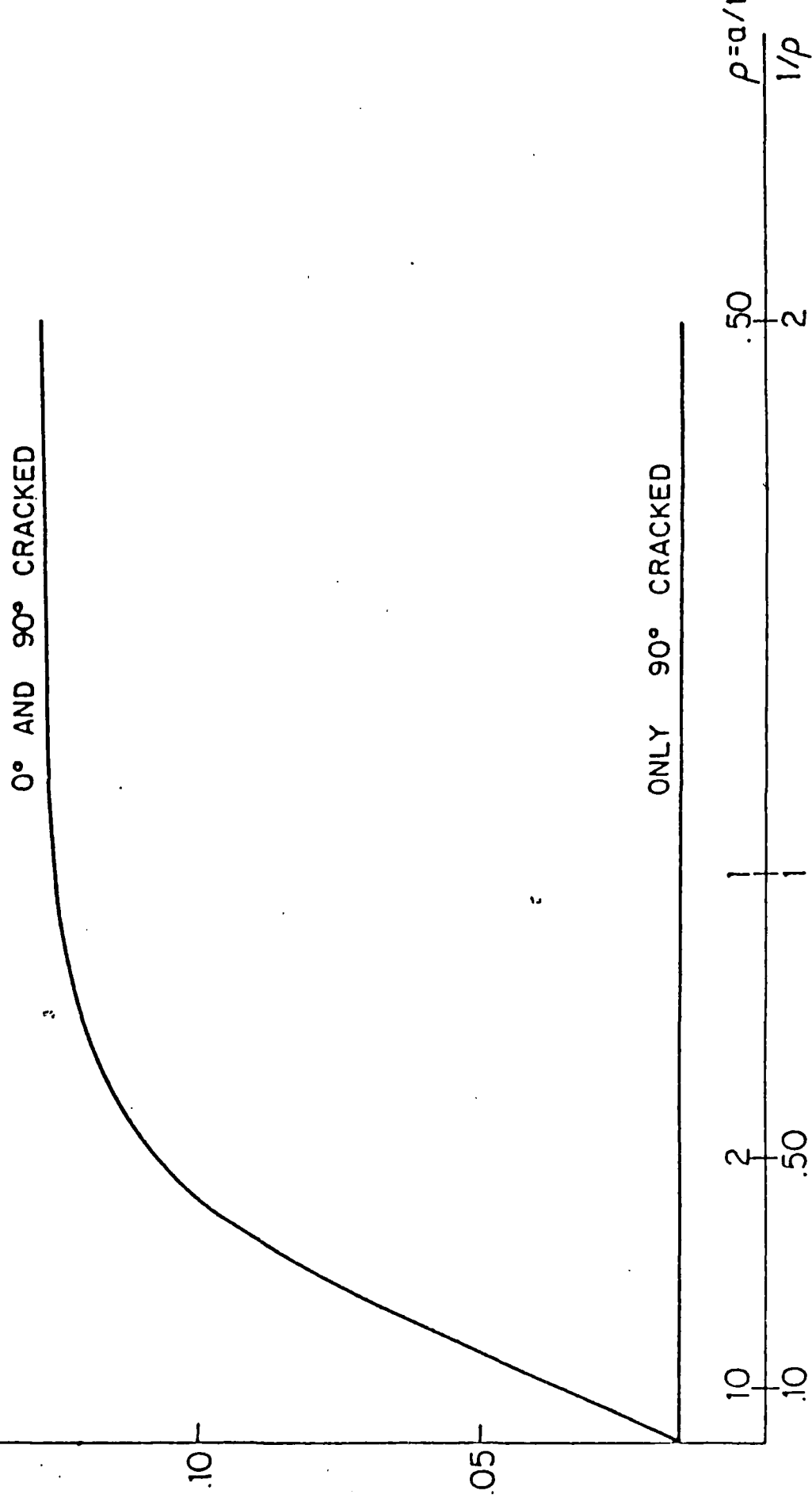


Fig. 12 - Variation of Poisson's ratio with crack density; singly and orthogonally cracked graphite/epoxy  $[0^\circ/90^\circ]_s$

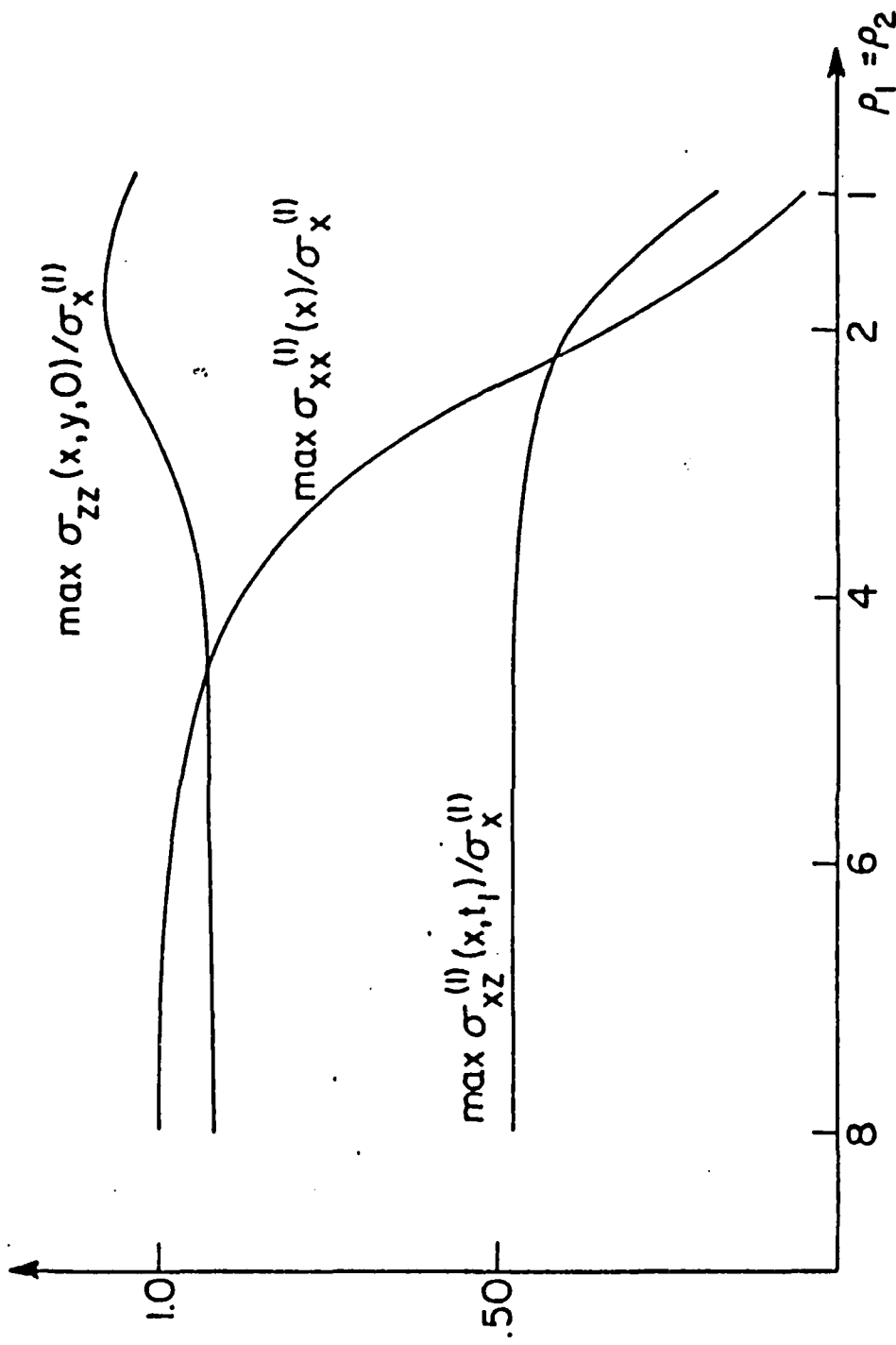


Fig. 13 - Maximum stresses versus crack density of orthogonally cracked graphite/epoxy [0°/90°]s

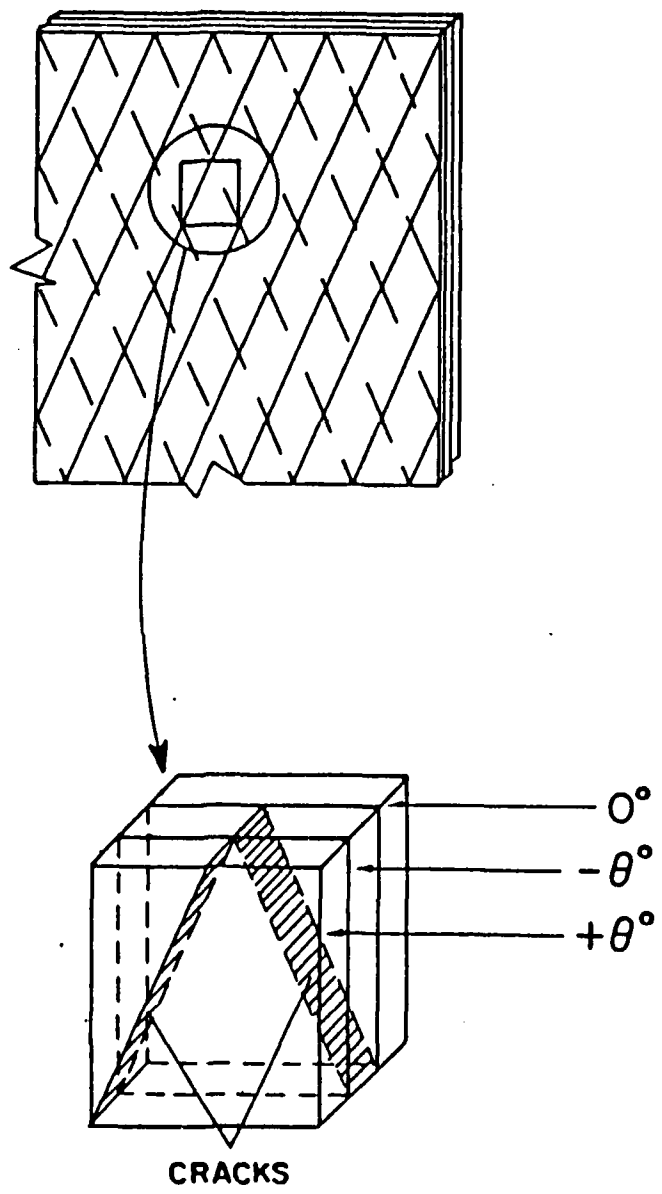


Fig. 14 - Repeating element for  $[0^\circ/0^\circ/-\theta^\circ]_S$

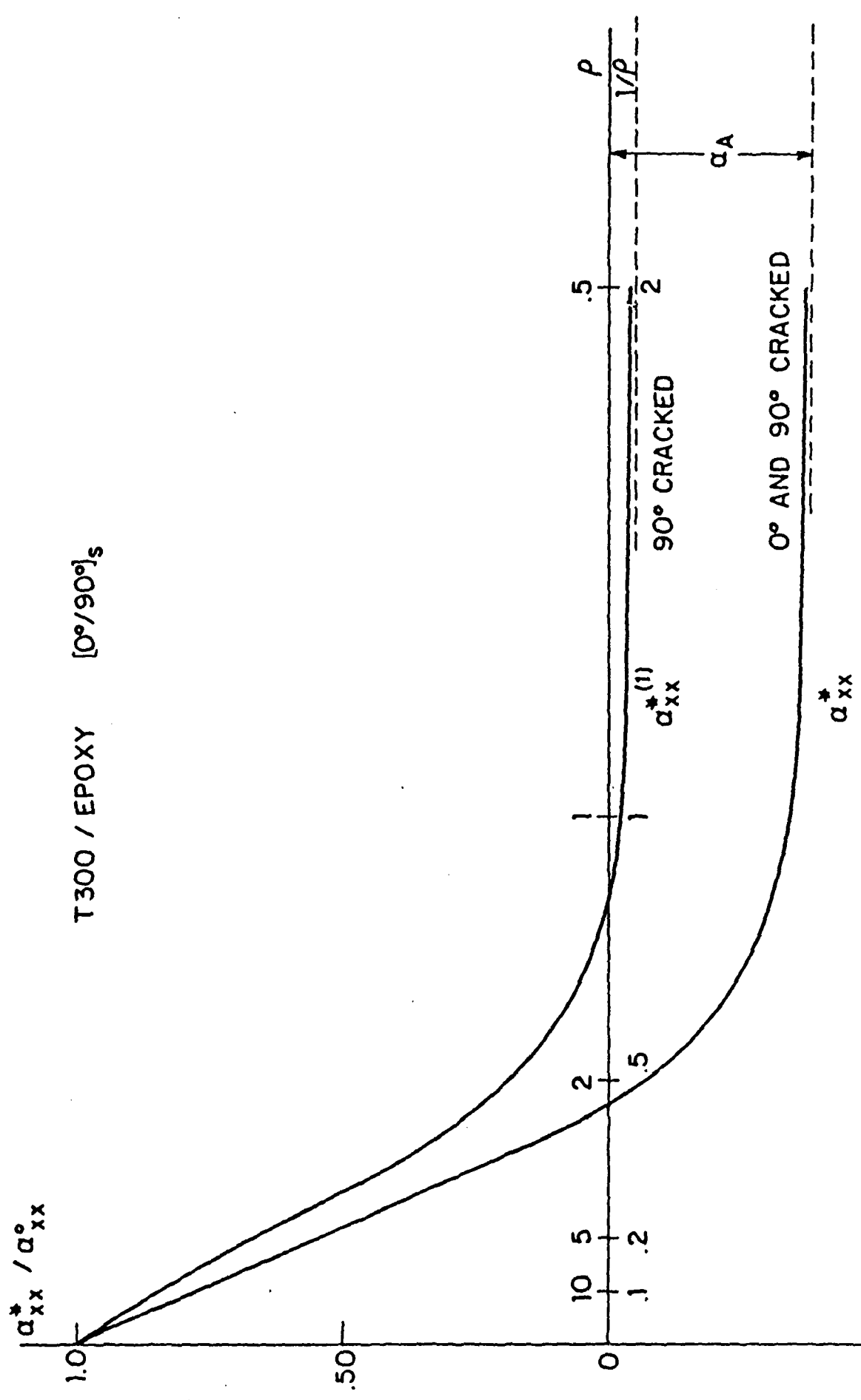
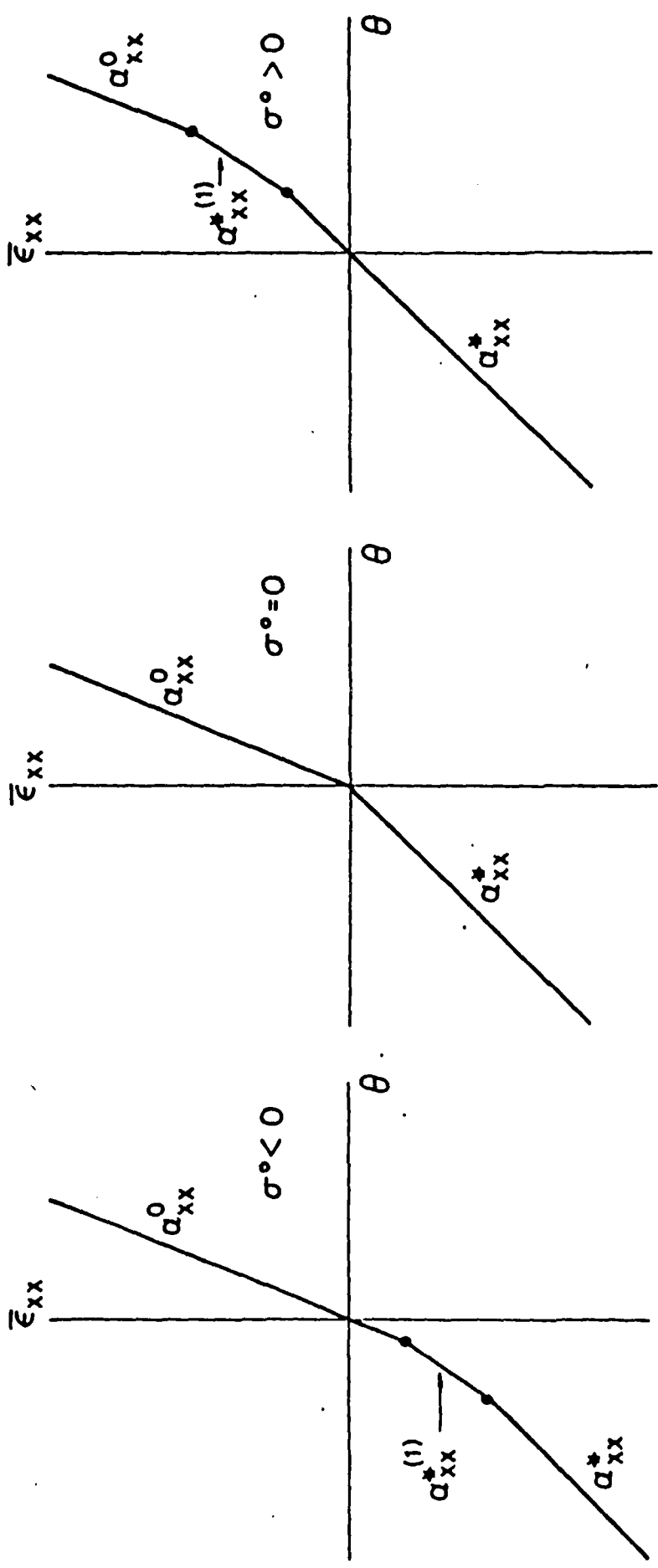


Fig. 15 - Thermal expansion coefficients versus crack density; singly and orthogonally cracked graphite/epoxy  $[0^{\circ}/90^{\circ}]_s$



16. Influence of nature of external load on thermal expansion coefficient of  $[0^\circ/90^\circ]_s$

THERMAL EXPANSION COEFFICIENTS OF CRACKED LAMINATES

by

Z. Hashin

Department of Solid Mechanics, Materials and Structures,

Tel-Aviv University,

Tel-Aviv, Israel.

ABSTRACT

Effective thermal expansion coefficients of cross-ply laminates containing many intra-laminar ply cracks are evaluated as functions of ply thermo-mechanical properties and crack density. The method employed is applicable to any cracked laminate if internal stress fields due to mechanical loads are known. Results obtained demonstrate strong reduction of expansion coefficients due to cracks. It is shown that because of opening of cracks by tension and closing by compression the laminate has several different expansion coefficients, each valid for a different load-temperature combination.

## 1. INTRODUCTION

There has been considerable interest in recent years in the analysis of property deterioration of damaged laminates. The primary damage consists of many intra-laminar ply cracks, in fiber directions, and the major research effort has been devoted to evaluation of stiffness reduction. Reifsnider and coworkers have applied simple shear lag methods (see e.g. Highsmith and Reifsnider [1]); Laws and Dvorak [2] have used so-called self consistent approximations to estimate cracked ply properties and on that basis the cracked laminate stiffness. Highsmith and Reifsnider [3] gave a numerical analysis of internal stresses and stiffness of cross-ply laminates in which both plies are cracked, based on higher order laminate theory. The same problem has been treated by Wang [4] with finite elements. Hashin [5,6] used variational methods to analyze stiffness reduction and internal stresses in cross-ply cracked in one or in two directions.

By contrast the practically very important problem of the modification of thermal expansion coefficients (TEC) by intra-laminar cracks has received only scant attention. Indeed the only published work on this subject known to us is a finite element numerical analysis by Herakovich and Hyer [7] who gave results for a cross-ply cracked in two directions.

In the present work we show that in order to evaluate the TEC of any cracked laminate it is sufficient to know the internal stresses produced by mechanical load. Thus the TEC of a cross-ply cracked in two directions are evaluated in simple fashion on the basis of the stresses obtained in ref. [6].

Since temperature changes produce both tensile and compressive internal ply stresses in laminates and since compression closes cracks, the effective

TEC of a cracked laminate will have different values depending on whether all cracks are open, some are closed or all are closed. This complex situation will be illustrated for the cross-ply laminates to be analyzed.

## 2. GENERAL DEVELOPMENT

To derive the effective TEC of a composite material let a body made of such material be subjected to the homogeneous traction boundary conditions

$$T_i(S) = \sigma_{ij}^0 n_j \quad (2.1)$$

where  $\sigma_{ij}^0$  is a constant stress tensor and  $n_j$  are the components of the outward normal, and to a uniform temperature change  $\theta$  relative to a uniform reference temperature  $T_0$ . Then from the average stress theorem (see e.g. Hashin [8])

$$\bar{\sigma}_{ij} = \sigma_{ij}^0 \quad (2.2)$$

where overbar denotes volume average. Then the average strain is given by

$$\bar{\epsilon}_{ij} = S_{ijkl}^* \bar{\sigma}_{kl} + \alpha_{ij}^* \theta \quad (2.3)$$

where  $S_{ijkl}^*$  is the effective compliance tensor and  $\alpha_{ij}^*$  is the effective thermal expansion tensor.

Let the stresses due to load (2.1) only, with no temperature change, be denoted  $\sigma_{ij}^s$  and let the stresses due to unit uniform temperature rise only, with zero boundary tractions  $T_i(S)=0$ , be denoted  $\sigma_{ij}^t$ . It follows by

superposition that the stress field in the composite material due to load and temperature change can be expressed in the form

$$\sigma_{ij}(\underline{x}) = \sigma_{ij}^s(\underline{x}) + \theta \sigma_{ij}^t(\underline{x}) \quad (2.4)$$

Levin [9] has proved a remarkable theorem which states

$$\int_V \alpha_{ij}(\underline{x}) \sigma_{ij}^s(\underline{x}) dV = \alpha_{ij}^* \sigma_{ij}^0 V \quad (2.5)$$

For a multiphase body with homogeneous constituents (2.5) assumes the form

$$\sum_m \alpha_{ij}^{(m)} \sigma_{ij}^{(m)} v_m = \alpha_{ij}^* \sigma_{ij}^0 \quad (2.6)$$

where  $m$  is the phase index,  $v_m$  the volume fraction of  $m$ th phase and

$$\bar{\sigma}_{ij}^{(m)} = \frac{1}{V_m} \int \sigma_{ij}^{(m)}(\underline{x}) dV \quad (2.7)$$

The effective TEC can be explicitly expressed from (2.6) in the form

$$\alpha_{ij}^* = \sum_m \alpha_{kl}^{(m)} B_{kl,ij}^{(m)} v_m \quad (2.8)$$

where  $B_{kl,ij}^{(m)}$  is defined by the linearity relation

$$\bar{\sigma}_{kl}^{(m)} = B_{kl}^{(m)} \sigma_{ij}^0 \quad (2.9)$$

The remarkable aspect of the relations (2.5), (2.6), (2.9) is in that they depend only on the mechanical stresses  $\sigma_{ij}^s$  and not on the thermal stresses  $\sigma_{ij}^t$ .

The relation (2.9) has been exploited by Levin (1967) to derive direct relations between the effective elastic properties and effective TEC of two-phase materials. In the case of composite materials which consist of more than two phases such direct relations cannot be established, but evaluation of effective elastic properties is still sufficient for evaluation of effective TEC for the former requires determination of  $\sigma_{ij}^s(x)$  which from (2.5) and its corollaries is sufficient to determine  $\alpha_{ij}^*$ .

We shall now consider the application of these relations to evaluation of TEC of damaged laminates. For sake of simplicity we consider only symmetric laminates which are thermoelastically orthotropic. Generalization to more complicated cases is a straightforward matter.

A laminate of rectangular plan form with orthotropy axes parallel to the sides of the rectangle is subjected to membrane loads

$$N_{xx} = 2h\sigma^0 \quad N_{yy} = N_{xy} = 0 \quad (2.10)$$

where  $2h$  is laminate thickness, fig. 1. The present loading is a special case of (2.1) when the only surviving component of  $\sigma_{ij}^0$  is  $\sigma_{11}^0 = \sigma_{22}^0 = \bar{\sigma}_{11}$ .

Let the internal stress field in the damaged laminate be represented as

Let the internal stress field in the damaged laminate be represented as

$$\sigma_{ij}^s(x) = \sigma_{ij}^l(x) + \sigma_{ij}'(x) \quad (2.11)$$

where  $\sigma_{ij}^l(x)$  is the stress field in the undamaged laminate and  $\sigma_{ij}'(x)$  is the change in stress due to the internal defects. Introducing (2.11) into (2.5) we have

$$\alpha_{xx}^* = \frac{1}{V_{\sigma}^0} \int \alpha_{ij} \sigma_{ij}^l dV + \frac{1}{V_{\sigma}^0} \int \alpha_{ij} \sigma_{ij}' dV \quad (2.12)$$

Since (2.5) is also valid for the undamaged laminate we identify the first integral in (2.12) as the TEC  $\alpha_{xx}^0$  of the undamaged laminate.

It is well known that the  $\sigma_{ij}^l$  are constant in each layer or ply. Let these stresses in the  $m$ th layer be referred to the material axes of the unidirectionally reinforced ply material and be expressed in the form

$$\sigma_{ij}^{(m)} = \sigma^0 k_{ij}^{(m)} \quad (2.13)$$

It follows at once that

$$\alpha_{xx}^0 = \sum_{ij}^m \alpha_{ij}^{(m)} k_{ij}^{(m)} \quad (2.14)$$

and it is readily realized that  $k_{ij}^{(m)}$  are components of the B tensor in (2.9)

for the present case.

In a more general sense we conclude that for a damaged laminate, and indeed for any damaged composite material

$$\alpha_{ij}^* \sigma_{ij}^0 = \alpha_{ij}^0 \sigma_{ij}^0 + \frac{1}{V} \int \alpha_{ij} \sigma'_{ij} dV \quad (2.15)$$

where  $\sigma'_{ij}$  is the stress perturbation due to defects.

We arrive at an immediate interesting consequence by noting the well known fact that interior interlaminar cracks have no effect on the stress distribution in symmetric laminates under membrane loading since such cracks have no effect on the states of plane stress in the layers. It follows that  $\sigma'_{ij}=0$  and therefore from (2.15)  $\alpha_{ij}^* = \alpha_{ij}^0$  and thus the effective TEC in the laminate plane are not affected by interlaminar cracks.

### 3. EVALUATION OF THERMAL EXPANSION COEFFICIENTS

We shall here be concerned with the case of a symmetric cross-ply laminate, denoted  $[0_m^0/90_n^0]$  in usual laminate notation in which one kind (e.g.  $90^0$ ) or both kinds of plies contain distributions on intra-laminar cracks, fig. 1. The case of cracked  $90^0$  occurs when the laminate is loaded normal to the  $90^0$  layer. The case of both plies cracked occurs when the laminate is subjected to heating/cooling temperature cycles, for in such a case the stresses normal to the fibers in the different plies are equal and opposite in sign. Since cracks are produced by tensile stresses heating can produce cracks in one ply and cooling can produce cracks in the other.

Another way to produce orthogonal cracks in both plies is to subject a  $\pm 45^\circ$  laminate to cyclic tension-tension load in direction of the bisector of the  $\pm 45^\circ$  directions.

To evaluate effective TEC we need the  $\sigma_{ij}^s$  stress field in an orthogonally cracked cross-ply laminate. This problem has been treated on the basis of finite elements by Wang [4] and on the basis of a higher order laminate theory by Highsmith and Reifsnider [3], both of these treatments being numerical. An analytical approximate variational treatment of the problem has been given by Hashin [6] and we shall use these results to evaluate effective expansion coefficients analytically. It is of interest to note that the stress field used is admissible in the sense of the principle of minimum complementary energy and it can thus be used to obtain a strict lower bound on effective Young's modulus of the cracked laminate, ref. [6]. The present use of this stress field does not necessarily produce a bound on the effective TEC. To establish such bounds the thermal stress field  $\sigma_{ij}^t$  is also needed and this will be discussed elsewhere. The justification for the present analysis is outstanding agreement of previous results for Young's modulus of a cracked laminate with experimental results, [5].

It is assumed for the sake of simplicity that the cracks in both plies are equidistant. In the following the inner ply is assigned the  $90^\circ$  direction and is labelled by index 1 while the outer plies are assigned the  $0^\circ$  direction and are labelled by index 2. The intercrack distances in the 1 and 2 plies are denoted  $2a$  and  $2b$  respectively. If the load (2.10) is applied to the laminate it follows from symmetry that the stress field is periodic. The repeating element for the stress field may be chosen as the region of the laminate defined by 4 plane cuts along any two intersecting crack pairs and the two

planes  $z=0, h$ , fig. 2.

The perturbation stresses due to cracks as defined in (2.11) are denoted  $\sigma_{ij}^{(1)}$  and  $\sigma_{ij}^{(2)}$  in the regions 1 and 2 respectively. The ply materials are transversely isotropic with TEC  $\alpha_A$  in fiber direction and  $\alpha_T$  transverse to the fibers. It follows that the last integral of (2.15) can be expressed in the form

$$\int_V \alpha_{ij} \sigma_{ij}^i dV = \int_{-a}^a \int_{-b}^b \int_0^{t_1} (\alpha_T \sigma_{xx}^{(1)} + \alpha_A \sigma_{yy}^{(1)} + \alpha_T \sigma_{zz}^{(1)}) dx dy dz +$$
$$\int_{-a}^a \int_{-b}^b \int_{t_1}^h (\alpha_A \sigma_{xx}^{(2)} + \alpha_T \sigma_{yy}^{(2)} + \alpha_T \sigma_{zz}^{(2)}) dx dy dz \quad (3.1)$$

According to the analysis given in ref. [6] the stresses entering into (3.1) have the form

$$\sigma_{xx}^{(1)} = - \sigma_x^{(1)} \phi(x) \quad \sigma_{yy}^{(1)} = - \sigma_y^{(1)} \psi(y) \quad (a)$$

$$\sigma_{zz}^{(1)} = [\sigma_x^{(1)} \phi''(x) + \sigma_y^{(1)} \psi''(y)] \frac{1}{2} (ht_1 - z^2) \quad (b)$$

(3.2)

$$\sigma_{xx}^{(2)} = \frac{1}{\lambda} \sigma_x^{(1)} \phi(x) \quad \sigma_{yy}^{(2)} = \frac{1}{\lambda} \sigma_y^{(1)} \psi(y) \quad (c)$$

$$\sigma_{zz}^{(2)} = \frac{1}{\lambda} [\sigma_x^{(1)} \phi''(x) + \sigma_y^{(1)} \psi''(y)] \frac{1}{2} (h - z)^2 \quad (d)$$

$$\lambda = t_2/t_1 \quad (e)$$

where  $\sigma_x^{(1)}$  and  $\sigma_y^{(1)}$  are the stresses in the 1 ply of the undamaged laminate and the functions  $\phi$  and  $\psi$  are defined by linear integro-differential equations, [6], and the boundary conditions

$$\phi(\pm a) = 1 = \psi(\pm b) \quad (a)$$

(3.3)

$$\phi'(\pm a) = 0 = \psi'(\pm b) \quad (b)$$

Since

$$\int_{-a}^a \phi''(x)dx = \phi'(a) - \phi'(-a)$$

$$\int_{-b}^b \psi''(y)dy = \psi'(b) - \psi'(-b)$$

These integrals vanish in view of (3.3b) and therefore the  $\sigma_{zz}$  stresses do not contribute to (3.1). Defining the mean values

$$\bar{\phi} = \frac{1}{2a} \int_{-a}^a \phi(x)dx \quad \bar{\psi} = \frac{1}{2b} \int_{-b}^b \psi(y)dy \quad (3.4)$$

It then follows in straightforward fashion from (3.1) and (2.12) that

$$\alpha_{xx}^* = \alpha_{xx}^0 + \frac{\alpha_A - \alpha_T}{1+\lambda} (k_x^{(1)} \bar{\phi} - k_y^{(1)} \bar{\psi}) \quad (a)$$

(3.5)

$$k_x^{(1)} = \sigma_x^{(1)} / \sigma^0 \quad k_y^{(1)} = \sigma_y^{(1)} / \sigma^0 \quad (b)$$

The values of  $\bar{\phi}$  and  $\bar{\psi}$  have been determined in ref. [6] and are given in the appendix.

We now consider some special cases. The first is a laminate in which only one kind of plies is cracked. Let it be assumed that there are no cracks in the outer plies. This implies that intercrack distance  $b$  is infinitely large, thus by definition (A-2) in the appendix,  $\rho_2 \rightarrow \infty$ . It follows from (A-7) and (A-9) that in this case  $\omega_2 \rightarrow 0$ , then from (A-10)

$$\bar{\phi} = \frac{\omega_1}{1 - m_1 m_2 (1 - \omega_1)} = \bar{\phi}^{(1)} \quad (3.6)$$

$$\bar{\psi} = - m_2 \bar{\phi}^{(1)}$$

and these values have to be introduced into (3.5) to obtain the TEC.

Similarly, if the inner ply is not cracked and the outer ones are, then

$$\bar{\phi} = - m_1 \bar{\psi}^{(2)} \quad (3.7)$$

$$\bar{\psi} = \frac{\omega_2}{1 - m_1 m_2 (1 - \omega_2)} = \bar{\psi}^{(2)}$$

Then from (3.5) and (A-5) the TEC in the two cases are

$$\alpha_{xx}^{*(1)} = \alpha_{xx}^0 + \frac{\alpha_A - \alpha_T}{1+\lambda} (1 + B_0/C_0) k_x^{(1)} \bar{\phi}^{(1)} \quad (a)$$

(3.8)

$$\alpha_{xx}^{*(2)} = \alpha_{xx}^0 + \frac{\alpha_A - \alpha_T}{1+\lambda} (1 + B_0/A_0) k_y^{(1)} \bar{\psi}^{(2)} \quad (b)$$

where the constants  $A_0$ ,  $B_0$  and  $C_0$  are defined in (A-3).

The TEC assume asymptotic limit values for large crack density. Theoretically this implies that either one or both of the ratios  $\rho_1$ ,  $\rho_2$  in (A-2) goes to zero. This does not really happen in practice since the crack patterns generally reach saturation for some definite intra-crack distances. Still the limiting values are of interest as lower bounds and it will also be seen that they are quite quickly approached as the crack density increases.

It is easily shown that when  $\rho \rightarrow 0$ , the quantity  $\omega$  as defined by (A-7) and by (A-9) approaches the limit 1. It then follows from (A-10) that

$$\left. \begin{array}{l} \lim \bar{\phi} = 1 \\ \lim \bar{\psi} = 1 \end{array} \right\} \quad \rho_1, \rho_2 \rightarrow 0 \quad (3.9)$$

Rather than inserting (3.9) into (3.5) it is more convenient to use (2.12) with (3.9). It then easily follows that

$$\alpha_{xx}^* = \alpha_A \quad \rho_1, \rho_2 \rightarrow 0 \quad (3.10)$$

In the event when only the inner or outer plies are cracked we have from (3.8)

$$\alpha_{xx}^{*(1)} \Big|_{p_1 \rightarrow 0} = \alpha_{xx}^0 + \frac{\alpha_A - \alpha_T}{1+\lambda} (1 + B_0/C_0) k_x^{(1)} \quad (3.11)$$

$$\alpha_{xx}^{*(2)} \Big|_{p_2 \rightarrow 0} = \alpha_{xx}^0 + \frac{\alpha_A - \alpha_T}{1+\lambda} (1 + B_0/A_0) k_y^{(1)}$$

Evaluation of the TEC  $\alpha_{yy}^*$ ,  $\alpha_{yy}^{*(1)}$  and  $\alpha_{yy}^{*(2)}$  is of course quite similar. For this purpose the TEC with subscripts  $xx$  in (3.5) and (3.8) should be replaced with the corresponding TEC with subscripts  $yy$  and  $k_x^{(1)}$  and  $k_y^{(1)}$  should be interpreted as (3.5b) when the loading (2.10) is replaced by

$$N_{yy} = 2h\sigma^0 \quad N_{xx} = N_{xy} = 0 \quad (3.9)$$

Figs. 3,4 show the variation of TEC  $\alpha_{xx}^*$  with crack density for Glass/Epoxy and for Graphite/Epoxy (T300 fibers) cross-ply. In each case  $t_1=t_2$ ,  $\lambda=1$  and results are given for orthogonal cracking,  $a=b$ , and also when only the inner layer cracked. Ply elastic properties and stress coefficients are given in table 1. It is seen that the cracks have significant effect on the TEC of the laminate, especially in the case of T300/Epoxy; that for orthogonal cracking the TEC are lower than for only one ply cracked and that for  $a=b=t_1$ , TEC values are already very close to large crack density asymptotic limits.

When a cracked laminate is subjected to loading and temperature change the internal ply stresses can be tensile or compressive. Since tensile transverse (normal to fibers) stresses open the cracks and compressive transverse stresses close them, the thermal deformation of the laminate will

be governed by abruptly changing TEC during the load-temperature process. This will now be illustrated for a cross-ply laminate in which all plies are cracked.

The transverse-stresses are  $\sigma_{xx}^{(1)}$  and  $\sigma_{yy}^{(2)}$  and the signs of these stresses due to load  $\sigma^0$  in x direction or due to temperature change, for uncracked laminates, can be seen in table 1. It is probably safe to assume that these stresses will retain their signs (but of course not their values) when the laminate is cracked. Consider first the case when a stress-free and load free cracked cross-ply is heated. In this case the transverse stresses in both plies are compressive. Therefore the cracks close and the TEC is that of the uncracked laminate. On the other hand, when the laminate is cooled from stress-free state, the transverse stresses are tensile, the cracks open up and the TEC are given by (3.5).

Next consider the same laminate which is heated under tension  $N_{xx} = 2\sigma^0 h$ . The load alone produces tensile transverse stresses. Therefore in the initial heating stage the TEC in x direction is  $\alpha_{xx}^*$ . At some temperature the compressive thermal stresses will close the cracks in one ply, ply 2 say. At this stage the TEC becomes  $\alpha_{xx}^{*(1)}$ , eq. (3.8a). Further heating will increase the thermal compressive transverse stresses to the point where the cracks in ply 1 will also close and from thereon the TEC is  $\alpha_{xx}^0$ . For cooling the TEC is always  $\alpha_{xx}^*$  since the thermal transverse stresses are tensile and are added to the tensile mechanical stresses.

Similar reasoning can be applied to the case of temperature change with compression. The nature of the thermal deformation for this and the previous cases is schematically shown in fig. 5.

#### 4. DISCUSSION AND CONCLUSION

It has been shown that the effective TEC of cracked laminates can be determined in simple fashion if the internal stress fields produced by constant membrane loads are known. Such stress fields can be utilized in this fashion whether known analytically or numerically. In this work we have utilized simple approximate stress fields, obtained elsewhere.

It has been found that intralaminar cracks significantly reduce the TEC of the laminate and this is in agreement with the numerical results given in ref. 7. When both plies of a cross-ply laminate are cracked the limit of reduction of TEC is the axial TEC of a ply. Therefore the TEC reduction is particularly significant for Graphite/Carbon fiber materials since in these cases the axial TEC of the ply is very small and often negative. This is illustrated in fig. 4.

An interesting phenomenon occurs due to the fact that thermal stresses in the plies are both tensile and compressive. In a cracked ply under compression the cracks close and therefore such a ply behaves as an uncracked ply. Therefore the laminate TEC during a load-temperature program will have different values and it is necessary to evaluate the thermal stresses to determine which TEC is appropriate, the choice being TEC for both plies cracked, one ply cracked or none. A variational analysis of thermal stresses will be presented elsewhere.

Since a cross-ply is hardly a laminate of practical importance it is appropriate to inquire into the problem of TEC modification by cracks in laminates of more complex configuration. On the basis of present treatment this problem is resolved when the stresses due to membrane loads are known and it is therefore in this direction where we have to look for the answers.

Obviously balanced symmetric  $0/90^{\circ}$  and  $+45/-45^{\circ}$  laminates with same crack density in all plies are isotropic in thermal expansion with same TEC. It is therefore to be expected that balanced symmetric  $0/90^{\circ}/+45/-45^{\circ}$  laminates with same crack density in all plies will have these same TEC, at least approximately.

#### ACKNOWLEDGMENT

This research has been supported by the Air Force Office of Scientific Research (AFOSR), Division of Aerospace Sciences, under Contract 85-0342, monitored by Major George Haritos.

Appendix

Material properties of reinforced ply

$E_A$	- Axial Young's modulus (fiber direction)	
$\nu_A$	- Axial Poisson's ratio	
$E_T$	- Transverse Poisson's ratio	(A-1)
$\nu_T$	- Transverse Poisson's ratio	
$G_A$	- Axial shear modulus	
$G_T$	- Transverse shear modulus	

Geometrical parameters

$$\rho_1 = a/t_1 \quad \rho_2 = b/t_1 \quad (A-2)$$

$$\lambda = t_2/t_1$$

Laminate parameters

$$A_0 = 1/\lambda E_A + 1/E_T \quad C_0 = 1/E_A + 1/\lambda E_T$$

$$B_0 = -(1+1/\lambda)\nu_A/E_A$$

$$A_1 = (\lambda/G_A + 1/G_T)/3 \quad B_1 = (1/G_A + \lambda/G_T)/3 \quad (A-3)$$

$\epsilon_1$

$$A_2 = [(3\lambda+2)\nu_T/E_T - \lambda\nu_A/E_A]/3 \quad B_2 = [(3\lambda+2)\nu_A/E_A - \lambda\nu_T/E_T]/3$$

$$C = (\lambda+1)(3\lambda^2 + 12\lambda + 8)/60E_T$$

$$p_1 = (A_2 - A_1)/C \quad q_1 = A_0/C \quad (A-4)$$

$$p_2 = (B_2 - B_1)/C \quad q_2 = C_0/C$$

$$m_1 = k_y^{(1)} B_0 / k_x^{(1)} A_0 \quad m_2 = k_x^{(1)} B_0 / k_y^{(1)} C_0 \quad (A-5)$$

Case I  $4q > p^2$

$$\alpha = q^{1/4} \cos(\theta/2) \quad \beta = q^{1/4} \sin(\theta/2) \quad (A-6)$$

$$\tan \theta = \sqrt{4q/p^2 - 1}$$

$$\omega = \frac{2[\text{Ch}(2\alpha\rho) - \cos(2\beta\rho)]}{\rho(\alpha/\beta + \beta/\alpha)[\alpha\sin(2\beta\rho) + \beta\text{Sh}(2\alpha\rho)]} \quad (A-7)$$

Case II  $4q < p^2$   $p < 0$

$$\alpha, \beta = \sqrt{(-1 \pm \sqrt{1-4q/p^2})/2} \quad (A-8)$$

$$\omega = \frac{(\beta/\alpha - \alpha/\beta)\text{Sh}(\alpha\rho)\text{Sh}(\beta\rho)}{\rho[\beta\text{Ch}(\alpha\rho)\text{Sh}(\beta\rho) - \alpha\text{Sh}(\alpha\rho)\text{Ch}(\beta\rho)]} \quad (A-9)$$

$$\bar{\phi} = \frac{\omega_1 - m_1(1-\omega_1)\omega_2}{1 - m_1 m_2 (1-\omega_1)(1-\omega_2)} \quad (A-10)$$

$$\bar{\psi} = \frac{\omega_2 - m_2 (1-\omega_2) \omega^{(2)}}{1 - m_1 m_2 (1-\omega_1) (1-\omega_2)}$$

To evaluate (10), (4) must be submitted to the case I, II tests. This determines the choice of  $\alpha, \beta$  and  $\omega$  in each case, thus determines  $\omega_1$  and  $\omega_2$  in (10).

REFERENCES

1. A.L. Highsmith and K.L. Reifsnider, Stiffness-reduction mechanisms in composite laminates, in Damage in Composite Materials, K.L. Reifsnider, Ed., ASTM STP 775, ASTM (1982), pp. 103-117.
2. N. Laws and G.J. Dvorak, The loss of stiffness of cracked laminates, in Fundamentals of Deformation and Fracture, Proc. Eshelby Memorial Symposium (IUTAM), Cambridge University Press, London (1985), pp. 119-127.
3. A.L. Highsmith and K.L. Reifsnider, Internal load distribution effects during fatigue loading of composite laminates, in Composite Materials: Fatigue and Fracture, H.T. Hahn, Ed., ASTM, STP 907, ASTM (1986), pp. 233-251.
4. A.S.D. Wang, Fracture analysis of matrix cracking in laminated composites, Dept. of Mech. Engng. & Mechanics Report, Drexel University, Philadelphia, Pa. (1985).
5. Hashin, Z., Analysis of cracked laminates: a variational approach, Mechanics of Materials, 4, (1985), pp. 121-136.
6. Z. Hashin, Analysis of orthogonally cracked laminates under tension, J. Appl. Mech., to appear.
7. C.T. Herakovich and M.W. Hyer, Damage-induced property changes in composites subjected to cyclic thermal loading, Engineering Fracture Mechanics, 25, (1986), pp. 779-792.
8. V.M. Levin, On the coefficients of thermal expansion in heterogeneous materials, Mechanics of Solids (translation of Mekhanika Tverdogo Tela), 2, (1967), pp. 58-61.

Ply Properties

Material	$E_A$	$E_T$	$v_A$	$v_T$	$G_A$	$G_T$	$\alpha_A$	$\alpha_T$
Gf/Ep	41.7	13.0	.300	.420	3.40	4.58	6.72	29.32
T300/Ep	140.0	9.2	.300	.347	4.34	3.41	-.70	32.33

Laminate Properties

Material	$t_1/h$	$t_2/h$	$E_x^0$	$E_y^0$	$v_{xy}^0$	$\alpha_{xx}^0$	$\alpha_{yy}^0$
Gf/Ep	.75	.25	20.30	34.75	.113	18.20	9.46
	.50	.50	27.57	27.57	.143	12.83	12.83
T300/Ep	.75	.25	42.08	107.72	.0257	5.20	.50
	.50	.50	74.97	74.97	.037	1.85	1.85

Laminate Stress Coefficients

Material	$t_1/h$	$t_2/h$	$k_x^{(1)}$	$k_y^{(1)}$	$k_x^{(2)}$	$k_y^{(2)}$	$\ell_x^{(1)}$	$\ell_y^{(1)}$	$\ell_x^{(2)}$	$\ell_y^{(2)}$
Gf/Ep	.75	.25	.6364	-.0411	2.091	.1232	-.1377	.0733	.4131	-.2196
	.50	.50	.4644	-.0764	1.536	.0764	-.1960	.1960	.1960	-.1960
T300/Ep	.75	.25	.2182	-.201	3.345	.0603	-.2477	.0927	.7430	-.2783
	.50	.50	.1221	-.0325	1.878	.0325	-.2749	.2749	.2749	-.2749

MPa/ $^{\circ}$ C

Elastic Moduli

GPa

TEC

$10^{-6} 1/^{\circ}$ C

Temperature Stress Coefficients MPa/ $^{\circ}$ C (stress per unit temperature rise)

Table 1 - Thermo-elastic properties and stress coefficients

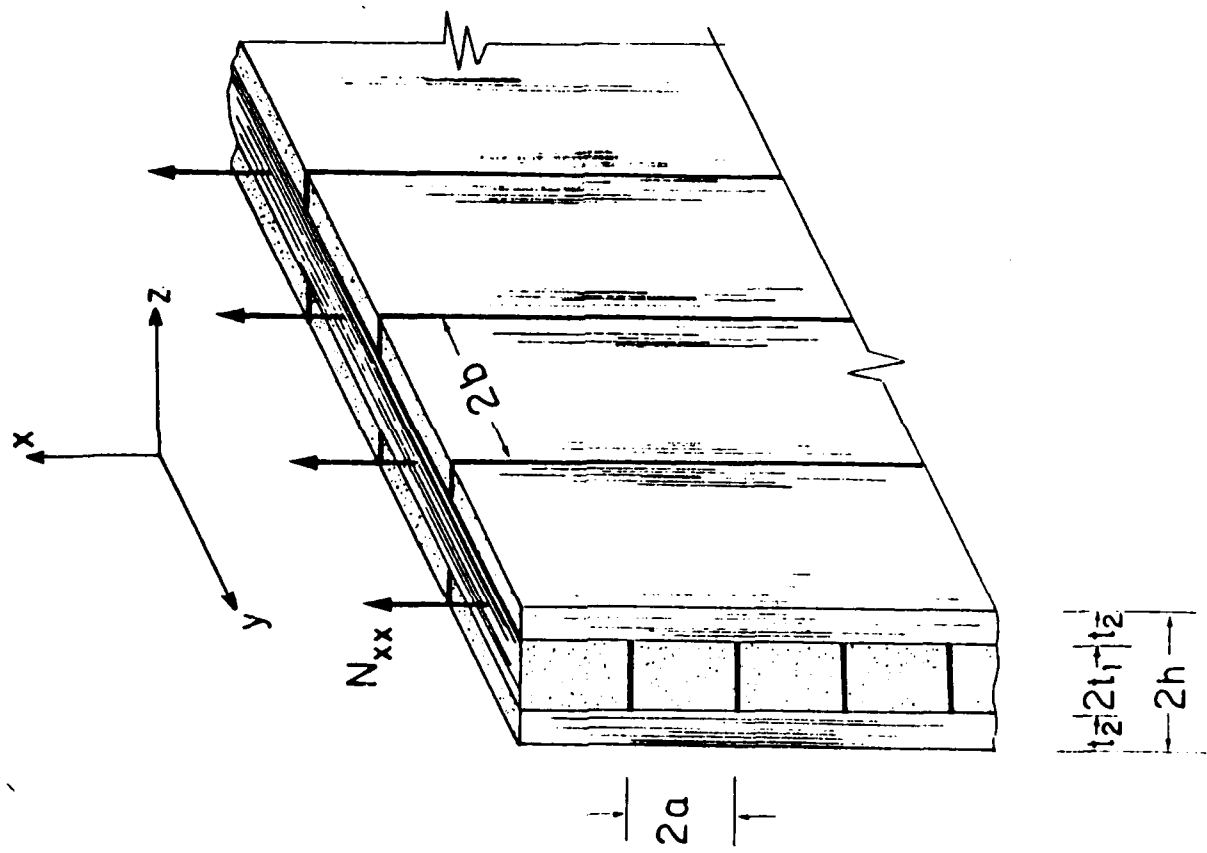


Fig. 1 - Laminate with all plies cracked.

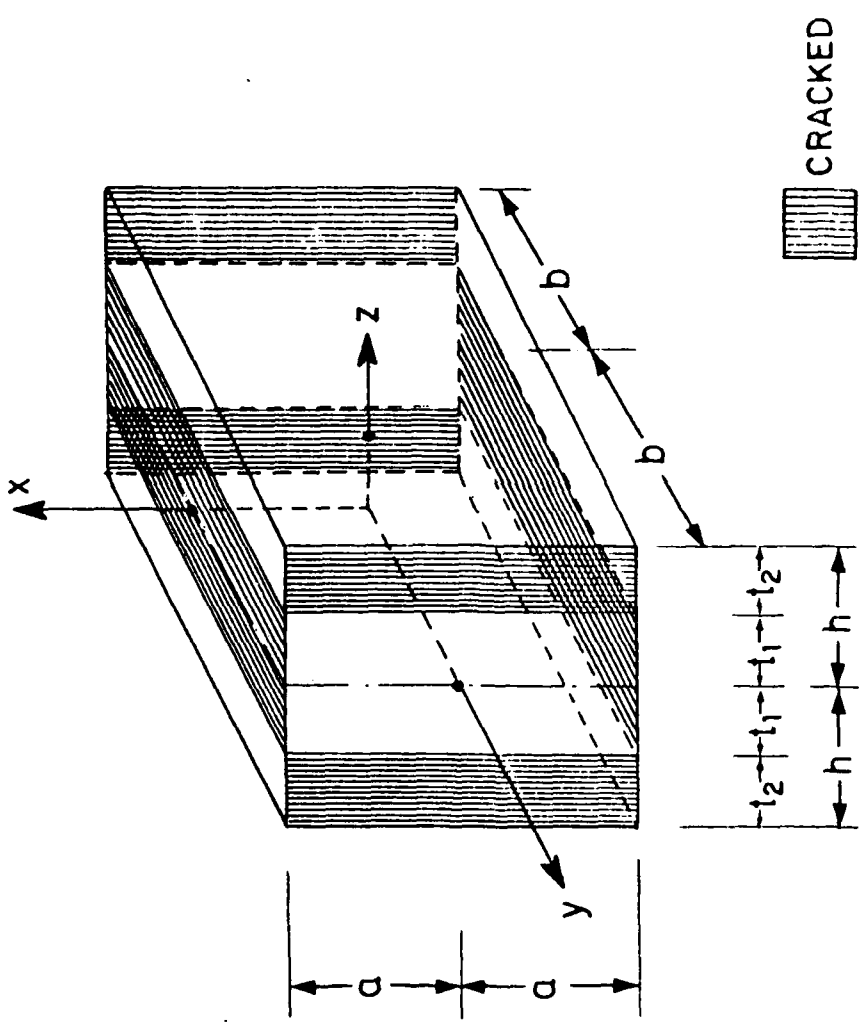


Fig 2. - Repeating element.

RD-A193 519

ANALYSIS OF STIFFNESS REDUCTION FAILURE AND STRESS  
CONCENTRATION IN FIBER. (U) PENNSYLVANIA UNIV  
PHILADELPHIA DEPT OF MATERIALS SCIENCE AND E.

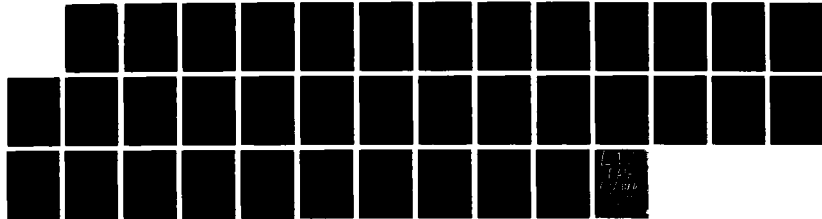
2/2

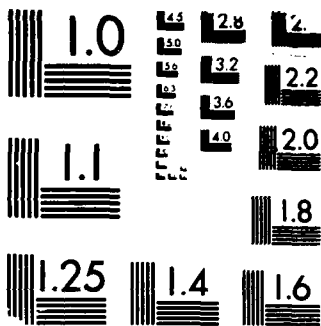
UNCLASSIFIED

Z HASHIN 31 DEC 87 AFOSR-TR-88-0367

F/G 11/4

NL





MICROCOPY RESOLUTION TEST CHART  
O'REAU STANDARDS 1963-A

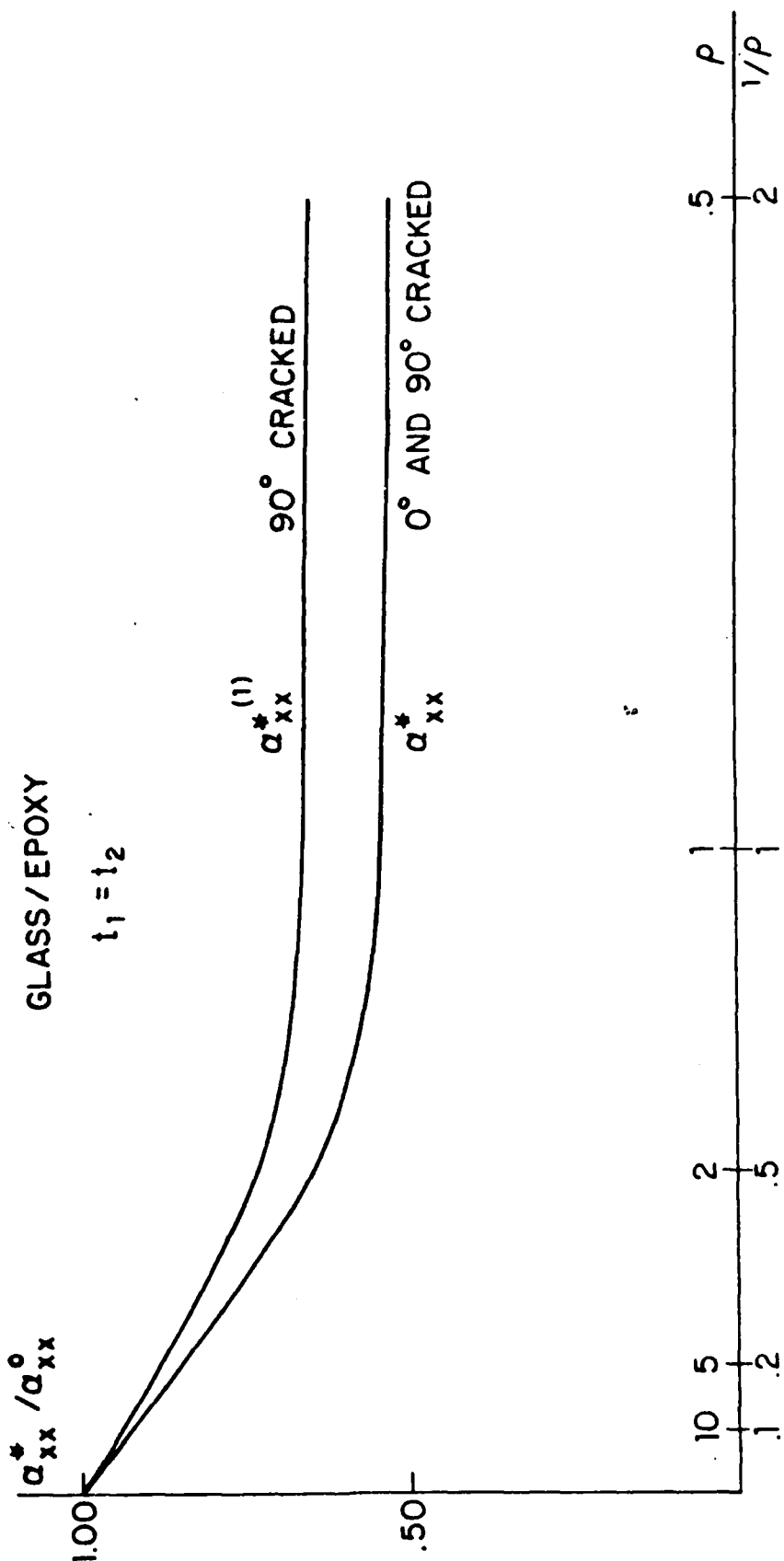


Fig. 3 - Variation of thermal expansion coefficient of Glass-Epoxy cross-ply with crack density

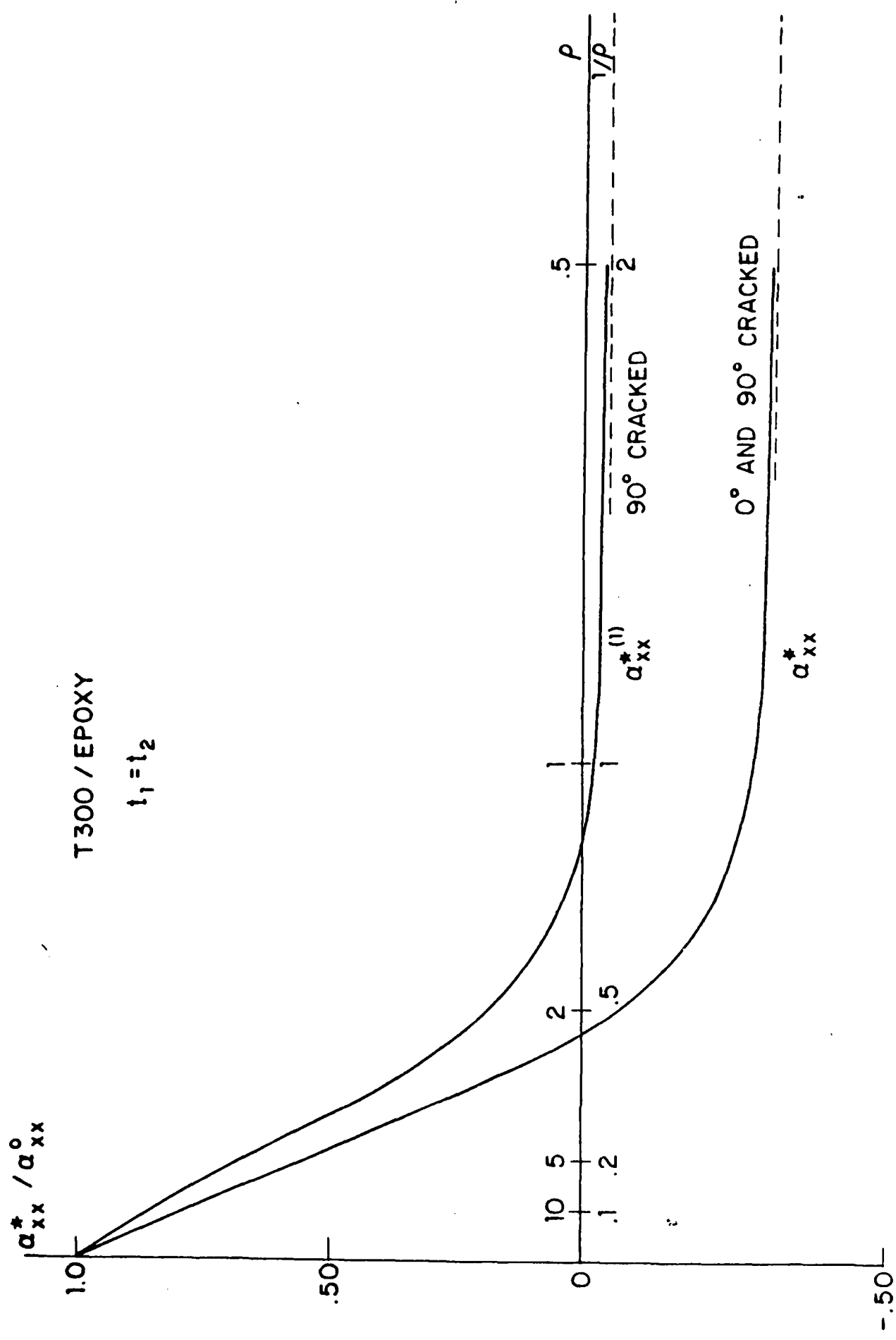


Fig 4 - Variation of thermal expansion coefficient of Graphite/Epoxy cross-ply with crack density.

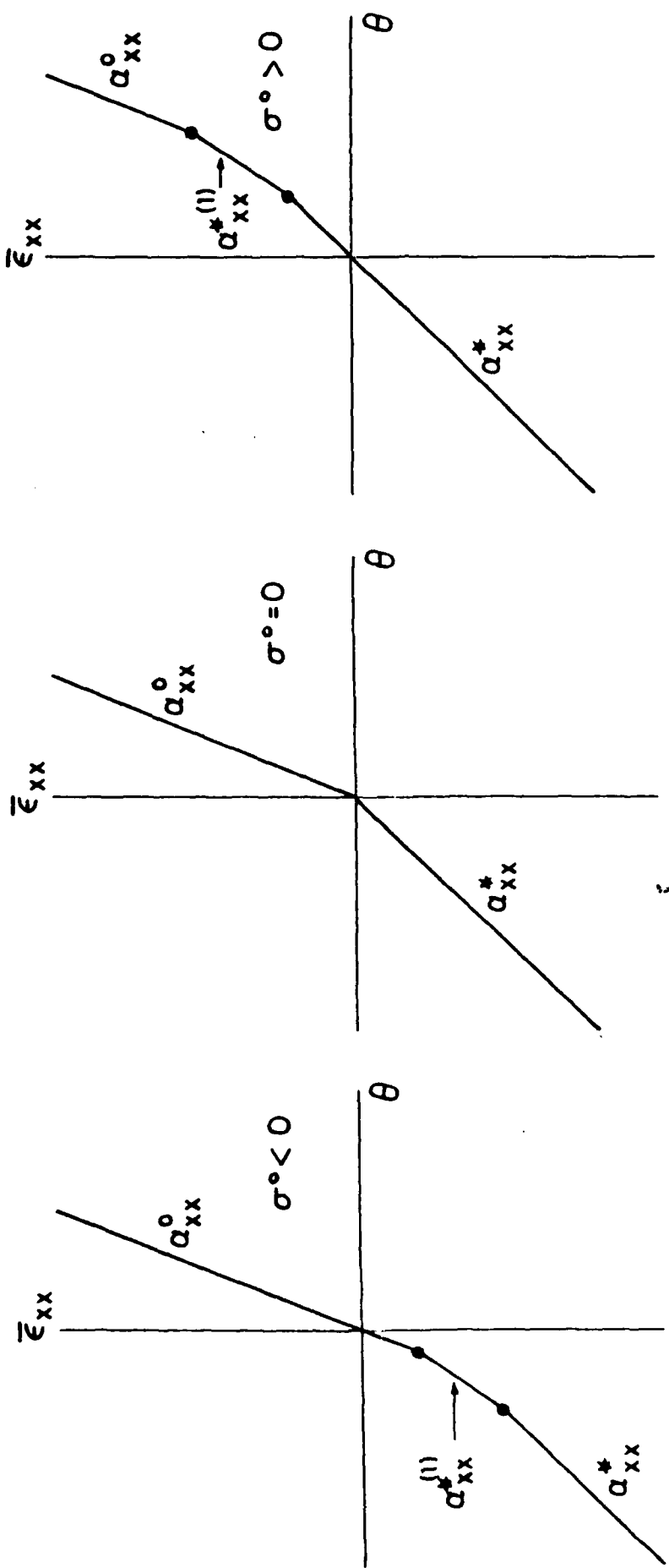


Fig 5- Effect of signs of load and temperature change on value of thermal expansion coefficient of cracked laminate.

**THE DIFFERENTIAL SCHEME AND ITS APPLICATION TO CRACKED MATERIALS**

by

**Zvi Hashin**

**Dept. of Solid Mechanics, Materials and Structures**

**Faculty of Engineering**

**Tel-Aviv University**

**Tel-Aviv, 69978, Israel**

**ABSTRACT**

A Differential Scheme (DS) approximation for elastic properties of cracked materials is established by a limiting process on the basis of the DS for porous materials. The method is applied to obtain stiffness reduction due to randomly oriented elliptical and penny shaped crack distributions in isotropic matrix, and to the case of aligned plane cracks in orthotropic sheets.

## INTRODUCTION

The problem of stiffness reduction of elastic bodies due to the development or presence of many disordered cracks is of significant scientific and engineering importance and has been the subject of many investigations. This appears to be a particularly difficult problem of the elastic behavior of heterogeneous media as is evidenced by the fact that the only exact results derived to date are for the case of small crack density, when the cracks do not interact. (Periodic crack arrays can be analyzed numerically to any desired degree of accuracy.)

Variational bounding methods which have proved so useful for composite media have been only sparsely applied to this problem: Gottesman (1980) for plane cracks and Willis (1981).

The approximate method known as the Self Consistent Scheme (SCS) has first been applied to this problem by Budiansky and O'Connell (1976) with special attention to randomly oriented elliptical and penny shaped cracks in isotropic matrix. This has been further developed by Horii and Nemat-Nasser (1983) to take into account friction between opposite crack surfaces. Hoenig (1979) has applied the SCS for aligned distributions of elliptical cracks and Gottesman et al. (1980) for aligned plane cracks in orthotropic sheet. Aboudi and Benveniste (1987) have used a generalized SCS, whereby a cracked circular disk is imagined to be embedded in the effective medium, rather than the crack directly, for randomly oriented plane cracks. Benveniste (1986) has also applied the Mori-Tanaka approximation to cracked materials. Other literature is cited and discussed in the above referenced papers.

Another approximate method of general nature is the so-called Differential Scheme (DS). This method is in a certain sense related to the SCS as will be explained further below. To the best of our knowledge both methods originate with Bruggeman (1935) in the context of conductivity and dielectrics of heterogeneous media. He named the SCS symmetric effective medium theory, since its results are insensitive to phase interchange, and the DS - effective medium theory. The former is a

more fortunate choice of words that self consistent scheme, for self consistency merely implies that the effective elastic moduli and effective elastic compliance tensors as predicted, separately, are mutually reciprocal. But this is only a minimal necessary requirement which must be imposed on any approximate theory and is therefore not a suitable label of identification.

The purpose of the present work is to establish a general DS formulation for cracked materials. To the best of our knowledge the only DS treatments of cracked materials in the literature are those of Salganik (1973), who applied the Roscoe (1952) interpretation of the DS to the case of randomly oriented penny shaped cracks in ad-hoc fashion, and of Henyey and Pumphrey (1982) who essentially reproduced the Salganik results.

The motivation for such a study are some inherent problems with the SCS results. For porous media with spherical voids the SCS predicts that the effective elastic moduli diminish linearly with void volume fraction until they vanish for 50% voids, Budiansky (1965), Wu (1966). This is theoretically unacceptable and is in disagreement with experimental results. It is a direct consequence of the phase symmetry of the SCS predictions as opposed to the considerable phase bias when one phase is matrix and the other inclusions. Similar problems are encountered in the SCS results for penny shaped cracks, Budiansky and O'Connell (1976). The effective Young's modulus diminishes linearly with crack density parameter (CDP) and the effective shear modulus nearly so, both moduli abruptly vanishing for CDP of value 9/16. This is not acceptable since the moduli should vanish asymptotically with increasing crack density. Furthermore, linear variation with CDP is restricted to small crack density when the cracks do not interact and can therefore not be valid for large density when the cracks do interact.

It has been shown by Boucher (1976) that the DS approximation for porous media does not exhibit the SCS problems and agrees quite well with experimental results. It would therefore seem worthwhile to develop the DS method for cracked materials.

## GENERAL DEVELOPMENT

The SCS and the DS may both be related to some fundamental results in the theory of elastic two phase media. It is well known, e.g. Hill (1963), that when such a material is subjected to average strain  $\bar{\epsilon}$  or to average stress  $\bar{\sigma}$  then the effective elastic moduli tensor  $C^*$  and effective compliance tensor  $S^*$  can be expressed in the form

$$C^* = C^{(1)} + (C^{(2)} - C^{(1)}) A v_2 \quad (a) \quad (1)$$

$$S^* = S^{(1)} + (S^{(2)} - S^{(1)}) B v_2 \quad (b)$$

where  $C^{(1)}$ ,  $C^{(2)}$ ,  $S^{(1)}$  and  $S^{(2)}$  are the moduli and compliance tensors, respectively, of the phases which have volume fractions,  $v_1$ ,  $v_2$  and the symmetric fourth rank tensors  $A$  and  $B$  are defined by the linearity relations

$$\bar{\epsilon}^{(2)} = A \bar{\epsilon} \quad \bar{\sigma}^{(2)} = B \bar{\sigma} \quad (2)$$

where  $\bar{\epsilon}^{(2)}$  and  $\bar{\sigma}^{(2)}$  are average strain and average stress over phase 2, the first when  $\bar{\epsilon}$  is prescribed and the second when  $\bar{\sigma}$  is prescribed. Eqs. (2) are equally valid when the phase indices are interchanged.

We introduce from now on the restriction that phase 2 is in the form of inclusions which are embedded in matrix 1. Then (2) becomes a convenient device for resolving the case of small concentration  $v_2 = c \ll 1$ , in which case it may be assumed that the inclusions are isolated. In this case the state of strain or stress in any of them is as if it were embedded all by itself in infinite matrix with far field  $\bar{\epsilon}$  or  $\bar{\sigma}$ . Eshelby has provided a well known solution for the general ellipso-

dal inclusion which amounts to determination of  $A$  or  $B$  in (2) now identified as  $A_s$  and  $B_s$  for this special case. Then the small concentration result can be expressed in the dual forms.

$$\begin{aligned} C^{*s} &= C^{(1)} + (C^{(2)} - C^{(1)}) A^s c & A^s &= A^s(C^{(2)}, C^{(1)}, g) \text{ (a)} \\ S^{*s} &= S^{(1)} + (S^{(2)} - S^{(1)}) B^s c & B^s &= B^s(S^{(2)}, S^{(1)}, g) \text{ (b)} \end{aligned} \quad (3)$$

where  $g$  symbolizes inclusion geometry.

In the most commonly used version of the SCS it is assumed that when inclusion volume concentration is not small the average state of strain or stress in any inclusion may be estimated as if it were embedded by itself in a homogeneous medium to which are assigned the effective elastic properties  $C^*$  and  $S^*$  of the composite. The consequence of this assumption is

$$\begin{aligned} C^* &= C^{(1)} + (C^{(2)} - C^{(1)}) A^* v_2 \\ A^* &= A^s(C^{(2)}, C^*, g) \end{aligned} \quad (4)$$

with an analogous result for  $S^*$ . There are as many eqns. (4) as there are components of  $C^*$ .

We mention in passing that there are other SCS versions in which a composite element is embedded in the effective medium. For discussion see e.g. Hashin (1983).

The DS is based on the notion of incremental construction of the composite material by gradual addition of infinitesimal amounts of inclusions. The fundamental assumption is that the effect of an increment  $dv_2$  on the effective properties at current  $v_2$  is governed by the small concentration results (3) in which the matrix is assigned the effective properties. But the equivalent of the small concentration  $c$  is not simply  $dv_2$  for since the composite must be statistically homogeneous at all stages of the construction process accommodation of new added inclusions requires rearrangement of

the current ones and because of this consideration it may be shown that the quantity  $dv_2/(1-v_2)$  is the proper equivalent of small concentration. This procedure results in differential initial value problems for effective moduli and compliances which may be expressed in the general tensor form, McLaughlin (1977),

$$\frac{dC^*}{dv_2} = (C^{(2)} - C^*) A^* / (1-v_2) \quad (5)$$

$$C^* \Big|_{v_2=0} = C^{(1)}$$

$$\frac{dS^*}{dv_2} = (S^{(2)} - S^*) B^* / (1-v_2) \quad (6)$$

$$S^* \Big|_{v_2=0} = S^{(1)}$$

Self-consistency of  $C^*$  and  $S^*$  as predicted by (5,6) has been stated by McLaughlin (1977). A proof is here given in appendix I.

The incremental procedure described above has been initiated by Bruggeman (1935) and has been further developed by Roscoe (1952), Boucher (1976) and McLaughlin (1977). In Roscoe's interpretation of the DS it is assumed that there are many inclusion sizes of many orders of magnitude. The filling process starts with the smallest inclusions and proceeds with increasing orders of magnitude. The mathematical expression of this procedure results again in eqns. (5,6). The reason for this interpretation is that if the added inclusions are much larger than the current ones then the fundamental assumption that they "see" an effective medium is quite accurate. But it should be noted that the requirements of infinitesimality of inclusion volume increment, large number of in-

clusions and increasing order of magnitude of inclusion size are mutually contradictory.

Norris (1985) has pointed out that there are many ways of incremental construction of a particulate composite, each of which leads to different effective elastic moduli. The physical fact is that the effective elastic properties of a composite are uniquely determined by its phase geometry (in all details) and by the phase properties. If the DS were an exact procedure then such "path dependence" would be unacceptable. Since, however, the DS is approximate its results are of uncertain accuracy, but it is an open question whether such uncertainty can be quantified by artificial variety in filling process. In any event the option of filling path dependence does not apply in the case of a cracked solid.

In preparation for cracks we first consider the case when the inclusions become voids. "This implies that  $C^{(2)} \rightarrow 0$ ;  $S^{(2)} \rightarrow \infty$ . Then (1a) assumes the form

$$C^* = C^{(1)}(I - A_0 v_2) \quad (7)$$

where  $I$  is the fourth rank symmetric unit tensor and  $A_0$  is  $A$  of (2a) for voids. The interpretation of  $\bar{\epsilon}^{(2)}$  in (2a) in this case follows from the average strain theorem

$$\bar{\epsilon}_{ij}^{(2)} = \frac{1}{2V_2} \int_{S_{12}} (u_i n_j + u_j n_i) ds \quad (8)$$

where  $S_{12}$  is the interface, thus the surface bounding the voids.

Modification of (1b) for voids needs some manipulation because  $S^{(2)} \rightarrow \infty$ . Introducing (2b) into (1b) and remembering that  $\bar{\sigma}^{(2)} \rightarrow 0$  for voids, we obtain

$$S^* = S^{(1)} + \bar{\epsilon}^{(2)} v_2$$

which can be written in the form

$$S^* = S^{(1)}(I + B_0 v_2) \quad (9)$$

where the tensor  $B_0$  is defined by

$$\bar{\epsilon}^{(2)} = S^{(1)} B_0 \bar{\sigma} \quad (10)$$

From (7,10) there immediately follow the small concentration results

$$C^* = C^{(1)}(I - A_0 c_2) \quad (11)$$

$$S^* = S^{(1)}(I + B_0 c_2)$$

where  $A_0$  and  $B_0$  are determined by evaluation of (8) for isolated voids for far fields  $\bar{\epsilon}$  or  $\bar{\sigma}$ , respectively.

Cracks are defined as very flat voids of vanishing thickness and thus also of vanishing volume. We multiply both sides of (8) by  $v_2$  and consider the limit of flattening out into cracks, which will from now on be identified as  $v_2 \rightarrow 0$ . Then the surface integral for each crack is confined to the two congruent crack surfaces and thus each component of normal appears, twice with opposite signs. Therefore

$$\lim_{v_2 \rightarrow 0} (\epsilon_{ij}^{(2)} v_2) = \frac{1}{2V} \int_{S_c} ([u_i] n_j + [u_j] n_i) ds = \gamma_{ij} \quad (12)$$

where  $S_c$  denotes the crack surface (once),  $[u_i]$  is the displacement jump across the crack surface,

usually called the crack opening displacement (COD), and  $n_i$  are the components of the normal with respect to one side of the crack.

The tensor  $\gamma$  in (12) is obviously linearly related to applied  $\epsilon$  or  $\sigma$ , whichever the case. We write these linearity relations in the form

$$\gamma^\epsilon = P\bar{\epsilon} \quad (a) \quad (13)$$

$$\gamma^\sigma = S^{(1)} Q\bar{\sigma} = R\bar{\sigma} \quad (b)$$

where the alternate forms (13b) will be used according to convenience.

It follows from (13), the left of (12) and from the definition of  $A_0$  and  $B_0$  that

$$\begin{aligned} P &= \lim (A_0 v_2) \\ Q &= \lim (B_0 v_2) \end{aligned} \quad \} v_2 \rightarrow 0 \quad (14)$$

It follows at once that for the case of cracks (7, 9) transform into

$$\begin{aligned} C^* &= C^{(1)} (I - P) \\ S^* &= S^{(1)} (I + Q) = S^{(1)} + R \end{aligned} \quad (15)$$

These are general results for cracked elastic bodies, expressing effective elastic properties in terms of COD. The case of small crack density is defined by non interacting cracks. This is a special case of (15) expressed as

$$C^{*S} = C^{(1)} (I - P^S) \quad (a)$$

$$S^{*s} = S^{(1)}(I + Q^s) = S^{(1)} + R^s \quad (b)$$

(16)

$$P^s = P^s(S^{(1)}, g_c) \quad (c)$$

$$Q^s = Q^s(S^{(1)}, g_c) \quad R^s = S^{(1)}Q^s(S^{(1)}, g_c) \quad (d)$$

where  $g_c$  is crack geometry. The tensors  $P^s$  and  $Q^s$  are determined by evaluation of (13) for non-interacting cracks.

It is easily realized that the SCS for cracked bodies can be written in terms of (15,16) in the alternative forms

$$C^* = C^{(1)}(I - P^*) \quad (a)$$

$$S^* = S^{(1)}(I + Q^*) \quad (b) \quad (17)$$

$$P^* = P^s(C^*, g_c) \quad Q^* = Q^s(S^*, g_c) \quad (c)$$

We now consider the DS and start with the case of voids. We can easily apply the reasoning leading from (3) to (5,6) for the case of voids by using small concentration versions of (11). Thus

$$C^{*s} = C^{(1)} \left[ I - A_0^s c_2 \right] \quad (18)$$

$$S^{*s} = S^{(1)} \left[ I + B_0^s c_2 \right]$$

$$A_0^s = A_0^s \left( C^{(1)}, g_0 \right) \quad B_0^s = B_0^s \left( S^{(1)}, g_0 \right)$$

where  $g_0$  is void geometry in the case of non-interacting voids. Then the DS for a porous material assumes the form

$$\frac{dC^*}{dv_2} = - C^* A_0^* / (1-v_2) \quad (a)$$

$$\frac{dS^*}{dv_2} = S^* B_0^* / (1-v_2) \quad (b) \quad (19)$$

$$A_0^* = A_0^s \left( C^*, g_0 \right) \quad B_0^* = B_0^s \left( S^*, g_0 \right) \quad (c)$$

Now multiply both sides of (19) by  $v_2$  and perform the limit of flattening out the voids into cracks. Then for example

$$\lim \left( v_2 \frac{dC^*}{dv_2} \right) = - C^* \lim \left( A_0^* v_2 \right) \quad v_2 \rightarrow 0$$

Since  $A_0^s$  is a special case of  $A_0$  it certainly satisfies (14) and therefore (19c) also satisfies (14).

Recalling (17c) it follows that

$$\lim_{v_2 \rightarrow 0} (A_0^* v_2) = R^*$$

with a similar reasoning for  $B_0^*$  we can finally write the modification of (19) to the case of a cracked solid in the form

$$\lim_{v_2 \rightarrow 0} \left( v_2 \frac{dC^*}{dv_2} \right) = -C^* P^* \quad (a)$$

$$v_2 \rightarrow 0$$

$$\lim_{v_2 \rightarrow 0} \left( v_2 \frac{dS^*}{dv_2} \right) = S^* Q^* = R^* \quad (b)$$

(20)

$$R^* = R^3 \left( S^*, g_c \right) \quad (c)$$

$$C^* \Big|_{v_2=0} = C^{(1)} \quad S^* \Big|_{v_2=0} = S^{(1)} \quad (d)$$

The limit on the left side cannot be carried out in a general sense and depends on the crack geometry as will be seen further below.

We specialize (20) to the important case when the cracked material is statistically isotropic. In this event all tensors appearing in (20) must be isotropic and we represent them in the convenient notation, Hill (1965), Walpole (1981)

$$C^* = 3K^* I^1 + 2G^* I^2 = (3K^*, 2G^*)$$

$$S^* = \left( \frac{1}{3K^*}, \frac{1}{2G^*} \right)$$

(21)

$$P^* = \left( 3P_1^*, 2P_2^* \right)$$

$$Q^* = \left( Q_1^*, 2Q_2^* \right)$$

where

$$\begin{aligned}
 I_{ijk\ell}^1 &= \frac{1}{3} \delta_{ij} \delta_{k\ell} & I_{ijk\ell}^2 &= \frac{1}{2} \left( \delta_{ik} \delta_{j\ell} + \delta_{i\ell} \delta_{jk} - \frac{2}{3} \delta_{ij} \delta_{k\ell} \right) \\
 I^1 I^1 &= I^1 & I^2 I^2 &= I^2 & I^1 I^2 &= I^2 I^1 = 0
 \end{aligned} \tag{22}$$

The great advantage of this notation is that a product such as in the right side of (20) assumes the simple form

$$C^* P^* = \left[ 9K^* P_1^*, 4G^* P_2^* \right]$$

Introducing these results into (20a) we have

$$\begin{aligned}
 \lim \left( v_2 \frac{dK^*}{dv_2} \right) &= -3K^* P_1^* \\
 \lim \left( v_2 \frac{dG^*}{dv_2} \right) &= -2G^* P_2^*
 \end{aligned} \tag{23}$$

with analogous results for (20b). Obviously, in the case of small crack density the material will also be statistically isotropic. Therefore, the tensors (16c) admit the representation (21) and thus

$$\begin{aligned}
 P_1^* &= P_1^s \left( K^*, G^*, g_c \right) \\
 P_2^* &= P_2^s \left( K^*, G^*, g_c \right)
 \end{aligned} \tag{24}$$

with a similar result for  $Q^*$ .

## APPLICATIONS

We consider first the case of randomly oriented elliptical cracks which have different sizes but identical ratio of minor to major axes  $a/b$ . The small crack density result is implicitly given in Budiansky and O'Connell (1976) and is here put into the form

$$K_s^* = K(1 - \kappa\alpha) \quad (25)$$

$$G_s^* = G(1 - \mu\alpha)$$

where  $K$  and  $G$  are matrix properties,

$$\alpha = \frac{\pi \sum a b^2}{V} \quad (26)$$

is the crack density parameter (CDP) which enters from evaluation of (12) and the sum indicates summation over all cracks. Furthermore

$$\kappa = \kappa(b/a, \nu) = \frac{8(1-\nu^2)}{9(1-2\nu)E(k)} \quad (27)$$

$$\mu = \mu(b/a, \nu) = \frac{16}{45} \frac{1-\nu}{E(k)} \left[ 1 + \frac{3}{4} \left( \frac{1}{1+\beta\nu} + \frac{1}{1+\rho\nu} \right) \right]$$

where

$$\beta = \left\{ k_1^2 K(k) - E(k) \right\} / k^2 E(k)$$

$$\rho = \left\{ k_1^2 [E(k) - K(k)] \right\} / k^2 E(k) \quad (28)$$

$$k^2 = 1 - b^2/a^2 \quad k_1^2 = b^2/a^2$$

Here  $\nu$  is the matrix Poisson's ratio and  $K(k)$  and  $E(k)$  are the complete elliptic integrals of first and second kind, respectively. Note that the bias towards  $b$  in (26) is due to the choice of representation in terms of the classical elliptic integrals.

The equivalence of (16a,c) and (25), utilizing the isotropy of all tensors, leads to the identification

$$P_1^s = \frac{1}{3} \kappa \alpha \quad P_2^s = \frac{1}{2} \mu \alpha \quad (29)$$

Therefore from (24)

$$P_1^* = \frac{1}{3} \kappa^* \alpha \quad P_2^* = \frac{1}{2} \mu^* \alpha$$

$$\kappa^* = \kappa(b/a, \nu^*) \quad \mu^* = \mu(b/a, \nu^*) \quad (30)$$

where

$$\nu^* = \frac{3K^* - 2G^*}{2(3K^* + G^*)} \quad (31)$$

is the effective Poisson's ratio. It remains to evaluate the limits on the left side of (23). Assume

that the elliptical cracks are obtained by flattening ellipsoidal voids which have the three axes  $a$ ,  $b$ ,  $pb$  where  $p$  can be made indefinitely small. Then the volume fraction of voids is

$$v_2 = \frac{\pi p \Sigma a b^2}{V} = p \alpha \quad (32)$$

where the last equality is due to (26). Remembering that  $dv_2$  is produced by adding voids it follows that

$$dv_2 = pd\alpha \quad (33)$$

Inserting (32,33) into (23),  $p$  cancels. Introducing (30) we obtain

$$\frac{dK^*}{d\alpha} = - K^* \kappa^* \quad (34)$$

$$\frac{dG^*}{d\alpha} = - G^* \mu^*$$

which in view of (31) are two simultaneous differential equations for  $K^*$  and  $G^*$ , with initial conditions

$$K^* \Big|_{\alpha=0} = K \quad G^* \Big|_{\alpha=0} = G \quad (35)$$

which can be easily integrated numerically.

In the special case of penny shaped cracks,  $a=b$ , these equations reduce to

$$\frac{dK^*}{d\alpha} = - \frac{19}{6} K^* \frac{1-\nu^*}{1-2\nu^*} \nu^*^2$$

$$\frac{dG^*}{d\alpha} = - \frac{32}{45} G^* \frac{(1-\nu^*)(5-\nu^*)}{2-\nu^*} \quad (36)$$

$$\frac{dE^*}{d\alpha} = - \frac{16}{45} E^* \frac{(1-\nu^*)^2(10-3\nu^*)}{2-\nu^*}$$

$$\alpha = \pi \sum a^3 / V$$

The first three equations are interdependent and any of them follows from the other two. These equations have already been stated by Salganik (1973) on the basis of the Roscoe (1952) interpretation of the DS according to which cracks added are always by an order magnitude larger than previous ones. The equations can be integrated in closed form as is shown in appendix II, and the results are

$$\alpha = \frac{5}{8} \ln \frac{\nu}{\nu^*} + \frac{15}{64} \ln \frac{1-\nu^*}{1-\nu} + \frac{45}{128} \ln \frac{1+\nu^*}{1+\nu} + \frac{5}{28} \ln \frac{3-\nu^*}{3-\nu}$$

$$\frac{E^*}{E} = \left( \frac{\nu^*}{\nu} \right)^{10/9} \left( \frac{3-\nu^*}{3-\nu} \right)^{1/9} \quad (37)$$

$$\frac{G^*}{G} = \frac{1+\nu^*}{1+\nu} \frac{E^*}{E}$$

These expressions have also been given by Zimmerman (1985).

Fig. 1 shows the variation of  $G^*/G$  and  $E^*/E$  with crack density on the basis of (36). Also shown are the SCS predictions for this case. The latter illustrate the difficulties mentioned in the introduction and it is seen that in contrast the DS results vanish asymptotically with increasing crack

density.

The calculations just performed reveal some noteworthy aspects. The first one is that in deriving (34) the CDP  $\alpha$  cancelled on both sides of the equation. It is believed that this is peculiar to elliptical cracks and stems from the strain uniformity in the ellipsoidal inclusion problem. For cracks of more general shape it cannot be expected that the limit on the left side and the mathematics involved in the right side of (23) should result in the same geometrical parameter.

The second observation is that the DS as interpreted here and by Roscoe (1952) give the same results for elliptical cracks with constant ratio  $a/b$  but not for cracks with different  $a/b$ . Therefore the two approaches are not necessarily equivalent.

The second example of DS application is concerned with the stiffness reduction of a plane orthotropic thin layer due to a distribution of parallel line cracks, fig. 2. This may be regarded as a possible model for a cracked ply inside a laminate consisting of unidirectional fiber composite plies and it is therefore of interest to consider the case of constant plane stress  $\sigma_{11}, \sigma_{22}, \sigma_{12}$ . Consider first the case of a single crack of length  $2a$  within an orthotropic ply, fig. 3. Stress-strain relations in plane stress are

$$\begin{aligned}\epsilon_{11} &= \frac{\sigma_{11}}{E_1} - \frac{\nu_{12}}{E_1} \sigma_{22} \\ \epsilon_{22} &= -\frac{\nu_{12}}{E_1} \sigma_{11} + \frac{\sigma_{22}}{E_2} \\ \epsilon_{12} &= \frac{\sigma_{12}}{2G_{12}}\end{aligned}\tag{38}$$

It is easily realized that application of  $\sigma_{11}$  by itself does not produce any COD. When only  $\sigma_{22}$  is applied the COD  $[u_1]$  vanishes because of symmetry and when only  $\sigma_{12}$  is applied the COD  $[u_2]$

vanishes because of antisymmetry. The surviving COD are well known; see e.g. Sih and Liebowitz (1970), and may be written in the form

$$\begin{aligned}
 [u_1] &= \sigma_{12} \eta \sqrt{a^2 - x^2} \\
 [u_2] &= \sigma_{22} \lambda \sqrt{a^2 - x^2} \\
 \eta &= \frac{2\sqrt{2}}{E_1} \left[ (E_1/E_2)^{1/2} + E_1/2G_{12} - \nu_{12} \right]^{1/2} \\
 \lambda &= (E_1)/(E_2)^{1/2} \eta
 \end{aligned} \tag{39}$$

Next we evaluate  $\gamma_{ij}$  as given by (12) for the case of small crack density, in which case all cracks have the COD (39). Noting that for the present case  $i,j=1,2$  and  $n_1=0$ ,  $n_2=1$ , it follows easily that

$$\gamma_{11} = 0$$

$$\gamma_{22} = \frac{\lambda \alpha}{2} \sigma_{22} \tag{40}$$

$$\gamma_{12} = \frac{\eta \alpha}{4} \sigma_{12}$$

where  $\alpha$  is the CDP given by

$$\alpha = \frac{\pi \Sigma a^2}{A} \tag{41}$$

$a$  is half crack length and  $A$  is the area of the ply considered of unit thickness. Identifying (40) with (13b) we realize that the only surviving components of the tensor  $R^s$  of (16) are

$$R_{2222}^s = \frac{\lambda\alpha}{2} \quad R_{1212}^s = \frac{\eta\alpha}{8} \quad (42)$$

The effective stress-strain relations of the cracked ply are

$$\begin{aligned} \bar{\epsilon}_{11} &= S_{1111}^* \bar{\sigma}_{11} + S_{1122}^* \bar{\sigma}_{22} \\ \bar{\epsilon}_{22} &= S_{1122}^* \bar{\sigma}_{11} + S_{2222}^* \bar{\sigma}_{22} \\ \bar{\epsilon}_{12} &= 2S_{1212}^* \bar{\sigma}_{12} \end{aligned} \quad (43)$$

where

$$\begin{aligned} S_{1111}^* &= \frac{1}{E_1^*} & S_{1122}^* &= -\frac{\nu_1^*}{E_1^*} \\ S_{2222}^* &= \frac{1}{E_2^*} & S_{1212}^* &= -\frac{1}{4G_{12}^*} \end{aligned} \quad (44)$$

To set up the DS we employ (20b,c). We consider the line cracks as limiting case of elliptical cracks with major axis  $a$  and minor axis  $pa$ . Then

$$v_2 = \frac{p\pi \sum a^2}{V} = p\alpha \quad (45)$$

$$dv_2 = pd\alpha$$

From (20c) and (42) the only surviving components of  $R^*$  are

$$R_{2222}^* = \frac{\lambda^* \alpha}{2} \quad R_{1212}^* = \frac{\eta^* \alpha}{8} \quad (46)$$

where the asterisk implies that all properties in  $\eta$  and  $\mu$  of (39) are to be replaced by effective properties. It now follows from (20b), (43-46) that

$$\frac{dS_{1111}^*}{d\alpha} = \frac{dS_{1122}^*}{d\alpha} = 0 \quad (a)$$

$$\frac{dS_{2222}^*}{d\alpha} = \frac{\lambda^*}{2} \quad (b) \quad (47)$$

$$\frac{dS_{1212}^*}{d\alpha} = \frac{\eta^*}{8} \quad (c)$$

Eqs. (47a) imply that these properties are not function of crack density and therefore they are equal to the properties of the uncracked material. Thus

$$E_1^* = E_1 \quad \nu_{12}^* = \nu_1 \quad (48)$$

This is of course an exact result which is easily deduced from first principles. It follows that

$$\eta^* = \frac{2\sqrt{2}}{E_1} \left[ \left( E_1/E_2^* \right)^{1/2} + E_1/2G_{12}^* - \nu_{12} \right]^{1/2}$$

(49)

$$\lambda^* = (E_1^* / E_2^*)^{1/2} \eta^*$$

and therefore from (44,47)

$$\frac{dE_2^*}{d\alpha} = -\sqrt{2} \frac{E_2^{*3/2}}{E_1^{1/2}} \left[ \left( \frac{E_1}{E_2^*} \right)^{1/2} + \frac{E_1}{2G_{12}^*} - \nu_{12} \right]^{1/2} \quad (50)$$

$$\frac{dG_{12}^*}{d\alpha} = -\sqrt{2} \frac{G_{12}^{*2}}{E_1} \left[ \left( \frac{E_1}{E_2^*} \right)^{1/2} + \frac{E_1}{2G_{12}^*} - \nu_{12} \right]^{1/2}$$

Eqs. (50) are easily integrated in closed form. If the equations are divided one by another we obtain a simple differential relation between  $E_2^*$  and  $G_{12}^*$  whose integral is

$$\frac{2}{\sqrt{E_1 E_2^*}} - \frac{2}{\sqrt{E_1 E_2}} = \frac{1}{G_{12}^*} - \frac{1}{G_{12}} \quad (51)$$

Expressing  $E_2^*$  from (51) and substituting into the second (50) we obtain a simple differential equation with integral

$$\left[ \frac{E_1}{G_{12}^*} + \left( \frac{E_1}{E_2^*} \right)^{1/2} - \frac{E_1}{2G_{12}^*} - \nu_{12} \right]^{1/2} - \left[ \left( \frac{E_1}{E_2^*} \right)^{1/2} + \frac{E_1}{2G_{12}^*} - \nu_{12} \right]^{1/2} = \alpha / \sqrt{2} \quad (52)$$

On the other hand the SCS leads to the simultaneous equations, Gortesman et al. (1980)

$$\frac{1}{E_2^*} = \frac{1}{E_2} + \frac{2}{\sqrt{E_1^* E_2^*}} \left[ \left( \frac{E_1^*}{E_2^*} \right)^{1/2} + \frac{E_1^*}{2G_{12}^*} - \nu_{12} \right]^{1/2} \alpha \quad (53)$$

$$\frac{1}{G_{12}^*} = \frac{1}{G_{12}} + \frac{2}{E_1^*} \left[ \left( \frac{E_1^*}{E_2^*} \right)^{1/2} + \frac{E_1^*}{2G_{12}^*} - \nu_{12} \right]^{1/2} \alpha$$

It is easily seen that (53) imply the relation

$$\frac{1}{G_{12}^*} - \frac{1}{G_{12}} = \left( \frac{E_2^*}{E_1^*} \right)^{1/2} \left( \frac{1}{E_2^*} - \frac{1}{E_2} \right) \quad (54)$$

and substituting for  $G_{12}^*$  from (54) into (53) we obtain an equation for  $E_2^*$ .

Fig. 4 shows plots of  $E_2^*/E_2$  and  $G_{12}^*/G_{12}$  as functions of CDP for a graphite/epoxy ply, according to the DS and the SCS. Note that in this case, unlike the case of penny shaped cracks, there is no dramatic difference between the two predictions. Note also that shear modulus reduction is much smaller than transverse Young's modulus reduction. This is apparently due to the large stiffness in fiber direction which inhibits the shear COD which is also in fiber direction

## CONCLUSION

A differential scheme (DS) approximation to obtain the elastic properties of solids containing distributions of many cracks has been established in a general sense. The necessary information for application of the method is the COD of a typical single member crack of the distribution when isolated in infinite homogeneous medium with elastic symmetry identical to the macro symmetry of the cracked material.

Specific results have been derived for randomly oriented elliptical and penny shaped cracks in elastic matrix and for aligned plane cracks in orthotropic sheet. There is a drastic difference between the DS and SCS results for penny shaped cracks and much milder difference for aligned plane cracks.

The method can be readily applied to many other cases of interest.

## ACKNOWLEDGEMENT

Support by the US Air Force Office of Scientific Research under Contract 85-0342, Major George Haritos contract monitor, is gratefully acknowledged.

## REFERENCES

Aboudi, J. and Benveniste, Y.	1987	Engng. Fract. Mech., 26, 171-184.
Benveniste, Y.	1986	Mech. Res. Comm., 13, 193-201.
Budiansky, B.	1965	J. Mech. Phys. Solids, 13, 223-227.

Budiansky, B. and O'Connell, R.J. 1976 Int. J. Solids Structures, 12, 81-97.

Boucher, S. 1976 Revue M., 22, 31-36.

Bruggeman, D.A.G. 1935 Ann. der Physik, 24, 636-679.

Gottesman, T. 1980 Dissertation, Tel-Aviv University

Gottesman, T., Hashin, Z. and Brull, M.A. 1980 in Advances in Composite Materials, Proc. ICCM 3, Pergamon Press, 749-758.

Hashin, Z. 1983 J. Appl. Mech., 50, 481-505.

Henyey, F.S. and Pumphrey, N. 1982 Geophys. Res. Letters, 9, 903-906.

Hill, R. 1963 J. Mech. Phys. Solids, 11, 357-372.

Hill, R. 1965 J. Mech. Phys. Solids, 13, 213-222.

Hoenig, A. 1979 Int. J. Solids Structures, 15, 137-154.

Horii, H. and Nemat-Nasser, S. 1983 J. Mech. Phys. Solids, 31, 155-171.

McLaughlin, R. 1977 Int. J. Engng. Sci., 15, 237-244.

Norris, A.N. 1985 Mech. of Materials, 4, 1-16.

Roscoe, R. 1952 Brit. J. Appl. Phys., 3, 267-269.

Salganik, R.L. 1973 Mekh. Tverd. Tela (Mech. Mats.), 8, 135-143.

Sih, G.C. and Liebowitz, H. 1970 in Fracture, Vol. II, Liebowitz Ed., Academic Press, 67-190.

Walpole, L.J. 1981 in Advances in Applied Mathematics, 21, Academic Press, 169-241.

Willis, J.R. 1981 in Advances in Applied Mathematics, 21, Academic Press, 1-78.

Wu, T.T. 1966 Int. J. Solids Structures, 2, 1-8.

Zimmerman, R.W. 1985 J. Mats. Sci. Letters, 4, 1457-1460.

## APPENDIX I

### SELF-CONSISTENCY OF DIFFERENTIAL SCHEME

It is required to prove that  $C^*$  and  $S^*$  as predicted by (5,6) are mutually reciprocal. Thus

$$C^* S^* = I$$

(I-1)

and therefore,

$$\frac{dC^*}{dv_2} S^* + C^* \frac{dS^*}{dv_2} = 0$$

Substituting from (5,6) into the second of (I-1) we have

$$(C^{(2)} - C^*) A^* S^* + C^* (S^{(2)} - S^*) B^* = 0 \quad (I-2)$$

Recall the definition (4) of  $A^*$  and analogous definition of  $B^*$  as small concentration tensors in which matrix properties have been replaced by effective properties. The left eqs. (3) must be mutually reciprocal. Carrying out the multiplication to order  $c_2$  we have

$$(C^{(2)} - C^{(1)}) A_s S^{(1)} + C^{(1)} (S^{(2)} - S^{(1)}) B_s = 0 \quad (I-3)$$

Replacing  $C^{(1)}$  and  $S^{(1)}$  by  $C^*$  and  $S^*$  in (I-3) proves (I-2) and thus the second of (I-1). This implies that the product  $C^* S^*$  is a constant tensor which must however be equal to  $I$  because of the known reciprocity of  $C^{(1)}$  and  $S^{(1)}$  in the initial conditions of (5,6).

This completes the self-consistency proof.

## APPENDIX II

### SOLUTION OF THE DS EQUATIONS FOR RANDOMLY ORIENTED PENNY SHAPED CRACKS

Write the second and third eqs. (36) in the form

$$\frac{dE^*}{E^*} = F(\nu^*)d\alpha \quad (II-1)$$
$$\frac{dG^*}{G^*} = H(\nu^*)d\alpha$$

By definition

$$E^* = 2(1 + \nu^*)G^* \quad (II-2)$$

Combination of the differential of (II-2) with (II-1) yields

$$d\alpha = \frac{d\nu^*}{(1+\nu^*)(F(\nu^*) - H(\nu^*))} \quad (II-3)$$

and thus

$$\alpha = \int_{\nu}^{\nu^*} \frac{d\nu^*}{(1+\nu^*)(F(\nu^*) - H(\nu^*))} \quad (II-4)$$

Introducing (II-3) into (II-1) with the definitions

$$e = E^* / E \quad g = G^* / G \quad (\text{II-5})$$

we have

$$\ln e = \int_{\nu}^{\nu^*} \frac{F(\nu^*) d\nu^*}{(1+\nu^*)(F(\nu^*) - H(\nu^*))} \quad (\text{II-6})$$

$$\ln g = \int_{\nu}^{\nu^*} \frac{H(\nu^*) d\nu^*}{(1+\nu^*)(F(\nu^*) - H(\nu^*))}$$

Introducing  $F(\nu^*)$  and  $H(\nu^*)$  from (36) the results (37) follow by elementary integration. There is of course no difficulty to employ (II-4,6) to analyze the case of elliptical cracks in accordance with (25) and (27,28). In this case it is best to carry out the integrations numerically.

## APPENDIX II

### SOLUTION OF THE DS EQUATIONS FOR RANDOMLY ORIENTED PENNY SHAPED CRACKS

Write the second and third eqs. (36) in the form

$$\frac{dE^*}{E^*} = F(\nu^*)d\alpha \quad (II-1)$$

$$\frac{dG^*}{G^*} = H(\nu^*)d\alpha$$

By definition

$$E^* = 2(1 + \nu^*)G^* \quad (II-2)$$

Combination of the differential of (II-2) with (II-1) yields

$$d\alpha = \frac{d\nu^*}{(1+\nu^*)(F(\nu^*) - H(\nu^*))} \quad (II-3)$$

and thus

$$\alpha = \int_{\nu}^{\nu^*} \frac{d\nu^*}{(1+\nu^*)(F(\nu^*) - H(\nu^*))} \quad (II-4)$$

Introducing (II-3) into (II-1) with the definitions

RANDOMLY ORIENTED PENNY SHAPED CRACKS

$$\begin{aligned}
 e &= E^*/E & g &= G^*/G \\
 \nu &= 0.30 & \alpha &= \pi \sum a_n^3 / V
 \end{aligned}$$

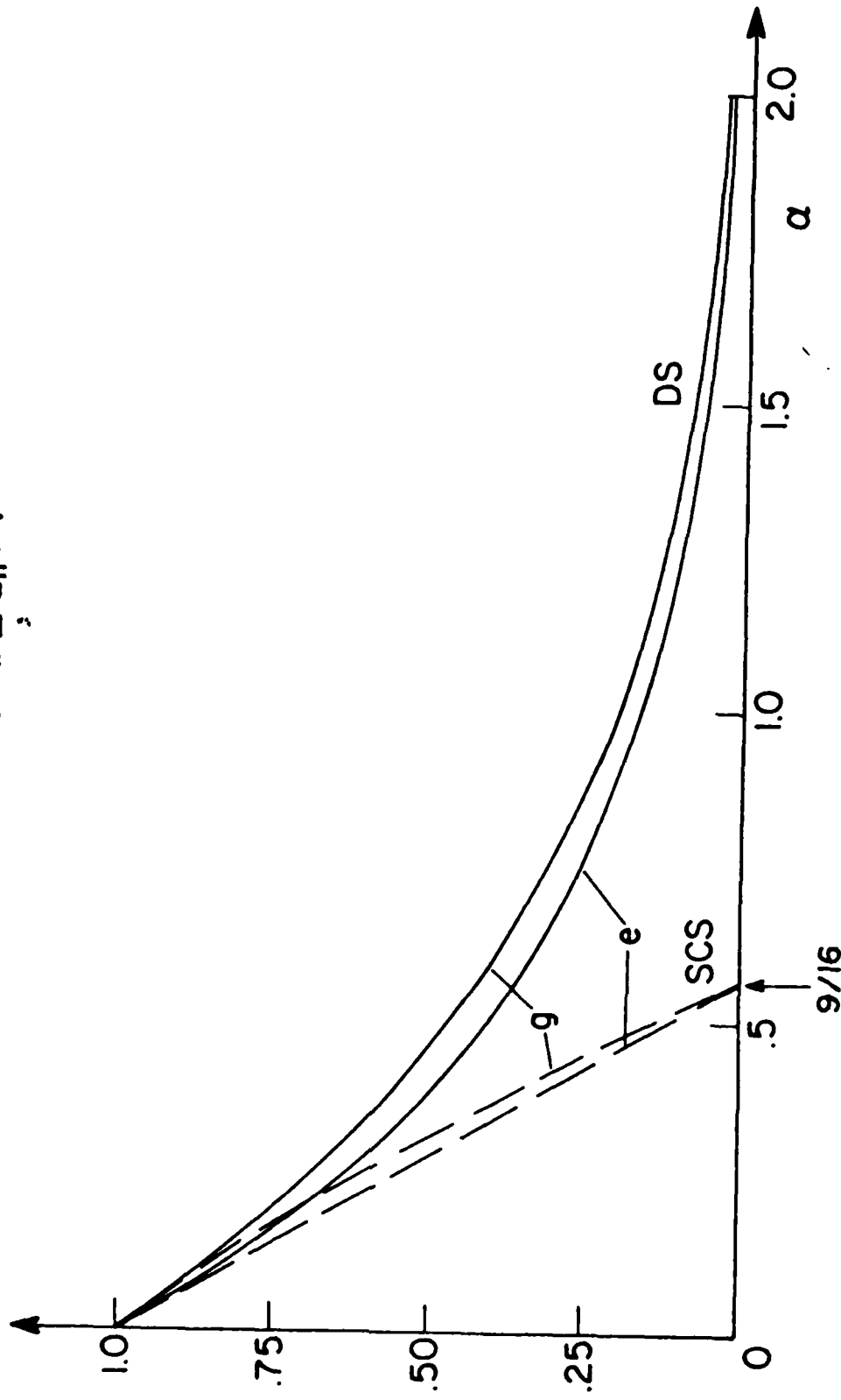


Fig. 1 - Stiffness reduction of isotropic solid with randomly oriented penny shaped cracks according to DS and SCS.

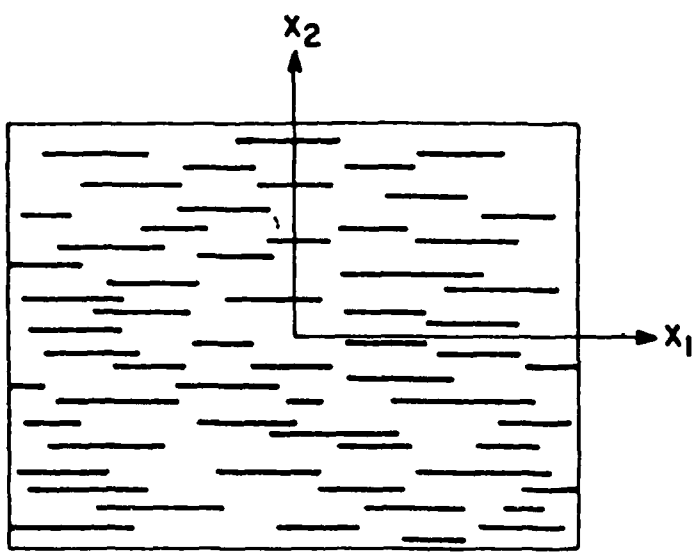


Fig. 2 - Orthotropic sheet with aligned cracks.

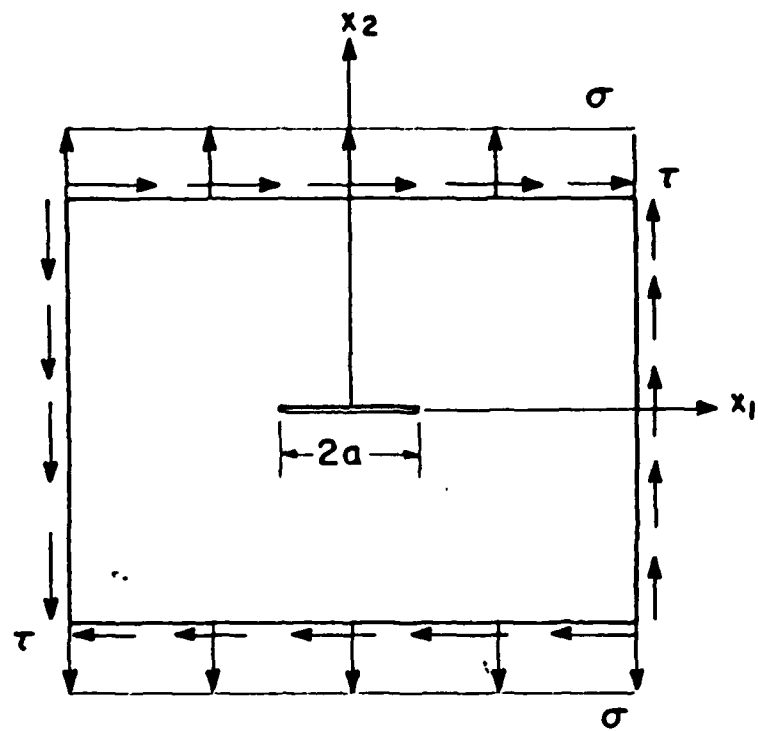


Fig. 3 - Isolated crack under transverse tension and shear.

## CRACKED UNIDIRECTIONAL T300/ EPOXY

$$E_1 = 140.0 \text{ GPa}$$

$$E_2 = 9.2 \text{ GPa}$$

$$G_{12} = 4.34 \text{ GPa}$$

$$J_{12} = 0.30$$

$$e = E_2^* / E_2$$

$$g = G_{12}^* / G_{12}$$

$$\alpha = \pi \sum a_n^2 / A$$

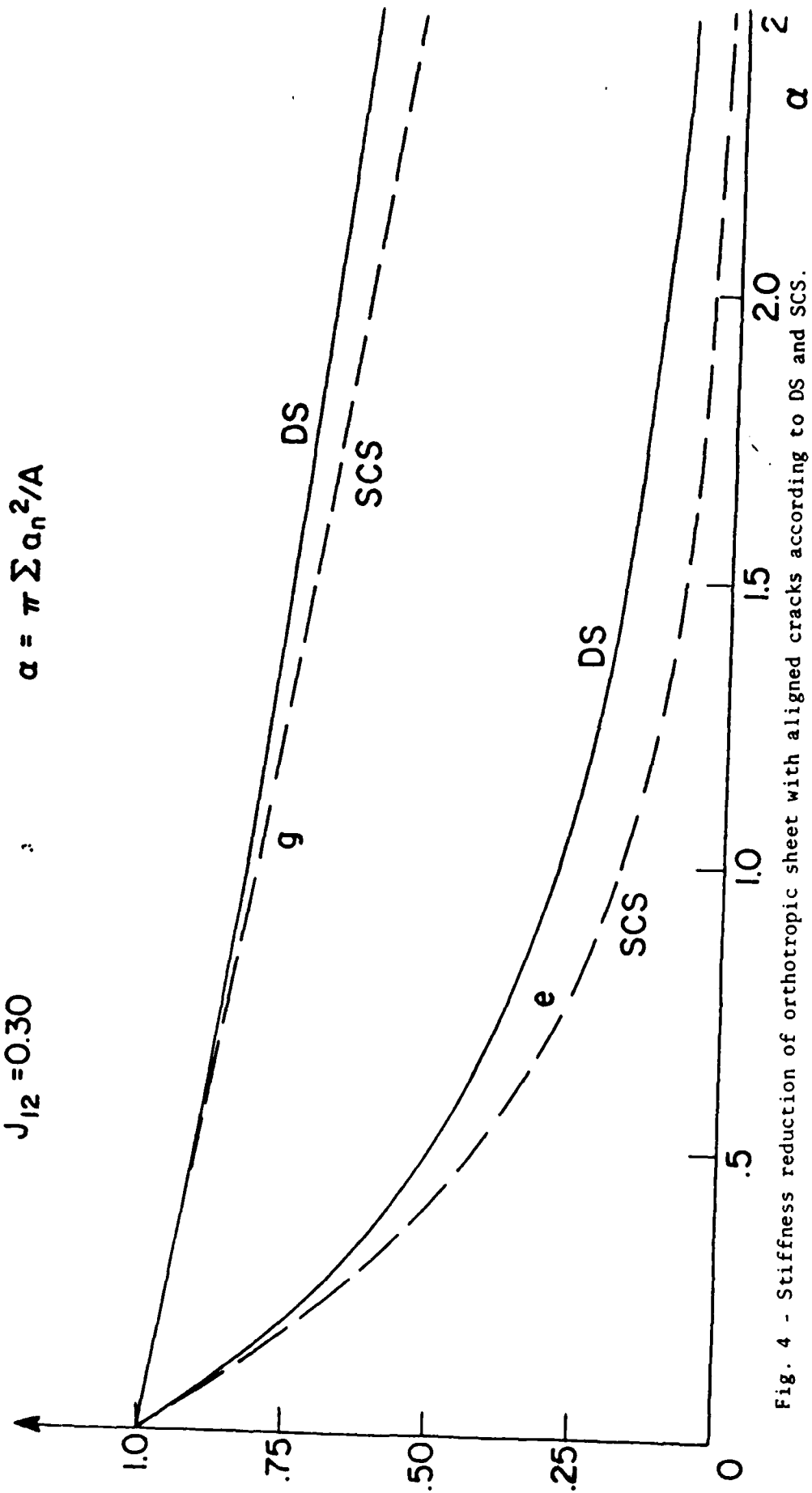


Fig. 4 - Stiffness reduction of orthotropic sheet with aligned cracks according to DS and SCS.

END

DATE

FILMED

7-88

Dtic